University of Novi Sad

Association of Centres for Interdisciplinary and Multidisciplinary Studies and Research (ACIMSI)

Medical Physics and Medical Engineering

Effective dose estimation and risk assessment in patients treated with iodine ^{131}I using Monte Carlo simulations

Doctoral thesis

Mentor: Prof. dr. Vesna Spasic Jokic

Author: Marina Zdraveska Kochovska

Novi Sad, 2014

University of Novi Sad

University of Novi Sad

ACIMSI

Key word documentation

Accession number: ANO	
Identification number: INO	
Document type: DT	Monograph documentation
Type of record: TR	Textual printed material
Contents code: CC	Doctoral thesis
Author: AU	Marina Zdraveska Kochovska
Mentor: MN	Prof. dr. Vesna Spasic Jokic
Title: TI	Effective dose estimation and risk assessment in patients treated with iodine ^{131}I using Monte Carlo simulation
Language of text: LT	english
Language of abstract: LA	eng. / srp.
Country of publication: CP	Serbia
Locality of publication: LP	Vojvodina
Publication year: PY	2014
Publisher: PU	Authors reprint
Publication place: PP	Univerzitet u Novom Sadu, Trg Dositeja Obradovica br.5 Novi Sad, Srbija

Physical description: PD	
Scientific field SF	Nuclear medicine
Scientific discipline SD	Medical physics
Subject, Key words SKW	Effective dose, dosimetry, risk estimation, Monte Carlo
UC	
Holding data: HD	
Note: N	
Abstract: AB	
Accepted on Scientific Board on: AS	
Defended: DE	
Thesis Defend Board: DB	president: member: member:

Univerzitet u Novom Sadu

Asocijacija centara za interdisciplinarne i multidisciplinarne studije i istraživanja – ACIMSI

Ključna dokumentacijska informacija

Redni broj: RBR	
Identifikacioni broj: IBR	
Tip dokumentacije: TD	Monografska dokumentacija
Tip zapisa: TZ	Tekstualni štampani materijal
Vrsta rada (dipl., mag., dokt.): VR	Doktorska disertacija
Ime i prezime autora: AU	Marina Zdraveska Kochovska
Mentor (titula, ime, prezime, zvanje): MN	Prof.dr Vesna Spasic Jokic Redovni professor tehnickog fakulteta, Univerzitet u Novom Sadu
Naslov rada: NR	Effective dose estimation and risk assessment in patients treated with iodine ^{131}I using Monte Carlo simulation
Jezik publikacije: JP	engleski
Jezik izvoda: JI	srp. / eng.
Zemlja publikovanja: ZP	Srbija
Uže geografsko područje: UGP	Vojvodina
Godina: GO	2014
Izdavač: IZ	autorski reprint
Mesto i adresa: MA	Univerzitet u Novom Sadu, Trg Dositeja Obradovica br.5 Novi Sad, Srbija

Fizički opis rada: FO	(broj poglavlja / stranica / slika / grafikona / referenci / priloga)
Naučna oblast: NO	Nuklearna medicina
Naučna disciplina: ND	Medicinska Fizika
Predmetna odrednica, ključne reči: PO	Efektivna doza, dozimetrija, procena rizika, Monte Carlo
UDK	
Čuva se: ČU	
Važna napomena: VN	
Izvod: IZ	
Datum prihvatanja teme od strane NN veća: DP	
Datum odbrane: DO	
Članovi komisije: (ime i prezime / titula / zvanje / naziv organizacije / status) KO	predsednik: član: član:

ACKNOWLEDGEMENTS

I would like to express my deep gratitude to my supervisor, Professor Vesna Spasic Jokic, for her inside and direction as the ideas for this work developed and for her continued guidance and support throughout my time at these studies.

I would like to thank you to colleagues from Institute of pathophysiology and nuclear medicine.

I would be remiss not to thank my parents for all of their support they have given me over the years and guidance in allowing me to follow my passions.

And finally, none of this would have been possible without the love and support of my husband, Ljupcho and my lovely daughter Elena, for being patient, understanding and supportive as I strove to complete this work.

CONTENT

Chapter 1

1. INTRODUCTION

1.1 Aim of the study

According to the literature radioactive iodine ^{131}I has been used for many years to treat benign thyroid disease. Also, treatment of thyroid cancer with $Na^{131}I$ is the most common application of radionuclide therapy in nuclear medicine and has been in use for many decades. At the Institute of pathophysiology and nuclear medicine this kind of radiotherapy is performed since 1956 y [1].

Whenever radiation is used in the treatment of the benign or cancer diseases, dosimetry is essential. The treatment must deliver the right dose to the target tissue of thyroid gland in the case of hyperthyroidism or residual thyroid volume in the case of the thyroid cancer patients, without harming other organs.

The main aim of this study is to simulate dosimetry of internal organs and risk assessment using MCNP 4b code in the case of performing radioiodine therapy either for hyperthyroid or thyroid cancer patients [2]. To search a safety optimization in this kind of therapy, it was recognized the necessity of more accurate knowledge of dose levels received by stomach and other organs. The study is focused on the dose determination due to ^{131}I administration in thyroid treatment in internal organs. Very important is to know the effective dose that will be reached in gastric. The main aims of this thesis are:

1. To calculate dose equivalents, effective doses for internal organs under the risk during therapy application of radioiodine using numerical simulations and to confirm all introduced assumptions.
2. To perform external measurement of dose rates (μSv/h) of thyroid cancer and hyperthyroid patients at 0.25 m, 0.5 m, 1.0 m and 2.0 m different distances.
3. To estimate with TLD's effective dose at the surface of the skin above region of gastric for 15 minutes after administration and during three days of hospitalization of patients.
4. To determinate additional risks of lifetime mortality of hyperthyroid and thyroid cancer patients.

An additional aim of this study was to provide information to be used in the improvement of radiation therapy, radiation safety practices and improvement of the fundamentals of radiation protection as defined by International Commission on Radiological Protection (ICRP): justification, optimization and application of dose limits.

1.2. Significance of the research

1.2.1 Objectives

The objective of this research was to determine the radiation – absorbed dose to the organs that were likely to receive significant doses from the capsule ^{131}I or in the form of capsule or solution for treatment of hyperthyroid and thyroid cancer patient. This was achieved by using computer codes that were executed with Monte Carlo N-particle-4b to calculate the doses to organs of interest [2].

1.2.2 Practical dosimetry: Benefits vs. risks

For many decades, radiation has been beneficial in both diagnostic and therapeutic nuclear medicine. Radiation was used to diagnose and treat the cancer with processes such as ablation as in ^{131}I therapy to treat thyroid cancer.

The long-term benefit of undergoing this treatment is the minimized probability of reoccurring tumors, adding years to the patient's lives and allowing them to proceed with their regular daily activities. Although there are significant benefits to undergoing this therapy, there are also certain issues that must be considered. These issues include side effects and radiation safety. The focus of this research is to the dose delivered to the stomach and other organs while undergoing this therapy since the capsule is dissolved and start absorption process. The dose delivered to the thyroid gland is expected to be high in these typical treatments. This research is important because, since the radiation dose to the thyroid gland should be large, the other organs and stomach are at risk of receiving high radiation doses.

As we study the details of dose calculations, it is possible to develop carefully the minimum requirements for performing an adequate calculation of radiation dose. With more and more data, constantly gathered the quality of the results and approaches will improve. The data analysis requires the time and attention of skilled professionals.

When only fixed dosages of radiopharmaceuticals are administered to all patients with no study whatsoever of radiation doses received, it is impossible to optimize individual subjects' therapies or to advance our understanding of dose–effect relationships and how to provide the best treatments for our patients. Although, gathering data and dosimetry modeling requires significantly more efforts and is difficult to implement day to day practice, it is worthwhile in providing the patient with a better quality of care and expectancy for a positive outcome from therapy [3].

The significance of this research is that the doses to internal organs can be determined and it worth to mention that such internal dosimetry calculation has been performed rare in the field of nuclear medicine.

We hope that in accordance with the calculations carried out during this study and reference available in the literature that we will improve therapy practice at Institute of pathophysiology and nuclear medicine, Faculty of medicine, “Ss. Cyril and Methodius” University, Skopje, Macedonia.

Designed quality programs will be useful also for regulatory and accreditation bodies in the process of accreditation and radiation protection strategy. The results of this investigation will improve safety culture in the health care system and also among authorities who make regulatory decisions.

1.2.3 Summary of this dissertation

This work is divided into interconnected chapters. Chapters 2 to 4 contain the literature review, history and theoretical background to the study. The basic physics and dosimetry theory applied in beta radiation, particularly to the ^{131}I are also discussed in chapter 2. Chapter 3 covers material and methods and aspects of the Monte Carlo transport code and focuses on the MCNP4b code which was used in this study. Chapter 4 provides the results and the discussion of the findings. Finally, the conclusions and recommendations and future research are discussed in Chapter 5.

Chapter 2

2. BASIC PHYSICS AND DOSIMETRY THEORY

2.1 Introduction

The physics of the interaction of radiation with matter is used in nuclear medicine, radiation therapy, diagnostic radiology and other areas of medical physics. In order to optimize treatment in radiotherapy, the way in which radiation energy is transferred to and absorbed by the patient's body must be investigated [4]. The main subject of interest in dosimetry is the mechanism of energy deposition in the matter by radiation [5].

Photons require an intermediate interaction stage of transferring energy first to atomic electrons before any transfer of energy to the medium can take the place since charged particles lose energy in a totally different manner to photons. Electrons start to lose energy immediately to the medium [5]. The basic physics of beta (β) particles, photons, dosimetry quantities and radiation dose distributions are discussed in the next sections.

2.2 Main types of ionizing radiation

Ionizing radiation can be divided into two categories. The first is called directly ionizing radiation and is composed of charged particles. Such charged particles include beta (β) particles, protons and alpha (α) particles, which require sufficient kinetic energy to produce collision and radioactive ionization when penetrating the absorber. The ionizing particles which are more important biologically are the alpha (α) and beta (β) particles [6]. The second category is named indirectly ionizing radiation, which is composed of uncharged particles such as neutrons and photons. The latter type of ionizing radiation can be detected by determining the ionization effects the charged particles produce during their interactions with matter [7, 8, 9, and 10]. As there are so many ionizing particles, only the most important will be discussed here.

2.2.1 Beta (β) – particles

The (β)-particles are fast, energetic electrons (high speed electrons) arising, not from orbital electrons but nuclear decay or transformations. They are ejected from the nucleus of unstable radioactive atom, with energies ranging from just above 0 MeV to the maximum energy ($E_{\beta\ max}$) available for particular radionuclide. This range of energies forms a continuous spectrum [10, 11]. The beta (β) particles are single, negatively charged and have a small mass. They cause ionization just like the primary electrons produced by photons [6].

The only difference between (β)-particles and electrons is their energy. The (β)-particles are deflected through a rather tortuous path [11], due to the light mass and high speed. They are more penetrating than (α)-particles, but can be stopped by a few millimeters of aluminum, so cannot penetrate deeply into tissues. ^{131}I is a beta emitter and hence is used for radiotherapy of hyperthyroid and thyroid cancer patients. Beta particles lose their energy in four ways: direct ionization, creation of delta rays by ionization, the production of Bremsstrahlung and Cerenkov radiation. Although all such mechanisms may occur, the most common are direct ionization and Bremsstrahlung production [11].

2.2.1.1 Transformation mode of beta particles

Radioactive nuclides, either naturally occurring or artificially produced by nuclear reactions, are unstable and strive to reach more stable nuclear configuration. These can be achieved through various processes of spontaneous radioactive decay. The radioactive transformation is chaotic process and defined as spontaneous nuclear transformations those results in the formation of new elements. This process is described as a change of radionuclide from one nuclear configuration to another [7]. Thus it is a process by which the nucleus attempts to achieve stability, it is not always successful at the first attempt and further transformation process may be necessary [4]. The rate of transformation is not affected by natural processes, such burning, freezing, solidifying, dilution, etc. with the exception of chemical change which can increase the electron density near the nucleus [11].

The process of radioactive transformation was first recognized by Rutherford. Commonly the term radioactive decay is used, but transformation is more accurate description of what is actually happening. Decay suggests a process of disappearance, what in reality happens is an atom with excess energy transforms itself to another atom that is either stable or one with more favorable conditions to proceed on stability [11]. The radioactive transformation of an atom occurs because of the constituents in the nucleus neither is nor arranged in the lowest potential energy state possible. Therefore, the rearrangement of the nucleus causes an excess energy to be emitted, and nucleus is transformed to an atom of a new isotope. This process may involve the emission of alpha particles, beta particles, orbital electron capture, negatrons, positrons , electromagnetic radiation in the form of X-rays or gamma rays and to a lesser extend neutrons, protons and fission fragments depending on the characteristics of the radionuclide [8.11].

In actual fact, the process is characterized by the transformation of an unstable nucleus into a more stable isotope that itself may be unstable, and will decay further through a series chain of decays until a stable nuclear configuration is reached [12]. In a stable nucleus, no particle ever acquires enough energy to escape, however, in radioactive nucleus it is possible for a particle by series of chance encounters to gain enough energy to escape from the nucleus. The ejection of a nuclear particle is pure chance, and there is no way to decide when any particular nucleus will disintegrate. However, if there are many nuclei, a certain percentage will disintegrate in a given time. Nuclei are characterized by the number of protons, Z and the number of neutrons in the nucleus.

$$(N=A-Z) \tag{1}$$

In such decay sequence, the nuclide which decays is frequently called the parent and its decay product the daughter. If both the parent and daughter nuclides are radioactive and the parent has a longer half-life than the daughter, the rate of decay of the daughter is determined not only by its own half–life but also by the rate at which it is produced. As a first approximation assumes that if the activity of the parents remains constant or is constantly replenished, so that the rate of production will at first exceed its rate of decay and equilibrium will be reached when rate of production is just equal to the rate of decay [4].

Two practical situations should be distinguished [4, 11, 13]:

1. Secular equilibrium: Occurs when the half-life of a parent is much longer than half life of daughter and $\lambda_d >> \lambda_p$. Thus daughter is much short lived than parent. In this case the parent and daughter activities are equal and both decay with the half life of parent radionuclide.

$$(A_d)_t = (A_p)_t \tag{2}$$

2. Transient equilibrium: Occurs when half-life of the parent is not that much longer than that of the daughter, both are almost equal in terms of activity and parent activity is not constant [14].

$$(A_d)_t = \frac{(T_{1/2})_p (A_p)_t}{(T_{1/2})_p - (T_{1/2})_d} \quad (3)$$

2.2.2 Gamma (γ) – rays

Gamma (γ) – rays are highly penetrating than (α) or (β) particles; electromagnetic rays (photons) emitted from the nucleus of an atom. They are highly energetic photons emitted from a radioactive source with a variety of monoenergetic energies, ranging from a low value of 100 keV to as high as 3 MeV. This means that each gamma ray has a precise energy corresponding to the discrete energy transformation within nucleus [15].

The energy of these rays is determined by the energy level structure of a particular radionuclide or the transition between the energy levels in the nucleus. Therefore, an emitted (Y)-ray is characteristic of that particular nucleus found that, in most (α) and (β) transformations, the (Y)-rays are emitted by the daughter nucleus during deexcitation and referred as if they were from the parent nucleus [10]. Practically, it requires several centimeters of lead to reduce their intensity appreciably. (Y)-rays offer the most practical approach to external beam radiotherapy [12]. ^{131}I has the yield percentage of 63 % for gamma rays with energy of 0,364 MeV.

2.2.3 X – rays

(X)-rays are electromagnetic radiation like (Y)-rays but are produced during the interaction of incident beta-particles with atomic orbital electrons of the target nucleus of interaction with a target nucleus. This produces characteristic radiation and “Bremsstrahlung” radiation, respectively. (X)-rays can be categorized in terms of their energy or clinical means as follows:

- Low energy: 0.1 – 20 keV
- Superficial x – rays: 10 keV – 100 keV
- Diagnostic range x rays: 10 keV – 150 keV
- Deep therapy or Orthovoltage X - rays: 100 keV – 500 keV
- Intermediate X- rays: 300 keV – 1 MeV
- Megavoltage X-rays: 1 MeV and above.

(X) – Rays are used mainly in diagnostic radiology for disease diagnosis, and in radiation therapy for disease treatment [12].

2.3 Interactions between ionizing radiation and matter

When a photon beam travels through any material, it interacts with the atoms and atomic electrons of this material by transferring some or all of its energy to the material. These photon interactions with matter or the absorber can lead to biological, chemical or physical changes, depending on the material type and photon beam quality [16]. The number of photons attenuated through matter depends on the number of incident photons, the type of material concerned and its density. The attenuation of photon beams follows an exponential relationship in a homogenous medium [17]. When considering a monoenergetic, narrow photon beam with (N) incident photons and the absorbing material of thickness (Δx), with (n) photons that interact with the attenuator and are removed from the beam, then (n) is expressed by:

$$\mathrm{n} = \mu \mathrm{N} \Delta \mathrm{x} \tag{4}$$

The proportionality constant (μ) is called the linear attenuation coefficient with dimensions cm^{-1}. It defines the fraction of photons that interact per unit thickness of attenuator (Δx). This coefficient depends on the photon and the nature of the material. Thus, this is the probability of whether or not particular photon will penetrate a given absorber. By considering the change in the number of photons (ΔN) in the beam passing through material thickness (Δx), the number of incident photons (N) is reduced by one for each interaction,

$$\Delta \mathrm{N} = -\mu \mathrm{N} \Delta \mathrm{x} \tag{5}$$

In order to determine the number of transmitted particles, last equation can be solved to

$$\mathrm{N} = \mathrm{N} o e^{-\mu x} \tag{6}$$

Equation (4) describes how incident photons (N) change as the beam passes through the attenuator, and equation (5) determines the number of interactions in the slab thickness bombarded by (N) incident photons.

The amount of attenuation depends on the number of atoms in any thickness of material which is material density. The linear attenuation coefficient divided by material density is referred to as the mass attenuation coefficient (μ/ρ) [8, 17].

Once a complicated series of processes has taken place, the average energy transferred (Etr) and the average energy absorbed (Eab) per interaction can be used to calculate the total energy transferred ($\Delta\mathrm{Etr}$) and the total energy absorbed ($\Delta\mathrm{Eab}$) in thickness (Δx). These total energies are defined by Johns & Cunningham (1983) as follows:

$$\Delta \mathrm{Etr} = \mathrm{Etr} \mu \mathrm{N} \Delta \mathrm{x} = \mu \left(\frac{\mathrm{Etr}}{\mathrm{h} \upsilon \Delta \mathrm{x}}\right) \mathrm{N} \mathrm{h} \upsilon \Delta \mathrm{x} \tag{7}$$

$$\Delta \mathrm{Eab} = \mathrm{Eab} \mathrm{N} \Delta \mathrm{x} = \mu \left(\frac{\mathrm{Eab}}{\mathrm{h} \upsilon \Delta \mathrm{x}}\right) \mathrm{N} \mathrm{h} \upsilon \Delta \mathrm{x} \tag{8}$$

Where ($\mathrm{N}\mathrm{h}\upsilon$) is the energy carried by the beam ratios ($\mathrm{Etr}/\mathrm{h}\upsilon$) and ($\mathrm{Eab}/\mathrm{h}\upsilon$) are energy transferred and energy absorbed respectively and ($\mu\mathrm{N}\Delta\mathrm{x}$) indicates the number of interactions occurring. The dimensions of $\mu(\mathrm{Etr}/\mathrm{h}\upsilon)$ and $\mu(\mathrm{Eab}/\mathrm{h}\upsilon)$ are the same and provide more fundamental coefficient called

transfer (μ_{tr}) and absorption (μ_{ab}) coefficient which can also be used to find total energies transferred and absorbed respectively in equation (7) and (8). The coefficients (μ_{tr}) and (μ_{ab}) are used in radiation dosimetry since (μ) explains only the local removal of photons from a beam without directly providing a measure of the energy transferred to or absorbed around the removal site.

Other more fundamental attenuation coefficients are electronic coefficient ($_e\mu$) and the atomic coefficient ($_a\mu$) defined by:

$$e\mu = \frac{\mu A}{\rho N a Z} \tag{9}$$

$$a\mu = \frac{\mu A}{\rho N a} \tag{10}$$

Where (μ/ρ) is the mass coefficient which is more fundamental and independent of density. (Na) is the Avogadro's number and (ρ), (Z) and (A) are density, atomic number and atomic mass of attenuating material, respectively [8].

Since the mass, electronic and atomic coefficients are measured in terms of area per gram, area per electron and area per atom, the coefficients are often referred to as cross sections. The cross-section can be defined as the ratio of probability of interaction occurring from the photon beam incident on a slab of material containing a number of atoms per unit area.

2.3.1 Photon interactions

Photons are far more penetrating in matter than other known types of radiation. They have no specific depth range, and their interaction with matter is based only on cross sections. In a matter, photons may undergo scattering or may have no interaction with matter (transmission), or they may be completely absorbed (absorption) and disappear. Photons demonstrate five important types of interaction which will be dealt with in the following subsections. These interactions are the Photoelectric effect, Compton Effect, Thompson scattering, Coherent scattering and Pair production.

2.3.1.1 Photoelectric Effect

The photoelectric effect process, also known as the photo effect is the interaction that might take place between an incident photon beam and one of the tightly bound electrons of K, L, M or N atomic shells in matter. It occurs mostly in the K-shell as illustrated in Figure 1.

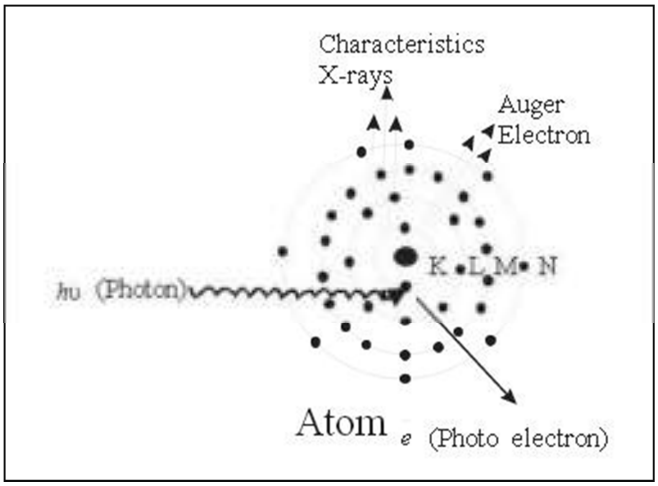

Figure 1. Illustration of photo effect (Khan 2003)

During the process, the photon disappears, and its energy is absorbed by the atomic electron. The requirement for the process to occur is that the incident photon energy $(\mathrm{h}\upsilon)$ must be greater but in order of binding energy of the orbital electron. In addition, this $(\mathrm{h}\upsilon)$ must be totally absorbed. The reason for this is that the electron must first absorb enough energy to overcome the binding energy (Eb) of its shell, and remaining photon energy is then given to the electron in the form of kinetic energy (Ek). The electron is ejected and is now called a photo-electron, leaving the atom with kinetic energy of:

$$\mathrm{Ek} = \mathrm{h}\upsilon - \mathrm{Eb} \tag{11}$$

An atom is left in an ionized state with vacancy created in the shell; thus the atom is left highly unstable. Very quickly the vacancy will be filled by one of the outer shell L, M or N orbital electrons. During this transition, energy will be released as electromagnetic radiation and this process is known as Characteristic radiation.

This radiation is the binding energy difference between the two shells with the exact specific characteristic value which is different for different elements. The energy of characteristic radiation depends on the energy of the photon and atomic number (Z) of the material and is found to be very low in biological absorbers.

The atom may also undergo a process known as the Auger effect where the energy released during the filling of the vacancy is absorbed by an orbital electron instead of being released from the atom. This excited and mono-energetic electron is then emitted from the atom. The emitted electron is called an Auger electron. Both Characteristic radiation and Auger electrons are emitted by all

elements, but heavy elements are more likely to emit radiation rays (Characteristic radiation) while light elements are more likely to emit electrons (Auger electrons).

The angular distribution of photoelectrons depends on incident photon energy: as the photon energy increases the photo-electrons are emitted in a more forward direction although momentum and energy are conserved. The photo-electron is quickly brought to rest by surrounding atoms and delivers its energy to them in the process. A similar process occurs in Auger electrons.

The probability of the occurrence of the photoelectric interactions depends on photon energy ($h\nu$). Also the photoelectric attenuation depends strongly on the binding energy (Eb) of the atomic electrons (which is the atomic number Z of absorbing material). The photoelectric attenuation coefficient is zero when ($h\nu << Eb$) and is inversely proportional to ($h\nu$). Hence, the following relationship between the mass photoelectric attenuation coefficient (σ/ρ), atomic number (Z) and incident photon energy ($h\nu$) holds true:

$$\frac{\sigma}{\rho} = \frac{z^3}{h\nu^3} \tag{12}$$

The last equation applies to energies up to 200 keV. At higher energies the term ($h\nu^3$) approximates to ($h\nu^2$) and eventually to ($h\nu$) [7, 9].

2.3.1.2 Compton effect

Compton scattering is an incomplete absorption of a photon's energy or the scattering of photon radiation. It is also defined as incoherent scattering. This process involves the inelastic interaction of photons with free or loosely bound outer orbital shell electrons, as shown in Figure 2.

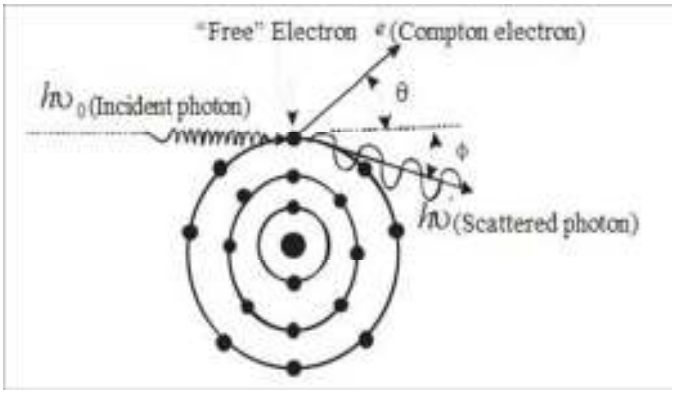

Figure 2. Compton effect (Khan 2003)

This interaction is inelastic in that the photon energy is not conserved, although the total energy of the interaction is. By free electron, it is meant that the electron has a much smaller binding energy, fraction than the incident photon energy [19]. The Compton Effect appears as a collision between a photon and a free electron [14]. In the process, some of the incident photon energy ($h\nu_0$) is absorbed while the scattered photon continues with a reduced energy. Then an emission of an electron (recoil or Compton electron) from the atom at recoil angle (Θ) occurs. This angle lies between the incident

photon direction and the direction of the recoil electron. Thus energy of the incident photon is shared between the scattered photon and the Compton electron. The sharing of energy depends on the scattering angle (ϕ) and the energy of the incident photon ($h\nu_0$) relative to the energy equivalent of the rest mass of the electron (m_0c^2) [19]. The energy of scattered photon ($h\nu'$) is related to the angle of deflection (ϕ) and by applying the laws of conversation of momentum and energy, as expressed in Figure 2, the following relationships can be derived:

$$E = h\nu_0 \frac{\alpha(1-\cos\phi)}{1+\alpha(1-\cos\phi)} \tag{13}$$

$$h\nu' = h\nu_0 \frac{1}{1+\alpha(1-\cos\phi)} \tag{14}$$

Where (ϕ) is the scattering angle at which the photon scatters which lies between the incident photon direction and the scattered photon direction. (E) is the energy of the recoil or Compton electron, which may also be expressed by:

$$E = h\nu_0 - h\nu' \tag{15}$$

And $\alpha = \frac{h\nu_0}{m_0c^2}$ and (m_0c^2) is the rest mass of the electron. The scattering angle (ϕ) depends greatly on the amount of energy received by the scattered photon. For each collision the amount of the energy transferred to both recoil electron and scattered photon, depends on the energy of the incident photon and scattering angle. For a high energy incident photon the Compton electron acquires most of the energy, and the scattered photon will carry away only small fraction of energy. So, most of the energy is deposited in forward direction. For low energy incident photon very little energy is transferred to the recoil electron, and most is entirely scattered. The probability of photon being scattered forward and being scattered backward are almost equal, depending on the amount of incident photon energy. Thus, as energy of incident photon increases the greater the energy of scattered photons at all scattering angles [8, 9]. The scattering angle determines the decrease in energy of the scattered photon thus the amount of energy ejected by the scattering photon depends only on the scattering angle. The greater the scattering angle the lower the energy of the photon will be scattered. Therefore, the lowest energy scattered photons occurs at 180 degrees, which occurs as a back-scatter radiation photons.

If the photons makes a direct hit: the electron will travel straight forward, and the photon will be scattered straight back. During this process, the electron receives maximum energy compared to the scattered photon.

If the photon makes a grazing hit: the electron will emerge nearly at right angles and the scattered photon will move almost straight forward. During this process, the electron receives almost no energy and the scattered photon has essentially the full energy of the incident photon.

The Compton Effect depends strongly on incident photon energy and is independent of density, atomic number or any other property of the absorbing material. Hence it follows that the Compton mass attenuation coefficient (σ/ρ_o) is independent of atomic number and depends only on the total

number of electrons in absorbing material. In turn, the Compton mass attenuation coefficient depends on material density and the number of electrons per gram. The mass attenuation coefficient (σ/ρ_o) is thus a measure of the total energy removed from the primary beam.

2.3.1.3 Classical scattering (Thomson scattering)

This process is easily explained by classical electromagnetic theory, which states that when an electromagnetic wave passes near a free electron, the electron is sent into vibration and accelerated by the electrical field of the wave. The electron will then radiate an electromagnetic wave of the same wavelength (λ), and this wave will form the scattered radiation. According to Young et al. the intensity of the radiation which is scattered at an angle (Θ) to the direction of the incident radiation at a distance (r) from an electron of charge (e) and mass (m) is expressed as:

$$\frac{I}{2r^2}k^2(1+\cos^2\Theta) \tag{16}$$

The (I) denote the incident intensity and (k) is a constant.

If the fraction of the incident energy scattered by an electron into the solid angle $d\Omega = \frac{1}{r^2}$ at an angle (Θ) is denoted by $d\sigma_e$, then it follows that:

$$\frac{d\sigma_e}{d\Omega} = \frac{k^2}{2}\,(1+\,\cos^2\Theta) \tag{17}$$

Where $(d\sigma_e/\,d\Omega)$ is called differential electronic cross section for classical scattering. This can be defined as a classical scattering coefficient per electron and per unit solid angle. The later is the function that allows the correct amount to be scattered for zero energy photons. During this process no energy is transferred to the electron since the frequency as well as the wavelength of the scattered radiation is the same as that of the incident radiation.

Since $d\Omega = 2\pi \sin\sin\theta d\theta$ between cone of (θ) and $(\theta + d\theta)$, equation (17) becomes

$$\frac{d\sigma}{d\theta} = \frac{k^2}{2(1+\cos^2\theta)2\pi\sin\theta} \tag{18}$$

By integrating equation (18) over all values of (θ) that is from zero to 180 degrees, the total cross section (σ_e), defined as the Thomson classical scattering coefficient for free electrons can be obtained [8,19] as:

$$d\sigma_e = \frac{8}{3\pi k} = 66.525 \cdot\ 10^{-30}\,m^2 \tag{19}$$

This process occurs when the binding energy of the electrons is high which means that the atomic number of scattering material is high, while the quantum energy of the incident photon is relatively low.

2.3.1.4 Coherent Scattering (Rayleigh scattering)

In coherent (Rayleigh) scattering or elastic scattering the photon interacts with a bound orbital electron, i.e., with the combined action of the whole atom. The event is elastic in the sense that the photon loses essentially none of its energy and is scattered through only a small angle. Since no energy transfer occurs from the photon to charged particles, Rayleigh scattering plays no role in the energy transfer coefficient; however, it contributes to the attenuation coefficient [10]. The probability of coherent scattering occurring depends on the incident photon energy ($h\nu$) and the atomic number (Z) of the material. The cross section of coherent scattering decreases rapidly with the increase in photon energy, and is negligibly small for energy greater than about 100 keV in low atomic number materials. Hence the following relationship applies:

$$\frac{\sigma_{coh}}{\rho} = \frac{Z^2}{h\nu} \tag{20}$$

Where (σ_{coh}/ρ) is the mass attenuation coefficient or cross section resulting from elastic scattering. Elastic scattering may occur as a result of a photon interacting with the nucleus of an atom of the attenuator. But the effect is even less and so may safely be ignored in medical radiography or imaging. This process has an effect in slightly broadening the angular width of the beam [7, 8]. From the equation (20), it is clear that coherent scattering occurs mainly at low energies (about 50 keV) for larger atomic number values.

2.3.1.5 Pair production

When the gamma photon energy is greater than 1.02 MeV the photon interacts with the nucleus of the absorber atom during its passage through it, and a positive electron and negative electron are produced at the expense of photon. The energy in excess of 1.02 MeV appears as the kinetic energy of two particles. The process is called pair production. It varies almost linearly with Z^2 of the absorber and increases slowly with the energy of the photon. Positive electrons created by pair production are annihilated to produce two 0.511 MeV photons identical to those produced by positrons from radioactive decay.

2.4 Electron interactions

All radiation particles or ionizing radiations (α-particles, β-particles, γ-rays and X-rays) interact differently with matter or tissue, since they have different characters. As a high energetic particle such as a β-particle transverses matter, it interacts with matter through coulomb interactions with atomic orbital electrons and atomic nuclei. Through these collisions, these β-particles may lose their kinetic energy (collision and radiative losses) or change their direction of travel scattering [12], slowing down as they pass through matter as a result of these collisions with atoms and molecules. High energy electrons, which are also charged particles, are a by-product of these collisions. The energy losses, whereas those occurring in a charged particle, in ionization and excitation events, are called *collision losses*, whereas those occurring in nuclear encounters resulting in Bremsstrahlung production are called *radiation losses*.

The parameters used to describe the gradual loss of energy of a charged particle as it penetrates an absorbing medium are called *stopping powers*. Such parameters may be collisional (ionization) or radiative stopping powers. These parameters play an important role in radiation dosimetry and are dependent on properties of the charged particle such as mass, charge, velocity and energy as well as on the absorbing medium's properties, such as density and atomic number [9].

Energy losses are described in terms of stopping powers, while scattering is described in scattering powers [12]. When attenuation is focused on the absorbing medium, we are interested in the linear rate of energy absorption, linear energy transfer (LET) by the absorbing medium as the ionizing particle transverses the medium distance (dl). It is important to show the specific point at which the energy is absorbed. The energy transfer from the charged particle to matter in each atomic interaction is generally small, and the particle undergoes a large number of interactions before its kinetic energy is spent. The kinetic energy gained by the electron may be lost through the following processes:

- Bremsstrahlung (inelastic collision as the electron nears the nucleus)
- Ionization and excitation (inelastic collision with atomic electrons)
- Elastic collision in which the electron may lose a maximum of half its original energy
- Violent electron-electron interaction causing delta ray.

As a result of the above mentioned processes, electron tracks are tortuous, and their exact shape and length are unpredictable.

A given kinetic energy electron travels at a much higher speed than a heavy particle with similar energy. Such an electron thus spends a briefer time in the vicinity of an atom than a heavier particle and therefore less likely to interact with the atom. Such an electron also carries only one unit of electrical charge and thus exerts weaker forces on orbital electrons. These electrons experience less frequent interactions than heavy particles and lose their energy more slowly than heavy particles. Electrons are much less densely ionizing, and they travel further before they are stopped, compared with heavy particles of similar energy [13]. Transfer from the energy of a photon beam to the medium take places in two stages:

- First involves the interaction of the photon with the atom, causing an electron or electrons to be set in motion
- The second stage involves transfer of energy from the high energy electron to the medium through excitation and ionization [8].

2.4.1 Collision interaction

The collision that occurs between a charged (β)-particle and atoms involves electric forces of attraction or repulsion, rather than actual mechanical contact. In close encounters, the strength of coulomb forces may be sufficient to cause orbital electrons to separate from the atom during the interaction of (β)-particle with atom, thus causing ionization. The ionization interaction appears as a collision between the (β)-particle and an orbital electron, and the (β)-particle losses energy in the process. Part of this energy is used to overcome the binding energy of the electron from the atom and what remains is given to the ejected secondary electron as kinetic energy. Thus ionization involves the ejection of an individual electron to a higher energy orbital after gaining energy from a (β)-particle. The ejected electron may be sufficiently energetic to cause secondary ionizations on its own. Such an ejected secondary electron is called a delta (δ) ray and occasionally causes longer side tracks when it is energetic enough. The effects of delta ray are accounted for by using the energy limit Δ, below which the energy transfer is considered dissipative. Ionization, involving an inner shell electron, leads to the emission of characteristic x-ray or Auger electrons, as described in the photoelectric effect process. However, these effects are generally small since most ionization interactions involve outer shell electrons.

If the energy lost by the incident (β)-particle is not enough to eject an electron from the atom, it is used to raise the electron to a higher level by a process known as excitation, thus causing atomic or molecular excitation. These interactions result in smaller energy losses than in ionization events. The energy transferred to an atom in an excitation interaction is dissipated in molecular vibrations, atomic emissions of infrared, visible, ultraviolet light and so forth.

The inelastic collisions responsible for energy deposition locally in the irradiated medium result in excitation or ionization of an atom. The probability of their occurrence depends on the energy of the passing electron, the distance of closest approach and the atomic number (Z) of the medium [5].

2.4.2 Radiative interaction

Radiative interaction occurs when the high speed β-particle penetrates the orbital electron cloud of an atom and interacts with its nucleus. The particle is rapidly decelerated and may be deflected from its original path and through the process it loses energy. The energy appears as a photon of electromagnetic radiation, called Bremsstrahlung. The energy of Bremsstrahlung photon can range anywhere from nearly zero to maximum equal to the full energy of the incident particle.

Bremsstrahlung depends on the atomic number of the absorber and the energy of the beta particle. These photons are governed by the Larmor relationship [12], which is expressed by:

$$P = \frac{q^2 a^2}{6\pi\varepsilon_0 c^3} \tag{21}$$

(P) is the power in the emitted photon, (q) is the electronic charge, (a) is the acceleration of the(β)-particle, (ε_0) the permittivity of free space and (c) the speed of light in free space.

Radiation losses through Bremsstrahlung increase with increasing - particle energy, and with increasing atomic number (z) of absorbing medium. Hence, low atom number materials like plastic and aluminum are more efficient as protective shields for beta particle emitters such as ^{131}I. This is because they are poor Bremsstrahlung radiation emitters and at the same time, they are good absorbers of beta particles. This type of energy loss is characterized by radiative stopping power [12, 13]. An approximation of percentage radiation losses for beta-particles having maximum energy $(E_{\beta max})$ (MeV) is:

$$\text{Percentage radiation losses} = \left(\frac{zE_{\beta max}}{3000}\right) \cdot 100\% \tag{22}$$

(z) is the atomic number of the absorbing material. The approximation is accurate to within about 30%. The total kinetic energy (KE) loss by the beta particle per unit length (x) can be described as the total mass stopping power given by combination of collisional and radiative interactions as follows:

$$\left(\frac{s}{\rho}\right) \text{tot} = \frac{1}{\rho}\frac{d(KE)}{dx} = \left(\frac{s}{\rho}\right) \text{col} + \left(\frac{s}{\rho}\right) \text{rad} \tag{23}$$

Where $\left(\frac{s}{\rho}\right) \text{col}$ is the mass collision stopping power resulting from β-particle and orbital electron interactions (atomic excitation and ionizations) and $\left(\frac{s}{\rho}\right) \text{rad}$ is the mass radiative Stopping power resulting from beta particle and nucleus interactions (Bremsstrahlung).

2.4.3 Continuous Slowing Down Range (CSDR)

As a beam of (β)-particles passes through the matter, the interaction causes the particles to slow down and change direction. Eventually, particles will lose all their kinetic energy and come to rest. There will be a finite distance beyond which there will be no particles, and this distance is called the particle range. This gradual and continuous loss of kinetic energy is often referred to as the continuous slowing down approximation (CSDA). The CSDA is used to obtain the actual range covered by the particle, taking into consideration the variation of the total mass stopping power with respect to the energy. The path of the beta particle is tortuous or zigzag. The charge and small mass may easily be deflected from a straight line path. This deviation will lead to variations in actual penetration of beta particles into the absorbing medium depending on the initial energy of beta particles. Thus beta particles do not have a well defined range [20]. In CSDA energy loss fluctuation are neglected, and the beta particles are assumed to lose energy along its track according to the mean energy loss per unit path length given by stopping power. That is inelastic energy losses by

beta particles moving through a medium with density ρ are described by the total mass energy stopping power $(S/\rho)_{tot}$ (in $MeVcm^2/g$). Stopping power defines the effect of material in beta dosimetry [5]. The range of beta particle with initial energy (E_0) is given in following relation

$$R_{csda} = \int_0^{E_0} \left(\frac{S(E)}{\rho}\right)_{tot}^{-1} dE \quad (24)$$

and $\left(\frac{S(E)}{\rho}\right)_{tot}^{-1}$ is the total mass stopping power with respect to energy, specifically total unrestricted mass stopping power. In the restricted collision stopping power it is, generally accepted that beta particles lose their energy in a large number of interactions with small energy losses. Thus, during CSDA the energy transferred to the medium may be assumed to be absorbed locally in a small volume close to the point of interaction [5].

2.4.4 Mass scattering power

Collisions that occur between (β)-particles themselves, between (β)-particles and electrons or between (β)-particles and a nucleus not only contribute to the energy absorbed but also increase the scatter of beam of (β)-particles. The energy loss and change of direction by the (β)-particle as it passes through a medium are described respectively by the stopping and scattering power ratios. The scattering angle depends on the atomic number (Z) of the medium, as well as on the cross section of radiation loss of the (β)-particles. The mean square angle of scattering related to the mass of scattering material is recommended for characterizing the "angular scattering power" of a given medium. Multiple scattering of (β)-particles as they traverse a path length (l) of the absorbing medium is commonly described by the mean square angle of scattering (Θ^2) which is the proportional to the mass thickness (ρl) of the absorber. The mass scattering power (T/ρ) expresses the increase in the mean square angle of scattering $(d\theta^2)$ per unit mass thickness (ρl) and can be defined as follows [5, 12].

$$\frac{T}{\rho} = \frac{1}{\rho}\frac{d\theta^2}{dl} = \frac{\theta^2}{l} \quad (25)$$

This equation emphasizes that the scattering power is analogous to stopping power in a given medium [12). Khan (2003) observed that scattering power varies approximately as the square of kinetic energy (KE) of the incident electron (β)-particle [9].

$$\frac{T}{\rho} = \frac{z^2}{KE_e^2} \quad (26)$$

2.5 Thyroid gland

The thyroid is the largest endocrine gland and its function is to synthesize, store and secrete iodinated hormones. The thyroid cells both collect and transport iodine for synthesis of the hormones and release the thyroid hormones T3 (triiodothyronine) and T4 (tetraiodothyronine) into blood circulation. Smaller quantities of several other closely related iodinated hormones that have a profound effect on the metabolism of the body are produced by thyroid gland.

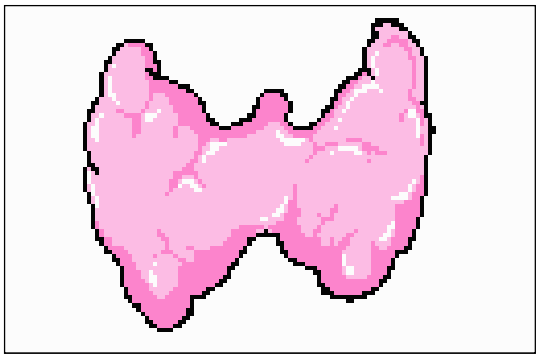

Figure 3. The Thyroid gland

The first step in the synthesis of thyroid hormones is the organification of iodine. Iodide is taken up, converted to iodine, and then condensed onto tyrosine residues which reside along the polypeptide backbone of a protein molecule called thyroglobulin. This reaction results in either a mono-iodinated tyrosine (MIT) or di-iodinated tyrosine (DIT) being incorporated into the thyroglobulin. This newly formed iodothyroglobulin forms one of the most important constituents of the colloid material, present in the follicle of the thyroid unit. The other synthetic reaction that is closely linked to organification is a coupling reaction, where iodotyrosine molecules are coupled together. If two di-iodotyrosine molecules couple together, the result is the formation of thyroxin (T4). If a di-iodotyrosine and a mono-iodotyrosine are coupled together, the result is the formation of triiodothyronine (T3).

From the perspective of the formation of thyroid hormone, the major coupling reaction is the di-iodotyrosine coupling to produce T4. Although T3 is more biologically active than T4, the major production of T3 actually occurs outside of the thyroid gland. The majority of T3 is produced by peripheral conversion from T4 in a deiodination reaction involving a specific enzyme which removes one iodine from the outer ring of T4. The T3 and T4 released from the thyroid by proteolysis reach the bloodstream where they are bound to thyroid hormone binding proteins. The major thyroid hormone binding protein is thyroxin binding globulin (TBG) which accounts for about 75% of the bound hormone.

In order to attain normal levels of thyroid hormone synthesis, an adequate supply of iodine is essential. The recommended minimum intake of iodine is 150 micrograms a day. Intake of less than 50 micrograms a day is associated with goiter. High iodine levels inhibit iodide oxidation and

organification. Additionally, iodine excess inhibits thyroglobulin proteolysis (this is the principal mechanism for the antithyroid effect of inorganic iodine in patients with thyrotoxicosis).

2.5.1 Hyperthyroidism

In hyperthyroidism, the level of thyroid hormones in the blood is increased while the level of TSH is depressed, and the thyroglobulin production is increased. The thyroid is depleted of iodine because of the hormones that are rapidly eliminated from the thyroid gland. The most common causes for hyperthyroidism are diffuse toxic goiter, also called Graves' disease, toxic multi nodular goiter and toxic adenoma (4) (Fig 4). The classic symptoms are weight loss, increase in appetite, weakness, palpitations, sweating, heat intolerance, tremor and irritability.

a b c

Figure 4. Examples of scintigrams after administration of ^{131}I-iodide showing the diagnosis a) Graves' disease; b) Multinodular goiter and c) Autonomous adenoma

Graves' disease (Figure 4-a) is caused by antibodies (IgG), which stimulate the TSH receptor. The cause of the disease is unknown, but stressful events in the life, like the death in the family or separation could trigger the disease [21]. A gamma camera image usually shows an enlarged thyroid and an uptake measurement of ^{131}I reveals a raised uptake of iodide.

The multi nodular goiter (Figure 4-b) is enlarged and has multiple nodules of various sizes. The growth of the nodules is often a slow process during several years. The gamma camera image will show an enlarged goiter with nodule-hot areas of different sizes. A nodular goiter is common in areas with iodine deficiency.

Autonomous adenoma (Figure 4-c) is functioning autonomously, and the rest of the normal thyroid tissue is suppressed. In gamma camera image, the nodule will show clearly, and the rest of the thyroid tissue will not be visible in the image. The frequency of the autonomous adenoma is higher in iodine – deficient areas then in iodine – sufficient areas [22].

2.5.2 Thyroid carcinoma

Although benign disease of the thyroid is relatively common, malignancy occurs relatively infrequently. Carcinoma of the thyroid represents approximately 1% of newly diagnosed cancers each

year and is the most common endocrine malignancy. Fortunately, for most individuals, the prognosis is excellent, and the most common types of thyroid cancer can be completely removed by surgical resection. There are four main varieties of thyroid cancer (papillary, follicular, medullary, and anaplastic).

Papillary Carcinoma representing approximately 65 % of cases, and are the most common thyroid malignancy. Papillary carcinomas are solitary or multifocal, slow growing tumors that arise from the thyroxin and thyroglobulin producing follicular cells of the thyroid. They typically present as asymptomatic thyroid nodules, however, the first manifestation may be enlargement of cervical lymph node, where metastases travel primarily. Distant spread of papillary carcinoma typically occurs to the lungs and bone. Approximately 5 % - 10 % of patients will develop distant metastases. These tumors are highly likely to take up radioiodine [22].

Follicular carcinoma is the second most common thyroid malignancy, constituting 20 % - 25 % of cases. They similarly arise from the follicular cells of the thyroid and present as slowly enlarging, painless masses. In contrast to papillary carcinoma, the rate of metastasis is somewhat higher (about 20%). Fortunately, well-differentiated metastases usually take up radioactive iodine, which can aid in identifying and ablating such lesions. Thyroid lobotomy and isthmusectomy or total thyroidectomy is both surgical options with very good prognoses.

Radioiodine is used for diagnostic, ablation and treatment. The initial diagnostic approach at thyroid cancer patients is the demonstration of residual normal thyroid tissue following removal of the tumor. At hyperthyroid patients, the diagnostic approach is to evaluate the size of thyroid tissue. The routine protocol in the treatment of thyroid cancer patients is if any thyroid tissue is visualized after removal of cancerous thyroid gland, ablation with radioiodine should be performed. After ten days from therapy, a whole body imaging is also performed.

2.5.3 Iodine ^{131} I

2.5.3.1 History

The first studies of iodide metabolism in thyrotoxicosis were made in 1927 when stable iodide was administered orally and the iodine in the urine determined after different intervals. It was found that most patients with thyrotoxicosis excreted less iodine than normal subjects and this method became one of the most frequently used diagnostic procedures, before production of radioiodine. The radioactive iodine was first produced in atomic-bomb experiments in USA, in the 1930's.The first production of radioiodine for clinical application was made by Robley Evans in 1937 [24]. He produced ^{128}I by the neutron irradiation of ethyl iodide. Evans administered an intravenous injection of ^{128}I into rabbits and demonstrated for the first time the rapid accumulation of radioiodine in the thyroid gland [25]. Radioactive iodine-131 was discovered by Glenn T Seaborg and John Livingood at the University of California-Berkeley [26] reported on the first use of ^{131}I in human subjects with thyroid disease. Some years later in 1940 it was introduced in the medical field. Hertz et al. (1940) introduced

the possibilities of radioactive isotope technique into the study of thyroid physiology and the investigations concerning thyroid diseases and iodide metabolism were enormously increased. Even though Fermi produced radioiodine already in 1934 by neutron bombardment of stable iodine, it was not made available until 1946 by actions of the United States Atomic Energy Commission, and ^{131}I became first available from a nuclear reactor at Oak Ridge, Tennessee [27]. The first report of the use of radioactive iodine for treatment of metastatic thyroid cancer was published by Seidlin et al. in 1946 [28]. ^{131}I was administered to a patient who was clinically hyperthyroid despite having had a thyroidectomy for thyroid cancer. A scan after therapy revealed uptake in pulmonary metastases. This report was followed by many case reports that confirmed that metastatic thyroid cancer lesions could concentrate the radioiodine. At Institute of pathophysiology and nuclear medicine^{131}I was used for the first time in 1950 when were done first experiments with rats [29.30]. Since then, ^{131}I has been used for diagnostic examination of the thyroid gland and became major therapeutic agent for hyperthyroidism and thyroid cancer.

2.5.3.2 Metabolism of ^{131}I

Iodine is an essential component of thyroid hormones, so the thyroid gland takes up iodine very easily. Normally, iodine is supplied to the body in foodstuffs and drinking water, and a normal dietary intake hardly ever results in excessive amounts of iodine intake. After intake, iodine will be concentrated in the thyroid tissue and used for the synthesis of hormones. If an additional amount of iodine is presented to the body, an average of about 25 % of this intake will be directly taken up by the thyroid. This amount is strongly dependent on the normal daily intake through the diet. With a low daily intake, the amount of uptake can be easily 50 %. Within daily intake, the uptake may be as little as 5 % - 10 %. The rest leaves the body quite quickly, within some days, mostly in the urine but also in other excretions, such as feces, sweat, saliva and breath. The iodine used by the gland is slowly released from the hormones into the body fluids and can recalculate. It is retained in a thyroid with a biological half-life of 120 days in the form of organic iodine. Organic iodine is assumed to be uniformly distributed in all organs and tissues of the body except the thyroid, and retained with a biological half-life of 12 days [31]. The committed dose is significantly reduced due to the short physical half-life of ^{131}I [31].

2.5.3.3 Radioactive iodine

As the body does not differentiate between stable and radioactive iodine -^{131}I, behaves in the same manner as stable iodine. This means that a large part of the intake will be concentrated in the thyroid within 24 hours to 48 hours. During the initial retention and recycling period that the radioactive iodine is in the body, it irradiates the thyroid tissue, resulting in death of tumor cells in the case of thyroid cancer or of a substantial amount of normal thyroid cells in the case of benign thyroid diseases. The half of the amount of the radioactive iodine will decay within 8 days. The main decay product is ^{131}Xe,

which is rapidly washed out of the body. In addition, damaged thyroid cells lose their capacity to organify iodine and consequently, the iodine is released back to the blood stream, resulting in excretion. Thus, radioactive iodine is removed from the body reasonably quickly, due either to radioactive decay or to metabolic excretion. The total amount of radioactive iodine reduces to half its original value at a rate which depends on the state of disease: between one day, in the case of thyroid cancer and total ablation of thyroid tissue, and seven days for patients with euthyroid goitre. In the case of hyperthyroidism, the effective half-life is about four to five days. It is well known that it is based on the physical half-life and the biological half-life, dependent on metabolism [32].

2.5.3.4 Radioactive decay products of ^{131}I

The original ^{131}I radionuclide, employed for studies of iodine metabolism, was produced by bombarding stable Tellurium with deuterons. Nowadays, ^{131}I is obtained primarily as a reactor byproduct from fission of ^{235}U atoms. Both methods produce ^{131}Te, which decays to ^{131}I according to the following [33].

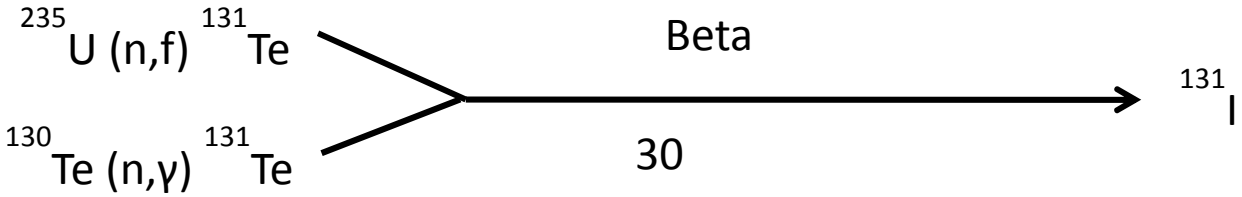

The nuclear material is processed to yield sodium iodide as a final chemical form. There are 37 known isotopes of iodine, and only one ^{127}I is stable. The isotopes of iodine have atomic masses from 108 to 144. The iodine ^{131}I nucleus is characterized by 53 protons and 78 neutrons, four neutrons more than the stable isotope ^{127}I.

The particles that are emitted as a result of radioactive decay, of an isotope, determine the potential usefulness in diagnostic and treatment of disease. The radioiodine ^{131}I fulfills many criteria as a radionuclide suitable for therapy. The ideal properties should one radionuclide have are as follows:

- Effective-half life in the range 5 h – 100 h (half-life should be relevant for the biokinetics procedure/treatment).
- Suitable modality of radiation (beta or alpha for therapy, gamma and other photons for imaging).
- Suitable energy range.
- Stable chemical bonds.
- Simple labeling procedure.
- Suitable metabolism of the radiopharmaceutical.

The iodine ^{131}I is used for treatment of hyperthyroidism and thyroid cancer as it has suitable physical half-life of 8.04 days, which is long enough for uptake by thyroid gland and is used in the metabolism and production of thyroid hormones it allows for an assessment of the function.
The simplified decay scheme is shown on Figure 5. As it is shown ^{131}I decays to stable ^{131}Xe [34], by negative beta decay according to the following nuclear transformation equation [35].

$$^{131}_{53}\mathrm{I} \rightarrow {}^{131}_{54}\mathrm{Xe} + \beta + \gamma + \check{\nu} \tag{27}$$

The mechanism of transformation is called “beta decay” because neutron is converted to a proton and an electron. In this decay process, an antineutrino is created and carries away part of the energy of this reaction.

$$^{1}_{0}\mathrm{n} \rightarrow {}^{1}_{1}\mathrm{p} + {}^{0}_{-1}\mathrm{e} + \check{\vartheta} \tag{28}$$

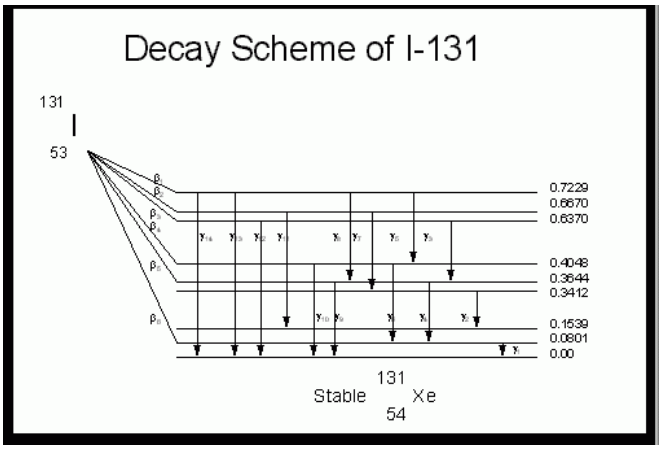

Figure 5. Decay Scheme of ^{131}I

The transition energy between ^{131}I and the ^{131}Xe ground state is 971 keV. The first emission product was an electron with a range in energy between 250 keV - 800 keV [35]. It is this product that makes ^{131}I useful for ablating normal thyroid tissue and treating differentiated thyroid cancers. Electrons in this energy range usually travel less than a millimeter before depositing their energy and causing an ionization event. This means that most of the damage from the electrons produced from the decay of ^{131}I occurs in the cells in which the ^{131}I is concentrated. This is the main point what we want to happen when we use ^{131}I to treat thyroid disease. The second decay product of ^{131}I is a moderate energy photon 364 keV. From the standpoint of treating thyroid disease, this emission product is undesirable because it travels far from its source before depositing its energy and thus increases total body dose with relatively little impact on thyroid tissue. The value of the 364 keV photon emitted from the decay of ^{131}I is that it makes iodine useful for diagnostic studies. In an iodine scan or uptake study it is photons that are not attenuated by the patient’s body that are being counted or processed into diagnostic images [36]. All iodine decay data is listed in Table 1.

Emissions	Energy / (MeV)	Yield (%)
Beta	0.248	2.12
“	0.334	7.36
“	0.606	89.3
Gamma	0.03	4.6
“	0.08	2.6
“	0.284	5.8
“	0.364	63.6
“	0.637	6.5
“	0.723	2.6
X-ray	0.030	3.9

Table 1. ^{131}I Decay Data (20)

The beta particles (Emax=0.606 MeV and Y=89.3%) are absorbed within a few millimeters of tissue and hence a very high, locally confined dose is delivered. Maximum range of beta in air is 165 cm [37]. There are three ways an individual other than the patient can be exposed to ^{131}I, external exposure from gamma rays, external beta contamination to the skin and eyes and internal contamination through ingestion or inhalation of radionuclide. Gamma emissions (E=0.364MeV, Y=82% and E=0.637MeV, Y=7%) can present a penetrating external exposure hazard. It is the exposure from these gamma rays that pose a radiation risk to medical staff, close friends, relatives and other individuals. ^{131}I is excreted through the urine, sweat, vomit and the saliva of the patient. This may pose a risk of external contamination if the patient is incontinent or nauseous as well as a small risk of internal contamination if the patient exchanges body fluids through kissing etc. Due to the high administered activity and the high energy of the ^{131}I gamma rays, the implementation of radiation protection guidelines, to protect the surroundings of the patient, are, therefore, crucial.

2.5.4 The Half life of ^{131}I

It is essential when selecting a therapy radionuclide, to match the physical half-life of the radionuclide with its biological half life in vivo. The half-life of the radioactive isotope is the time it takes for the isotope to decrease activity by 50%. There are three kinds of half life’s that should be considered when radioactive iodine is used to study or treat a hyperthyroid and thyroid cancer patient. The physical half-life is the time it takes for the amount of radioiodine to decrease by 50% purely as a result of radioactive decay. The biologic half-life is the time it takes, the amount of radioiodine in a person’s body to decrease by 50% purely as a result of the excretion of iodine in the sweat, saliva, feces and urine. In the thyroid gland or in thyroid cancers, the biologic half-life is mainly determined by

the time that the isotope remains in the normal or malignant follicular cell. The effective half-life is the combination of the effects of radioactive decay and physiologic excretion. The relationship between the three types of half-lives is given in following equation:

$$\mathrm{Te} = \frac{\mathrm{Tb} \times \mathrm{Tp}}{\mathrm{Tb} + \mathrm{Tp}} \tag{29}$$

Table 2 presents the physical, biological and effective half life of ^{131}I. The values for biologic and effective half- life are different for the thyroid and extra thyroidal compartment because thyroid follicle cells normally concentrate iodine to a much greater degree than many other tissues [36].

^{131}I Physical half life	**^{131}I Biologic half-life**		**^{131}I Effective half-life**	
	normal thyroid compartment	extra thyroid compartment	thyroid compartment	extra thyroid compartment
8.04 days	80 days	12 days	7,3 days	8 hours

Table 2. Physical, biological and effective half life of ^{131}I

2.5.4.1 Sodium Iodide (Na^{131}I)

Na^{131}I-sodium iodide is available for oral ingestion as sodium iodine of high specific activity as a liquid solution or in capsules, for oral ingestion. Sodium iodide (Na^{131}I), therapeutic capsule is prepared by absorbing a solution of carrier-free ^{131}I sodium iodide onto an inert filter that is contained within a gelatin capsule. Capsules are available from several manufacturers in a range of calibrated activities. At IPNM, we use products from CIS with following characteristics, given in Table 3.

Manufacturer	Information
Cis-US,Inc	Capsule (gelatin-white opaque): Sodium iodide ^{131}I absorbed onto inert filler. Sodium iodide Oral Solution: 0.1% sodium bisulphate and 0.2% edentate disodium (stabilizers), 0.5% sodium phosphate (buffer) Sodium hydroxide or hydrochloric acid (pH adjustment: 7.5-9.0).
Cis-US,Inc	Sodium Iodide ^{131}I Oral solution: 2.48 mg/ml sodium thiosulfate Antioxidant, 4.2 mg/ml phosphate buffer, sodium hydroxide (PH adjustment: 7.5-9.0).

Table 3. Formulation information of therapeutic - Sodium Iodide (Na ^{131}I)

Following oral administration in liquid form, iodine is rapidly and completely absorbed in the upper intestine. It is distributed primarily in the body's extravascular fluid within the first one hour. When patient takes a therapy in the form of a capsule Figure 6, it takes some time before absorption starts.

Figure 6. Capsule form of ^{131}I

Although, it is much safer to perform therapy in the form of capsule gastric and other surroundings organs receive certain internal absorbed dose. Very rare the intravenous route is used only in patients who are unable to ingest the solutions or capsules. From the view of radiation protection capsules are safer than liquid solutions, because less radioactivity is released into the air during the handling. We recommend to patients to ingest large amounts of water that attenuates the radiation dose that may be emitted to the gastric wall before dissolution of the capsule. The functioning thyroid tissue takes up part of the dose and is completed by 24 hours [33]. The rest is excreted, primarily in the urine. In some thyroid cancer patients, there may be very little uptake and much as 90 % of the dose can be excreted in the first 24 hours [34]. Contrary hyperthyroid patients may retain up to 80 % in the thyroid gland. A small amount of ^{131}I is present in other body fluids, including sweat and saliva.

Iodine is a precursor of thyroxine and is taken up into follicular cells of the thyroid where it is rapidly converted to protein-bound iodine. Its retention in the follicular cell is dependent on the metabolic activity of the cell, and in the thyrotoxic patient the biological half-life of iodine will be shorter than in the euthyroid patient. Following oral administration, about 40% of the activity has an effective half – life of 0.3 days and 60% has an effective half-life of 7.61 days [33]. In patients with differentiated thyroid cancer, the retention of iodine is variable but activity may still be visualized at the site of a thyroid tumor a month after treatment has taken place [33]. As the path length of the beta particle is about 0.5 mm - 0.8 mm, the toxic effects are limited to the thyroid, with sparing of adjacent tissues. The normal biodistribution of iodine includes salivary glands, stomach and renal tract including bladder. These organs also receive a radiation dose during therapy with ^{131}I, although this dose may be reduced by stimulating salivary flow and maintaining a high urine output during the early treatment period. The high-energy gamma emissions also contribute to an unwanted whole body radiation dose and also to the radiation protection problems associated with radiation therapy.

2.5.4.2 Organ of interest – Gastric

When performing radioiodine therapy especially for treatment of thyroid carcinoma a great dose has to be delivered to the unhealthy thyroid tissue as a target organ and to avoid or limit the expression undesired effects in other normal tissues of the patient. First critical organ during performing this kind of therapy is a gastric Figure 7. Of course, most of absorbed dose will be delivered to the thyroid tissue but of our interest is the dose that has been delivered to gastric and other organs. One of the goals of this thesis is to perform dose calculation and to estimate the absorbed dose to gastric. For that purpose, we have used several assumption, but first of interest is the anatomy and form of the gastric.

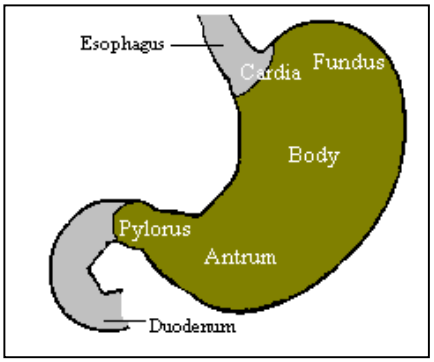

Figure 7. Gastric

The **stomach** is the most dilated part of the digestive tube and is situated between the end of the esophagus and the beginning of the small intestine. It lays in the epigastria, umbilical, and the hypochondriac regions of the abdomen, and occupies a recess bounded by the upper abdominal viscera and completed in front and on the left side by the anterior abdominal wall and the diaphragm. The radioiodine therapy is performed orally, and the patients take the therapy in the form of capsules or in the form of solution. When the therapy is performed in the form of the capsule, it takes some time before absorption start. The dissolving time of the capsule material is about 15 minutes [40]. This is long enough to make possible risky exposure to a part of the stomach wall and several surrounding organs. These doses are not measurable directly but could be easily estimated using numerical experiment as Monte Carlo technique is.

2.5.4.3 Isolation ward

After performed thyroidectomy, patient has to be treated with radioiodine therapy ^{131}I. Because ^{131}I emits gamma rays 364 keV the patient's represents radiation hazard to his surroundings i.e. family members and hospital staff. The patient has to be hospitalized in "isolation room" to avoid contamination of other persons. This room is specially designed of lead walls to avoid irradiation to bystander and allows management of radioactive waste produced by the patient by separate waste collection, storage and disposal after complete decay. Hospitalization time can be from three up to seven days when release criteria will be reached. Physicist performed every day measurements and when dose rate of 7 μSv/h at a distance of two meters will be reached, patient will be released from hospital. For his further behavior, written instructions will be given. It is local hospital rule according national regulation.

Figure 8. Isolation ward for patients

2.6 Internal dosimetry and basic dosimetry quantity

The need for quantitative measurements is necessary for all fields, especially in dosimetry is crucial to have understandable and precise quantities and units**.** Two International organizations are active in relation to quantities and units: The International Commission on Radiation Units and Measurements (ICRU) which mainly working with the physical aspects of dosimetry and The International Commission on Radiological Protection (ICRP) – assessment and quantification of the biological effects of radiation and provides recommendations and guidance on all aspects of radiation protection against ionizing radiation. The goal of current systems of a units is to assess the biological effects resulting from external and internal exposure to ionizing radiation in terms of stochastic (cancer induction, genetic effects) as well deterministic effects (tissue effects) in order to have sufficient mechanisms to control these effects [41].

2.6.1 Biologic effects of ionizing radiation

It is well known that the interaction between ionizing radiation and human tissues result in biological damage. The damage to tissues is primarily due to secondary charged particles, usually energetic electrons that result when the tissues are exposed to ionize radiation. The secondary ionizing particles yield highly reactive free radicals that interact with molecules in the tissue breaking chemical bonds and causing a variety of chemical changes. Most of the resulting damage is subsequently repaired, but some is not. There are two broad categories of radiation related effects in humans: ***stochastic*** and ***nonstochastic***.

Nonstochastic effects, (now deterministic effect, previously acute effects) are effects that are generally observed soon after exposure to radiation. The major characteristics of nonstochastic effects are:

- There is a threshold of dose below which effects will not be observed
- Above this threshold, the magnitude of the effect increases with dose
- The effect is clearly associated with the radiation exposure.

The amount of radiation required to produce these deterministic effects has been derived from studies in experimental cell cultures and animal studies as well as human epidemiology studies. From these studies, the dose thresholds have been established where the effect is observed in 1% of population (Table 4). This means these values represent the amount of radiation energy absorbed by the tissue where if 100 people were exposed to this level of radiation, only a single individual would experience this effect.

Tissue	Total acute dose threshold (Gy)	Time to develop effect
Lens of eye		
Detectable opacities	0.5-2	> 1 year
Cataract formation	5.0	> 1 year
Skin		
Skin reddening	3-6	1 - 4 weeks
Temporary hair loss	4	2 - 3 weeks
Skin death and scarring	5-10	1- 4 weeks
Testes		
Temporary sterility	0.15	3 - 9 weeks
Permanent sterility	3.5 - 6	3 weeks
Ovaries		
Permanent sterility	2.5 - 6	< 1 week
Gastrointestinal		
Mucosa lining loss	6	6 - 9 days
Bone marrow		
Reduction of blood cell production	0.5	1- 2 months
1% incidence level based on ICRP publication 103 (2007)		

Table 4. Dose Threshold for Deterministic Effects

Reviews of biological and clinical studies have shown that, below 0.1 Gy, no deterministic effects from radiation exposure have been proven. This is primarily that the cellular repair mechanisms occur continuously, and this prevents deterministic effects at low radiation exposure levels. Examples of these effects are erythematic, epilating, depression of bone marrow cell division central nervous system damage, damage to the unborn child etc. Some organs are more radiosensitive than others. The law of Bergonie Tribondeau [42], states that cells tend to be radiosensitive if they have three properties: high division rate, long dividing future, the type of cell is unspecialized. In other words, the law states that the radiosensitivity of a cell type is proportional to its rate of division and inversely proportional to its degree of especially. So, rapidly dividing and unspecialized cells as a rule are the most radiosensitive. One important no stochastic effect is death. This results from damage to the bone marrow, then to the gastrointestinal tract than to the nervous system.

Stochastic effects (earlier called late effects) are effects that are probabilistic. They may or may not occur in any given exposed individual. These effects generally manifest many years, even decades, after radiation exposure. Their major characteristics, in direct contrast with those for nonstochastic effects, are:

- Threshold may not be observed
- The probability of the effect increases with dose

- We cannot definitively associate the effect with radiation exposure.

Examples of this effect are *cancer induction* and *genetic effects*.

2.6.1.1 Cancer induction

The fact that ionizing radiation causes cancer is well established. At high enough doses, the rate of production clearly increases with increasing the dose. Radiation-induced cancer is indistinguishable from a "spontaneous" cancer. In the populations that have been studied to establish relationships between dose and risk, in most cases, the radiation doses them and the rates of cancer are subject to considerable uncertainty. For different types of cancer if we plot the cancer rate against the dose received; the data will show an upward trend Graph 1. The question that none of the data sets clearly answers is that of the shape of the curve at low doses and dose rates. The controversy continues to rage over whether the relationship between dose and the absolute or relative number of induced cancer should be extrapolated to zero dose. That means all exposure to radiation, no matter how small, is associated with some risk of cancer, or if there is a threshold.

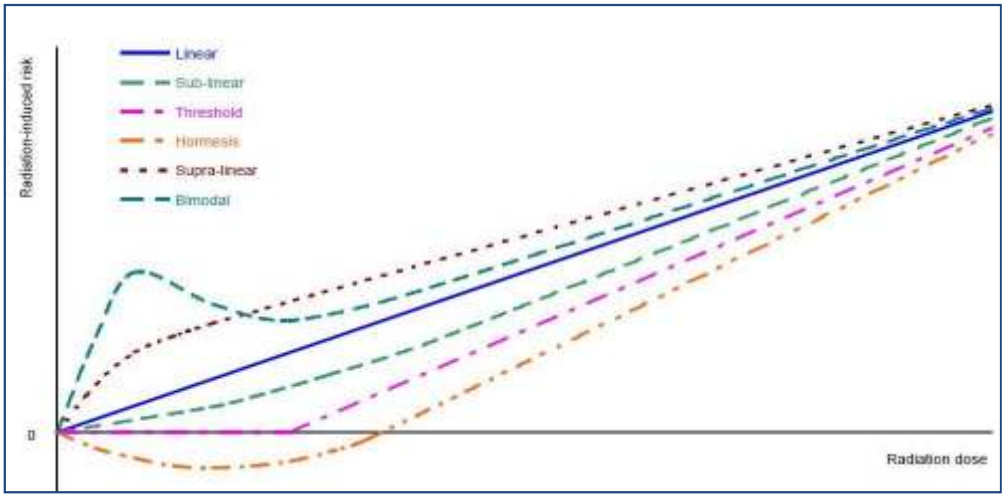

Graph 1. Possible dose-response curves describing the excess risk of stochastic health effects at low doses of radiation

There is evidence to support both views, even controversial theory of *hormesis*. According this theory exposure to low levels of radiation is associated with less cancer induction than in systems deprived of all radiation exposure. The possible mechanism here is that exposure to radiation stimulates cellular repair mechanism so called *adaptive response*. In individual, experiments, hormetic and adaptive response mechanisms have been demonstrated [43]. Very recent research has profoundly challenged conventional notions of the relationship between radiation dose and observed effects. In a report by the American Association of Physicists in Medicine, (AAPM) [44], it is noted that various cellular and organ studies have shown that low LET type effects have been seen when Auger emitters are present only in the cytoplasm of cells, whereas when Auger emitters may be incorporated into the DNA of cells. In that case, the resulting survival cells curves are similar to those seen for high-LET

alpha particles. The committee concludes that the absorbed dose from Auger emitters must be calculated at a level suited to the biological system employed. For that purpose, the target volume must be determined on a case by case basis.

Brooks point out that absorbed dose is often used too liberally as a direct indicator of radiation risk [45]. The simple concept of energy absorbed per unit mass of tissue has good predictive value at some dose levels, and if the activity is uniformly distributed throughout the organ, it is clearly not a good predictor of biological response when activity is not uniformly distributed and when energy deposited by high LET particles occurs in regions where it is difficult to distribute the energy over the appropriate target mass. The experimental evidence has shown that in some condition cells with no direct energy deposition from radiation may demonstrate a response so-called *bystander effect*.

The data available concerning the bystander effect fall into two quite separate categories, and it is not certain that the two groups of experiments are addressing the same phenomenon. First, there are experiments involving the transfer of medium from irradiated cells, which results in a biological effect in unirradiated cells. Second, there is the use of sophisticated single particle micro beams, which allow specific cells to be irradiated and biological effects studied in their neighbors; in this case communication is by gap junction. Medium transfer experiments have shown a bystander effect for cell lethality, chromosomal aberrations and cell cycle delay. The type of cell, epithelial vs. fibroblast, appears to be important. Experiments suggest that the effect is due to a molecule secreted by irradiated cells, which is capable of transferring damage to distant cells. Use of a single microbeam has allowed the demonstration of a bystander effect for chromosomal aberrations, cell lethality, mutation, and oncogenic transformation. When cells are in close contact, allowing gap junction communication, the bystander effect is much larger magnitude than the phenomenon demonstrated in medium transfer experiments. A bystander effect has been demonstrated for both high and low-LET radiations, but it is usually larger for densely ionizing radiation such as alpha particles. Experiments have not yet been devised to demonstrate a comparable bystander effect on a three-dimensional normal tissue. Bystander studies imply that the target for the biological effects of radiation is larger than the cell, and this could make a simple linear extrapolation of radiation risks from high to low doses of questionable validity [46].

Another mechanism called *genomic instability* also suggests that the effects from radiation may be felt in cells other than those directly irradiated. Cells irradiated with radiation have been shown to not have observable radiation damage, but subsequent generations of these cells may show DNA damage

In the scientific world, there is still no agreement concerning this issue. Most regulatory bodies in the United States and elsewhere follow and use the Linear No Threshold Model (LNT). LNT model of cancer risk prediction was validated by (Biological Effects of Ionizing Radiation) BEIR VII Committee, and still it is best working model. The problem arises when this model is used for scientific conclusions [47].

It is very important to notice that radiation induced cancer in a population and the cancers are always expressed at some long time after the exposure. This period of time between exposure and the expression of the disease is called the latent period. Large populations have to be considered to perform statistically valid studies. Leukemia has the shortest latency period before expression, (5 -15 years) after exposure. With most solid cancers, the latent period is more like 20 years. Late effects of radiation also occur due to environmental radiation. Since accurate information is lacking on the natural frequency of these effects, it is difficult to estimate the influence of low radiation doses on this increase. In addition sex, age, genetic history, geography and other socio-economic factors influence the frequency of natural occurrence. Therefore, it is very difficult to prove that a cancer is directly related to earlier radiation exposure, because the other factors encountered during the latency period may be the actual cause of the cancer.

An estimation of risks to a person at low radiation doses has been made from following sources:

- Human exposures – medical, occupational, military and accidental
- Experimental animal studies
- Experiments on mammalian cell cultures
- Prospective studies of the victims of the atomic bomb explosions in Nagasaki and Hiroshima
- The inhabitants of Bikini and other Pacific island who were exposed to radiation as a result of fall-out.

In the Table, 5 are presented the risk of the cancer as deducted from the currently available information.

Type	Male (rad per 10^6 persons)	Female (rad per 10^6 persons)
Leukemia	660	730
Nonleukemia	110	80
Total	770	810

Table 5. Excess cancer mortality-life time risk, single exposure (Chandra 1992)

2.6.1.2 Type of radiation, Amount of Tissue and Biological Variation

Even for the same absorbed dose, different type of radiation, have different abilities to damage tissue. A weighting factor (quality factor, ω_R) is introduced which represents the relative amount of damage likely to be caused to live cells by the same amount of different radiation types. Higher linear energy transfer (LET) is produced by alpha particles, protons and neutrons as a result of the production of recoil protons. Lower LET radiations are electrons and gamma rays and x-rays as a result of Compton and photoelectric interaction. High LET produces greater damage in a biological system than low LET. The relative biological effectiveness (RBE) of a radiation for producing a given biological effect is defined as follows [48].

$$RBE = D/D' \tag{30}$$

D - Dose of standard (x-ray) radiation needed to produce a biological effect.

D' - Dose of a second radiation needed to produce the same biological effect.

The biological response depends on the type of tissue (ex: thyroid, ovaries, testes, bone marrow, or nerve tissue) involved. All cells are not equally sensitive to radiation damage. In general, cells which divide rapidly and/or are relatively non-specialized tend to show effects at lower doses of radiation than those which are less rapidly dividing and more especially. Examples of the more sensitive cells are those which produce blood. This system (called the hemopoietic system) is the most sensitive biological indicator of radiation exposure. The risk of malignancy per Sv is different for various tissues of the body. Given the same radiation dose and dose rate, bone marrow is much more sensitive than nerve tissue to certain types of radiation damage. Biological factors like species, individual and cell sensitivity and the recipient's age are important. Injury to a biological system also depends upon the amount of tissue irradiated.

2.6.2 Internal radiation dosimetry

2.6.2.1 Dose Calculation

The radiation absorbed dose depends on several factors:

1. The amount of radioactivity administered
2. The physical and biological half-lives of the radioactivity
3. The fractional abundance of the radiation in question from the radionuclides
4. The biodistribution of radioactivity in the body
5. The fraction of energy released from the source organ that is absorbed in the target volume, which is related to the shape, composition and the location of the target.

The physical characteristics of a radionuclide are well established. Information about the biodistribution of the ingested radioactivity can be obtained from various experimental studies in humans and animals. Factors 4 and 5 vary from one individual to another and therefore they are approximated for a "standard" or "average" 70-kg man. Radiopharmaceuticals administered to patients are distributed in a different region of the body. The region of interest for which absorbed dose is to be calculated is considered the "target", whereas all other regions contributing to the radiation dose to the target are considered"sources". The source and the target become the same when the radiation dose due to the radioactivity in the target is calculated [49].

2.6.2.2 Absorbed dose

All dose quantities are based on the fundamental definition of absorbed dose in a point [50] as the quotient of $(d\varepsilon)$ by$(\ dm)$, where $(d\varepsilon)$ the mean energy is imparted to matter in an infinite volume (dV) at a point of interest in a material of density (ρ) during a certain period of time by ionizing radiation and (dm) is the mass in (dV)

The **absorbed dose (D)** is defined as the statistical average of the energy (E) imparted per unit mass at a point:

$$D = d\varepsilon/dm \tag{31}$$

The unit of absorbed dose is the Gray (Gy) and one Gy is equal to 1 joule of energy absorbed per kilogram of matter (1J/kg) [51]. The concept of absorbed dose applies to all categories of ionizing radiation dosimetry, to all materials, and to all forms of ionizing radiation.

Absorbed dose can be measured absolutely or relatively using advanced equipment, not at all suitable for daily radiation protection work. In all fields of radiation protection, there is an interest to estimate the risk to the individual or to a group of individuals of the exposure which they have undergone. Together with the basic quantity absorbed dose, there are two types of quantities defined for specific use in radiological protection: protection quantities (defined by the ICRP and used for assessing the exposure limits) and operational quantities (defined by ICRU and intended to provide a reasonable estimate for the protection quantities). The relationship between physical protection and operational quantities are given in the following Figure 9.

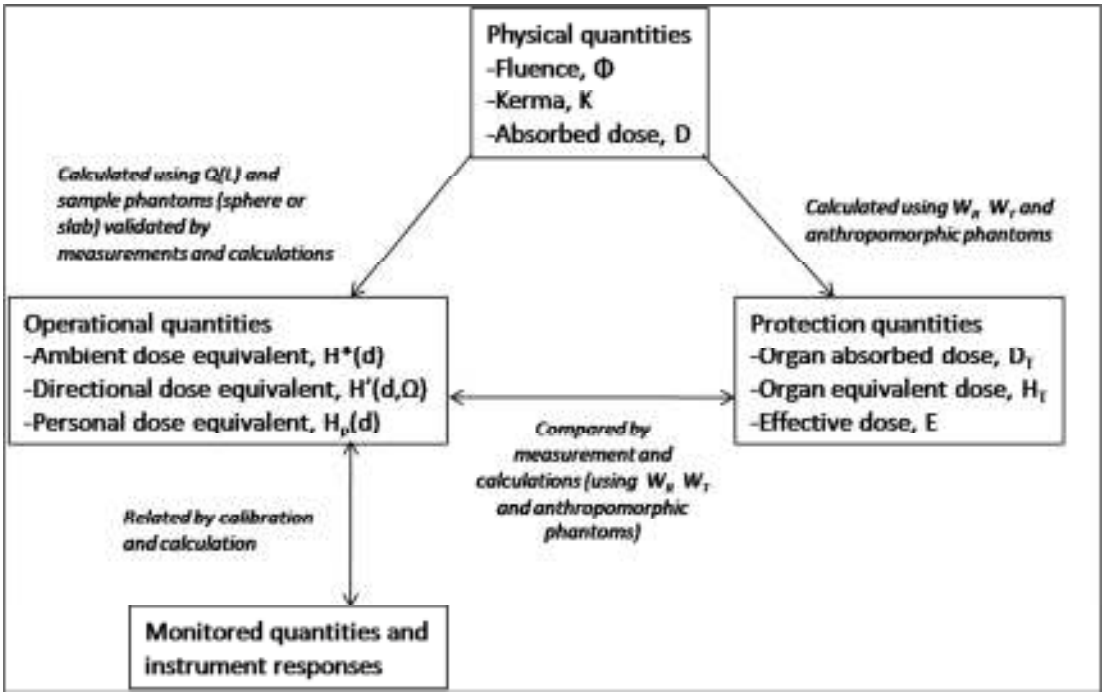

Figure 9. Relationship between physical protection and operational quantities (S.Mattsson 2013)

2.6.3 Protection Quantities

The protection quantities are mean absorbed dose to an organ or tissue (D_T), equivalent dose in tissues or organs (H_T) and effective dose (E).

2.6.3.1 Calculation of mean absorbed dose

To assess radiation exposure to humans and correlate it with the risk of exposure, mean absorbed dose in tissues or organ is used. The mean absorbed dose, to an organ from internally administered radiopharmaceuticals is dependent on the characteristics of both the radionuclide and pharmaceutical in terms of the type of radiation emitted and spatial and temporal distribution of the radionuclide in the body. The mean absorbed dose, D_T (Gy) averaged over the tissue or organ (T) is defined as:

$$D_T = \varepsilon_T / m_T \tag{32}$$

Where (ε_T) is the mean total energy imparted in a tissue or organ (T) and (m_T) is the mass of that tissue or organ.

2.6.3.2 Equivalent dose

In 1973, ICRU [52] defined **equivalent dose H,** which is used to take into account the fact that different particle types have biological effects that are enhanced per given absorbed dose. The absorbed dose can, however, result in different biological effects depending upon the type and energy of radiation causing the dose. The equivalent dose is expressed in a unit named the Sievert (Sv). Equivalent dose is equal to the absorbed dose multiplied by a factor that takes account of the way a particular radiation distributes energy in tissue, thus influencing its effectiveness in causing harm. The concept of equivalent dose is applied only to radiation exposures received by human beings. The dose equivalent (H_T) at a point of interest in tissue or organ (T) is given by the equation:

$$H_T = \sum w_R \, D_{T,R} \tag{33}$$

The (w_R) is the radiation weighting factor for radiation (R) and (D_{TR}) is the mean absorbed dose in organ or tissue (T) from radiation (R). For gamma rays, X-rays and beta particles, the factor is set at 1, therefore the absorbed dose and equivalent doses are numerically equal. For alpha particles, the factor is 20, so that an absorbed dose of 1 Gy from alpha radiation corresponds to a dose equivalent of 20 Sv, [53].The factor (ω_R) is defined to be a function of linear energy transfer (LET). LET is the radiation energy lost per unit length of path through a material. Different types of radiation have different LET. X-rays, gamma rays and electrons are known as low LET radiation. Higher LET is more destructive to biological material than low LET radiation at same dose. The radiation used in nuclear medicine is typically low LET radiation. LET is approximately equivalent to the stopping power for charged particles and is expressed in units of keV μm^{-1}. All of the radiation ultimately manifests itself through charged particles, so LET is a good measure of localized radiation damage to materials not limited to biological structures. For the common situation where a spectrum of energies and a mixture

of particle types are present, the value of (ω_R) for the complete radiation field is an average over spectrum of LET present weighted by the absorbed dose as a function of LET, D (LET).
The values of the new radiation weighting factors (ω_R) compared with previously recommended are given in the following Table 6.

Radiation type	Radiation weighting factors (ω_R)	
	ICRP 1990	ICRP 2007
Photons, electrons and muons of all energies	1	1
Protons and charged pions	5*	2
Alpha particles and heavy ions	20	20
Neutrons	Step and continuous function of neutron energy	Revised continuous function of neutron energy
*Pions were not considered		

Table 6. ICRP recommended radiation weighting factors (ICRP1990, 2007)

In general, the values of (ω_R) in the 1990 ICRP system are larger than those of (ω_R) used in 1973 system. The latest guidance found in ICRP publication 103 [54] has reduced the size of this increase in (ω_R) for neutrons in some energy intervals. Generally more serious effects are produced by high doses rather than low doses. Also, it is generally assumed that the dose and effect are linearly related even at low doses. There is no threshold radiation dose below which the two important effects – (production of genetic damage and the induction of cancer) are not produced [53].

2.6.3.3 Effective dose

When the body is irradiated after administration of radiopharmaceuticals, individual organs and tissues are likely to receive different equivalent doses. Since various tissues and organs have different radiation sensitivity, the quantity **effective dose E** is introduced, providing the possibility to express the radiation risk to patients undergoing different radio diagnostic procedures by means of a single figure. The effective dose is a revision of the effective dose equivalent (H_e) [55] which initially, was developed for occupationally exposed persons, and is defined as the sum of the equivalent doses (H_T) weighted by the tissue weighting factor (w_T). Effective dose (E), obtained as the sum of equivalent doses to each organ or tissue, weighted using defined tissue weighting factors (w_T), to take account of the contribution of the individual organs and tissues to overall detriment from cancer and hereditary effects is given by

$$E = \sum w_T H_T = \sum w_T \sum w_R D_{T,R} \quad (35)$$

The unit for effective dose is Sievert, Sv (J/kg). The basis for the weighting factors is the relative contribution of the organ to the total detriment, based on probability of fatal cancer; relative length of life lost; relative non fatal contribution and severe genetic effects [56, 37]. The (ω_T) values have been developed from the reference population of the equal number of both sexes and the wide range of ages. On the Graph 2 are presented the comparison between changing values of ICRP 26, ICRP 60 and ICRP 103.

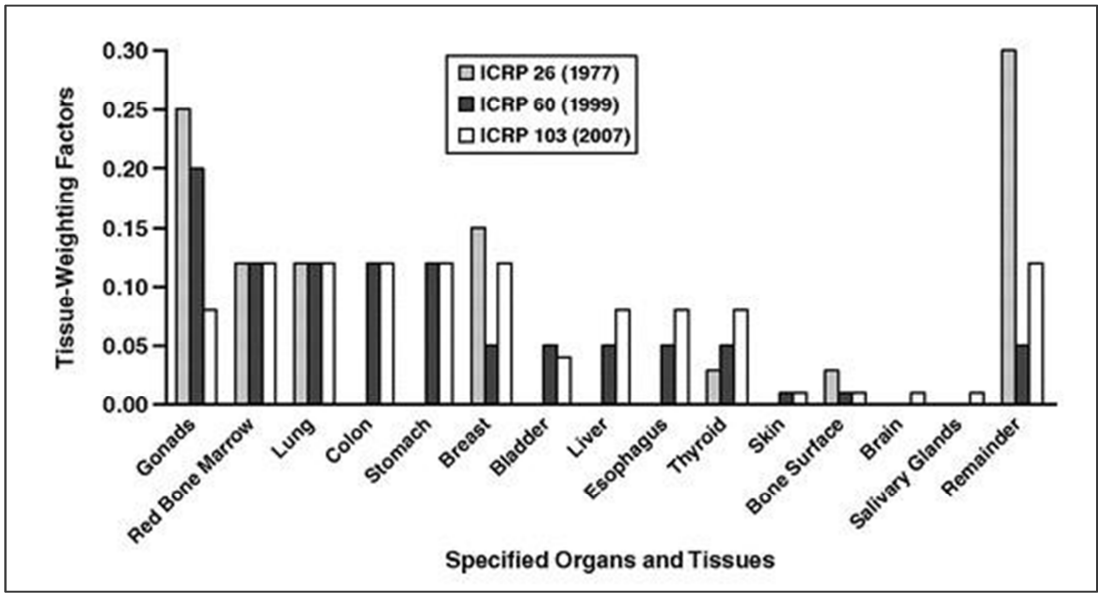

Graph 2. Tissue weighting factors according ICRP26, ICRP 60 and ICRP 103

The organ doses that are needed for calculation of effective dose are calculated for reference male and female persons using a family or reference phantoms of which the adult male and adult female phantom is already published [38]. Using the reference phantoms, dose conversion coefficients for external and internal exposure are calculated for reference conditions:

- Standard irradiation geometries for external radiations [39].
- Standard (ICRP) biokinetics models for internal emitters [40].

Tissue	w_T	$\sum w_T$
Bone marrow, breast, colon, lung, stomach and remainder tissues (13*)	0.12	0.72
Gonads	0.08	0.08
Bladder, esophagus, liver and thyroid	0.04	0.16
Bone surface, brain, salivary glands and skin	0.01	0.04
*Reminder tissues: adrenals, extra thoracic (ET) region, gall bladder, heart, kidneys, lymphatic nodes, muscle, oral mucosa, pancreas, prostate (male), small intestine, spleen, thymus and uterus/cervix (female).		

Table 7. ICRP recommended tissue weighting tissue factors, ICRP 2007 [36]

Effective dose is not based on data from any one individual person and does not provide individual specific dose but rather that for a reference person under a given exposure situation. Effective dose because of underlying approximations and simplifications is not suitable for risk assessment for individuals. It is, however, of practical value for comparing the relative doses related to stochastic effects from different diagnostic examinations, the use of different technologies for the same medical examination provided that the representative patients or patient populations for which the effective doses are derived are similar with regard to age and gender.

2.6.3.4 Absorbed dose rate

According to the publication ICRU No67 (2002) [57] when a radionuclide decays by emitting only one type of radiation the average absorbed dose rate in the target volume for the transformation volume source is given by:

$$D = \Delta \tilde{A} \Phi / m \quad (36)$$

Where (Δ) is the mean energy emitted per nuclear transformation, (Ã) is the accumulated activity of the source volume, (m) is the mass of the target volume, and (Φ) is the fraction of energy absorbed by mass of the target volume. Volume settings source and target volume are illustrated in Figure 10

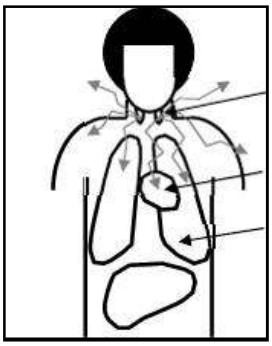

Figure 10. Representation of source and target volume

Depending on the metabolism they are associated to the incorporated radionuclides could decay in lungs, in gastrointestinal (GI) tract or other specific organs: these are known as source organs. The tissues in which energy is deposited following a nuclear decay are known as target organs. In the ICRP publication there are as many as 23 target organs listed.

2.6.3.5 Energy emitted per disintegration

This term is known as the mean energy emitted by nuclear transformation of a radionuclide. It is expresses by:

$$\Delta i = Kn_i Ei \quad (37)$$

(Ei) is the average energy of the (i) type of radiation, (n_i) is the average number of the (i^{th}) type of radiation emitted by nuclear transformation and (K) is a constant that depends on the chosen system. Generally this term is tabulated according to the type emission of radiation.

2.6.3.6 Absorbed fraction

According Sgouros [58] the absorbed fraction is the fraction of the energy emitted by the source volume which is absorbed in the target volume, according. The flux (Φ), equals the energy absorbed in the target volume for the i^{th} type radiation emitted by the source volume divided by the energy of the i^{th} type of radiation emitted by the source volume.

If the source volume emits electrons, alpha particles it is generally that these particles are completely absorbed by the tissue volume source.

Electron	Assume $(\mathrm{AFT} \leftarrow \mathrm{T}) = 1$ elsewhere = 0
Alpha	Assume $(\mathrm{AFT} \leftarrow \mathrm{T}) = 1$ elsewhere = 0

If the volume source emit photons depending on its energy, it will be absorbed not only the volume of tissue source as well as other organ tissues adjacent to the volume source. Photon data are found in Reference Man (MIRD Pamphlet). In this work, it was considered only the transport photon irradiation scenarios. Figure 11.

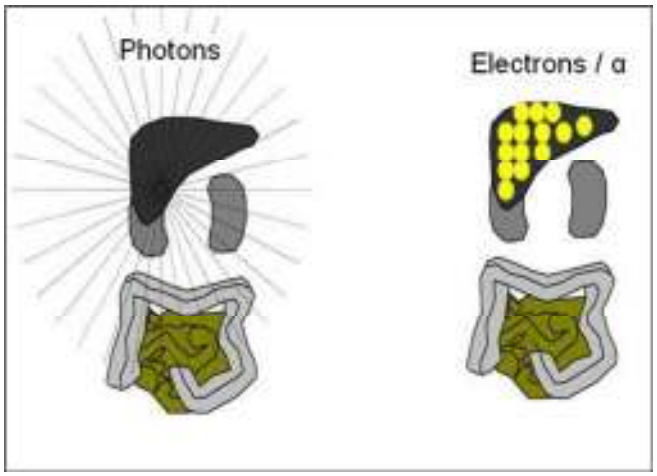

Figure 11. Different tissue absorption properties of photos versus electron or α- particle emissions of radio nuclide

Additional considerations are required for wall organs and bone. The computation of the values of $AF\ (T \leftarrow S)$ for each combination source to target organ is performed by means of Monte Carlo radiation transport calculations on anthropomorphic numerical phantoms.

2.6.3.7 Accumulated activity

Activity located in the source organ and the time that remains in this region depends on the properties and biological characteristics of the radiopharmaceutical and individual metabolism as well as the

physics half-life of the radionuclide. The total number of disintegration is the sum of all nuclear transformations in this organ within a time interval of interest is accumulated activity Ã and is defined as:

$$\tilde{A} = \int_{t1}^{t2} A(t)dt \tag{38}$$

Where A (t) is defined as activity function which is integrated in time interval interest. According Zanzonico et al. [59] measures of activity versus time are illustrated as shown in Graph 3.

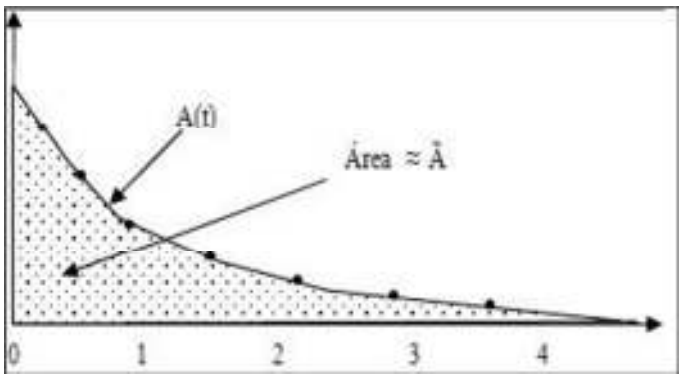

Graph 3. Time activity curve

The function activity can usually be described using a sum of exponentials, as can be seen from the following equation:

$$A(t) = \sum_j A_{max} * e^{-(\lambda+\lambda_j)*t} = \sum_j A_{max} * \ e^{-(\lambda_{ef})_j * t} \tag{39}$$

where (A_{max}) is the maximum activity in the organ, (λ) is the physical decay constant corresponding to the physical half-life of the radionuclide, (λ_j) is the elimination constant biological component of the exponential, $(\lambda_{ef})_j$ is the effective constant decay for the j-th component of the exponential, (t) is the total time radionuclide in a particular organ. The maximum activity captured by the residual thyroid tissue can be expressed by:

$$A_{max} = f * A_o \tag{40}$$

Where (f) is the maximum activity fraction captured by the residual thyroid tissue from administered activity to patient. For a simple model which considers only one compartment accumulated biological activity can be calculated by the following equation [60].

$$\widetilde{A} = \int_0^t A_{max} * e^{-\lambda_{ef} * t'} dt' = A_{max} * \left(1 - e^{-\lambda_{ef} * t'}\right)/\lambda_{ef} \tag{41}$$

Where $\lambda_{ef} = \ln(2)/T_{1/2ef.}$ As the accumulated activity until the complete elimination the radionuclide is obtained when the integral is calculated in the range of zero to infinity, the radionuclide is obtained when the integral is calculated in the range of zero to infinity, it has been:

$$\tilde{A} = A_{max}/A_{ef} = A_{max} * T_{1/2ef}/\ln(2) = 1{,}443 * A_{max} * T_{1/2ef} \quad (42)$$

2.6.3.8 Residence time

If the accumulated activity ($\tilde{A}$) is normalized by the administered activity (Ao), the activity units are canceled and new parameter residence time (τ) is obtained [57].

$$\tau = \tilde{A}/Ao \quad (43)$$

2.6.3.9 Specific absorbed fraction

It is defined as the fraction of energy by the radionuclide in the volume-source that is absorbed per unit mass of the target volume:

$$\Phi = \Phi/m \quad (44)$$

This equation can be used to specific target volume and surface [118]. The values of SAF's have been calculated and revised on the basis of the Oak Ridge series of analytical anthropomorphic phantoms. Recently new sets of data have been extensively calculated using "voxel" phantoms.

2.6.3.10 Average absorbed dose per unit accumulated activity "S" values

"S"-values are defined as average absorbed dose per unit cumulative activity. The physical aspects can be combined within magnitude in volume source, according to following equation:

$$S = \Delta * \Phi = \frac{\Delta * \Phi}{m} \quad (45)$$

This equation contains information regarding the radiation emitted by volume source, the geometry and composition of the source volume and target volume. Thus average absorbed dose can be simplified to the following equation:

$$\bar{D} = \tilde{A} * S \quad (46)$$

Equation (46) is considered only for radiation from a volume type source. When considering different source volumes, various types of radiation and various target volumes can be used another equation:

$$\bar{D}_K = \sum_h \tilde{A}_h \, S(r_k \leftarrow r_h) \quad (47)$$

Where $S(r_k \leftarrow r_h)$ indicates the average absorbed dose per unit accumulated activity of the target volume of the volume source, r_k, r_h. The subscript "h" represents the number of volumes source. When the target volume is a source volume, the dose is known as self-dose, when the source volume

is a target volume dose is known as cross-dose. Average absorbed dose per unit accumulated activity is given by:

$$S(r_k \leftarrow r_h) = \sum_i \Delta_i \Phi_i(r_k \leftarrow r_h) = \sum \frac{\Delta_i \Phi_i(r_k \leftarrow r_h)}{m_k} \quad (48)$$

The “S” values can be calculated from MIRD phantom as it was done in this work.

2.6.4 Anthropomorphic model

The evaluation of the dose in organs and tissues of the human body for various conditions of exposure to ionizing radiation has a very important role for radiation protection. However, due to the inability of the positioning of dosimeters in many cases is not feasible to measure the dose in organs and tissues of interest. To solve this problem, there is the possibility to use simulation models of human body, which aim is to represent, as best as possible external and internal structures enabling evaluation by the simulation of dose, irradiation conditions and exposure of individuals to external sources [61].

The anthropomorphic models used to evaluate the dose can be classified into three different types:

- **Physical models** constructed in whole layers, using materials presenting properties of interaction with matter similar to human tissues. In this type of model there are holes where it is possible to place dosimeters;
- Using **mathematical models** equations for the representation of several organs and tissues of a human body. These equations describe organs on geometric way as ellipsoids, cubes etc.
- **The models based on images** of the external and internal components of the human body of real people, mainly obtained through medical imaging techniques such as Computed Tomography (CT) and Magnetic Resonance Imaging (MRI).This model is known as voxel simulator. The voxel is defined as an elementary unit of volumetric digital image, or three dimensional pixel, which make up the structure of the simulator. These models are more realistic because they represent individual anatomical structures more faithfully in a computational context than the other models; therefore provide a better estimation of dose.

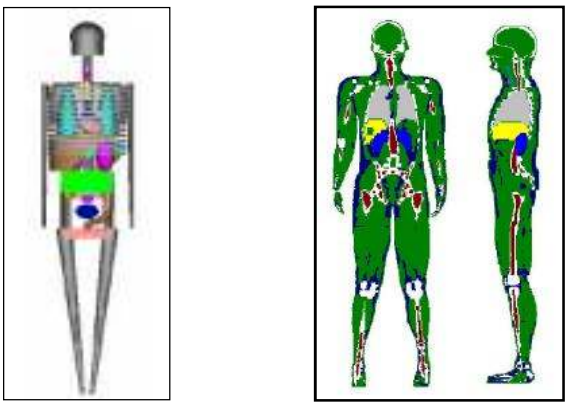

Figure 12. Differences between a mathematical simulator and a simulator voxel

The most popular analytical phantom is the so called MIRD phantom, which consists of three types of tissues: lung, skeletal and soft tissue (red bone marrow). Such phantoms are used in Monte Carlo radiation transport simulations where the source is usually located within each source organ. Models have been extended to take into account age groups other than adults.

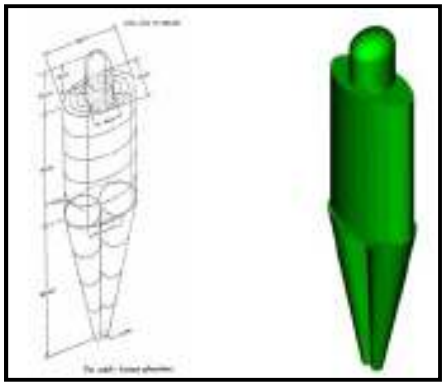

Figure13. The adult human phantom external dimensions (MCNP model of ADAM)

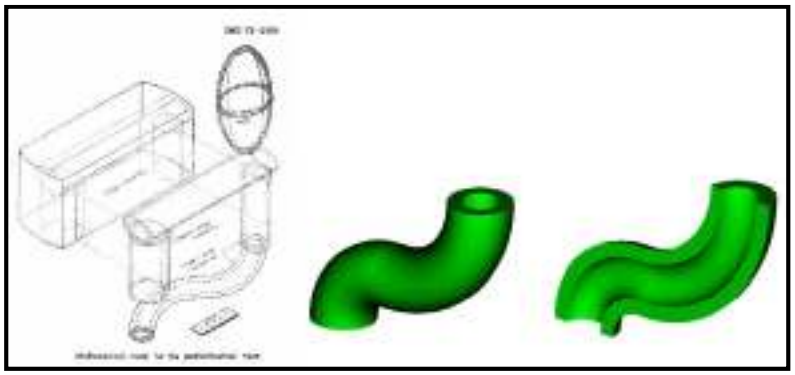

Figure 14. The adult human phantom

GI tract (an MCNP model of the sigma (Courtesy L. Casalini))

The model used in this work and data for the creation of this model was taken from MIRD and is explained in details in material and methods part. There are developed voxel models which are presented on Figure 15. Also, there are developed software's which might be used for dosimetry, but with well known individual based input data: MIRDOSE, OLINDA, RADAR etc.

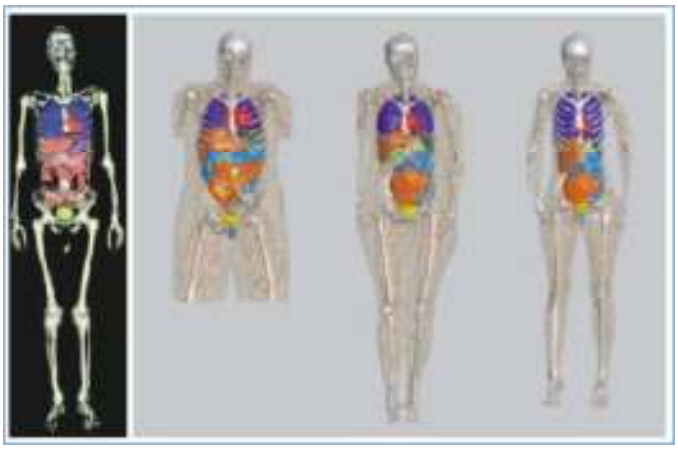

Figure 15. Voxel based phantoms: Golem, Holga, Donna and Irene Radiat. Env. Biophys (2001)

2.7 Monte Carlo Method

The Monte Carlo (MC) method was invented by Jon von Neumann, Stanislaw Ulam and Nicholas Metropolis, who gave it its name, and independently by Enrico Fermi. Originally it was not simulation method, but a mathematical approach aimed at solving a multidimensional integrodifferential equation by means of the stochastic process. When the method is applied to physical stochastic process, such as neutron diffusion, the model (in this case a random walk) could be identified with the process itself. Under those circumstances, the Monte Carlo method represents a simulation technique since every step of the model is aimed at mimicking an identical step physical process. Particle transport and interaction represent a typical stochastic process and is, therefore, perfectly suitable for Monte Carlo simulation. Many applications in high energy physics and medicine are based on Monte Carlo simulation in which the history of each particle (trajectory, interactions) is reproduced in detail. An important and useful feature of MC simulations is the possibility of studying parameters that cannot be measured experimentally. While, before 1990, the typical Monte Carlo approach was to simplify problems as much as possible, the modern Monte Carlo codes instead require fewer approximations and provide more accurate solutions [62].

2.7.1 Phase space

The concept of phase space is central to the understanding of the Monte Carlo method. Phase space is a concept of classical statistical mechanics. Each phase space dimension corresponds to a particle degree of freedom: three dimensions correspond to the position in real space (*x, y, z*), and three other dimensions correspond to the momentum: p_x, p_y, p_z, or to energy (*E, Θ, Φ*). More dimensions may correspond to other possible degrees of freedom: quantum numbers, particle type and so on. Each particle is represented by a point in phase space. Time can also be considered a coordinate, or it can be considered an independent variable. The variation of other phase space coordinates as a function of time constitutes a particle "history" [62].

2.7.1.1 Phase Space Density

The basic quantity describing a population of particles is the phase space density n (t, x, y, z, p_x, p_y, $p_{z)}$, which is the number of particles in an infinitesimal volume of phase space. The product (nv) of the space phase density and the particle velocity are important because they represents the rate of the path length density and therefore relates to the particle interaction rate with matter. The quantity Ψ = nv is called angular flux and is the most general radiometric quantity. (Ψ) Can also be defined as the derivative of the fluence (Φ) with respect to all phase space coordinates time, energy and solid angle (direction vector).

$$\Psi = \frac{\partial \Phi}{\partial t\, \partial E\, \partial \vec{\Omega}} = \dot{\Phi}_{E\vec{\Omega}} \tag{49}$$

The angular flux is a fully differential quantity, but most Monte Carlo solutions are integrals of (Ψ) over one or more phase space dimensions: coordinates, time, energy, angle. Fluency (Φ) on the other hand is the most integral radiometric quantity:

$$\Phi = \int_{\mathrm{E}}\int_{\vec{\Omega}}\int_{\mathrm{t}}\dot{\Phi}_{\mathrm{E}\vec{\Omega}}\mathrm{dE}\mathrm{d}\vec{\Omega}\mathrm{dt} \tag{50}$$

Often in Monte Carlo calculations the time dependence is not explicitly followed and the fluency differential with respect to energy Φ (E) = $\mathrm{d}\Phi/\mathrm{dE}$ is the quantity of interest [62].

2.7.1.2 Physical meaning of the elements of Boltzmann equation

Calculation using Monte Carlo method is different from the calculations based on deterministic methods [63]. When it is desired to describe the radiation transport using the deterministic method, it solves the Boltzmann transport equation which is balance equation in phase space. At any phase space point, the increment of particle density (*n)* in an infinitesimal phase space volume is equal to the sum of all "production terms" minus the sum of all "destruction terms".

$$\frac{1}{\mathrm{v}}\frac{\partial\Psi(\mathrm{x})}{\partial\mathrm{t}} + \vec{\Omega}\cdot\nabla\Psi(\mathrm{x}) + \Sigma_{\mathrm{t}}\Psi(\mathrm{x}) - \mathrm{S}(\mathrm{x}) = \int_{\Omega}\int_{\mathrm{E}}\Psi(\mathrm{x})\Sigma_{\mathrm{s}}(\mathrm{x}'\rightarrow\mathrm{x})\mathrm{dx} \tag{51}$$

where (x) represents all phase space coordinates: $\vec{r}$, $\vec{\Omega}$, E, t. The various elements of the Boltzmann equation have the following physical meaning:

- The $\frac{1}{\mathrm{v}}\frac{\partial\Psi(\mathrm{x})}{\partial\mathrm{t}}$ term represents the time dependent change of angular flux, due to particle decay
- $\vec{\Omega}\cdot\nabla\Psi(\mathrm{x})$ is the change due to translational movement without change of energy and direction.
- $\Sigma_{\mathrm{t}}\Psi(\mathrm{x})$Where Σ_{t} the total is macroscopic cross section, is a term representing absorption.
- $\mathrm{S}(\mathrm{x})$ represents the particle sources
- The double integral, where Σ_t is the macroscopic scattering cross section, refers to scattering, change in angular flux due to direction change without a change of particle position.

All Monte Carlo particle transport calculations are attempts to solve the Boltzmann equation in its integral form, carrying out the integration over all possible particle histories. According to the order described in the text, the Boltzmann equation has no analytical solution. In Monte Carlo calculations transport equations are not solved analytically, but to simulate processes of interaction of individual particles and record up some aspects of their behavior. The behavior medium is then inferred from the Central Limit Theorem and the average behavior of individual particles as described in Annex 1. The Monte Carlo method can in principle, simulate any problem particle transport in any geometry. The technique simulates the physical laws that acting on the particles. The accuracy of the results depends only on the approximation of physical theories with the "reality" of interactions, and the number of "stories" executed. Monitoring of the particle from

its creation until the end of his life is defined as “history”. According Laurel et al. main components of a Monte Carlo algorithm are described as follows:

- ***Probability distribution***: This method simulates the physical laws that act on the particles. These laws can be described by one or more distributions probability and the accuracy of the results depends only on the approximation of physical theories with the “reality” of interactions, and the number of “histories” executed. In other word, the physical system must be described by a set of pdf’s.
- ***Random Number Generator:*** The Monte Carlo method is based on randomness of physical processes. To provide this simulation process of randomness, random number generator was used. This generator should be capable of providing the random values, numbers, uniformly distributed between 0 and 1, short run time (speed of the algorithm) and period (sequence of random numbers) which produces numbers apparently independent, similar to figures from truly random occurrences.
- ***Marking, counting or scoring***: The results of each simulation must be accumulated. Counters are used to accumulate the number of attempts and successes. The outcomes must be accumulated into overall tallies or scores for the quantities of interest.
- ***Error estimation***: an estimate of the statistical error (variance) as the function of the number of trials and other quantities must be determined
- ***Variance reduction techniques:*** methods for reducing the variance in the estimated solution to reduce computational time for Monte Carlo simulation.
- ***Parallelization and vectorization*** algorithms to allow.

To perform the transport simulation of radiation that defines the probability of interaction of a particle per unit distance is Σ_t. The probability that an interaction occurs between x + dx follow the Poisson distribution, given by:

$$\mathrm{p(x)dx} = \mathrm{e}^{-\Sigma_t \mathrm{x}} \sum_{\mathrm{t}} \mathrm{dx} \tag{52}$$

For each random number uniformly distributed in the interval $0 \leq \eta < 1$ there is a variable x, a cumulative distribution function, which obeys the following relationship:

$$\eta = \int_0^{\mathrm{x}} \mathrm{p}(\mathrm{x}_1)\mathrm{dx}_1 \tag{53}$$

Substituting the value of p(x), and performing the integration

$$\eta = 1 - \mathrm{e}^{-\Sigma_t \mathrm{x}} \tag{54}$$

And

$$x = \frac{-\ln(1-\eta)}{\Sigma_t} \tag{55}$$

Since (1- η) is also uniformly distributed in the interval (0, 1) then value coincidence with the (η) and will result in the following equation:

$$x = \frac{-\ln(\eta)}{\Sigma_t} \tag{56}$$

The distance between interactions, (S) is derived by the following equation (57) where

$$S = -\lambda \ln(\eta) \tag{57}$$

$\lambda = \frac{1}{\Sigma_t}$ is the mean free path. The probability of interaction can be defined with attenuation coefficient being the same and may vary depending on the power photon, the composition and density of the medium in which it moves.

2.7.2 Determination of errors in the Monte Carlo technique

The result of a calculation using the Monte Carlo method is the average number of "histories" performed during the simulation (BRIEMEISTER et al 1986). The histories are generated by random sampling and a value of the quantity studied is allocated to each "history". Let p(x) be the probability function of a "history" of value x. Mx variable is given by p(x).

$$\mathrm{Mx} = \int_{\mathrm{a}}^{\mathrm{b}} \mathrm{x}\, \mathrm{p(x)}\, \mathrm{dx} \tag{58}$$

The values of p(x) and thus Mx are not known exactly, but the true mean; (x) can be estimated using the Monte Carlo method (59).

$$\bar{\mathrm{x}} = \frac{1}{\mathrm{N}} \sum_{\mathrm{i}=1}^{\mathrm{N}} \mathrm{x_i} \tag{59}$$

where $(\mathrm{x_i})$ value of corresponding to the "history" (i), and (N) is the total number of "histories". The variance (σ^2) can be estimated using following formula (60).

$$\sigma^2 = \frac{1}{\mathrm{N}-1} \sum_{\mathrm{i}=1}^{\mathrm{N}} (\mathrm{x_i} - \bar{\mathrm{x}})^2 \tag{60}$$

The square root of (σ^2) is defined as the standard deviation of the population(x_i) obtained using the values (x_i) that were generated by random sampling. For (N) large, the variance of the distribution averages of $(\sigma_{\bar{x}}^2)$ can be calculated by the equation: (61)

$$\sigma_{\bar{\mathrm{x}}}^2 = \frac{\sigma^2}{\mathrm{N}} \tag{61}$$

Thus

$$\sigma_{\bar{\mathrm{x}}} = \frac{\sigma}{\sqrt{\mathrm{N}}} \tag{62}$$

To reduce $\sigma_{\bar{x}}$ half is the need to run four times the number of "histories" which is the problem inherent in the Monte Carlo method. Using Central Limit Theorem, when N>>1:

A) $\bar{x} - \sigma_{\bar{x}} < Mx < \bar{x} + \sigma_{\bar{x}}$, interval of confidence is 68%.

B) $\bar{x} - 2\sigma_{\bar{x}} < Mx < \bar{x} + 2\sigma_{\bar{x}}$, interval of confidence is 95%.

C) $\bar{x} - 3\sigma_{\bar{x}} < Mx < \bar{x} + 3\sigma_{\bar{x}}$, interval of confidence is 99.7%.

If we associate the greatness absorbed dose to be allocated to each “history” we can calculate the standard deviation SD of the absorbed dose in each organ using equation (62) where N is the number of simulated photons, (Di) is the dose absorbed by the i-th photon, (D) is the average absorbed dose deposited in each organ. Then calculated coefficient of variation (CV) is given by (63).

$$S_{\bar{D}}^2 = \sum_{i=1}^{N} (D_i - \bar{D})^2 / N(N-1) \tag{63}$$

$$CV = \frac{S_{\bar{D}}}{\bar{D}} \tag{64}$$

BRIESMEISTER 1986 presented a way to verify the degree of reliability of the radiation transport calculations using the method of Monte Carlo, as it is shown in Table 8.

Coefficient of variation (CV) values	Rating the calculated magnitude
0.5 to 1	Disposable
0.2 to 0.5	Unreliable
0.1 to 0.2	Questionable
<0.10	Generally trustworthy, except for point detectors
<0.05	Generally trustworthy

Table 8. Values of coefficients of variation (CV) provided by BRIESMEISTER (1986)

2.8 Risk assessment of the nuclear medicine patient

Diagnostic and therapeutic applications of radioiodine in hospitals worldwide have continued to grow, so the general public awareness of the hazards of ionizing radiation and their tendency to question clinical management has increased. Recent recommendations have identified an increased risk from radiation and contain reduced occupational and public dose limits [56, 64]. Therefore, a key factor in sustaining this growth in clinical activity while retaining the confidence of the referring clinician, the patient and the public, is for nuclear medicine practitioners to maintain and up-to-date knowledge of the radiation risks associated with their procedures. The need to understand the methodology used to assess these risks and to appreciate the associated limitations is of great importance. Two types of risk are identified following the administration of radiopharmaceutical to the patient: the risk to the patient and risk to critical groups exposed to the patient. Administered radioactivity presents a risk to the patient who should be balanced against the benefit from obtaining a diagnosis or carrying out the treatment. A method for quantifying the risk to the patient is described in terms of estimating the effective dose. The main limitations in these estimates are uncertainties in the biokinetics data and the assumption of a uniform distribution of activity in each organ. Contact with radioactive tissue from the patient or exposure to radiation emitted from radioactivity retained by the patient presents a risk to hospital staff and to members of the public. Also, member's of patient's family, particularly young children and breast-fed infants, are of particular concern, and their associated risks require careful assessment [65].

2.8.1 Risk evaluation

It is essential to explain the patient which sets out to evaluate the risk associated with nuclear medicine procedure; it is also essential to advise the patient of the risk associated with not carrying out the procedure.

2.8.2 Relative risk

A very simple method of explaining the risk associated with the procedure is to compare the effective dose with that from a more familiar radiation source such as diagnostic X-ray procedures Table 9 [64]. Comparison with the average dose from background radiation or with the dose from a change in lifestyle yielding a background dose higher than the average value can also provide a simple way of placing the nuclear medicine risk into a meaningful context. For example in Macedonia, the average dose from natural background radiation is 2.0 mSv/y.

Procedure	Effective dose (mSv)
Plain film	
Chest	0.04
Skull	0.1
Pelvis	1.0
Thoracic spine	1.1
Abdomen	1.4
Lumbar spine	2.2
Intravenous urogram	4.6
Barium enema	8.7
Ctomography	
Head	1.8
Cervical spine	2.9
Thoracic spine	5.8
Pelvis	7.3
Chest	8.3

Table 9. Effective dose

2.8.3 Absolute risk

Expressing the risk in absolute terms not only allows an estimate to be made of the probability of radiation induced injury. It allows comparison with the risks associated with the natural occurrence of these effects and with risks associated with occupational, personal and recreational activities. ICRP gives a risk for severe hereditary effects, the fatal cancer and non-fatal cancer of 1.3, 5 and 1.0×10^{-2} Sv^{-1} respectively (total 7.3×10^{-2} Sv^{-1}) for the whole population [63]. These values correspond to the risk for each effect of 1 in 77 000, 1 in 20 000 and 1 in 100 000, respectively, for an ED of 1 mSv, which is the annual limit for members of the public recommended by ICRP. These risks can be compared with an estimated natural frequency of 1-3 in 100 for genetic diseases manifesting at birth, and a cumulative risk of 1 in 1300 for fatal childhood cancer up to the age of 15 years [64].

In the Table 10. are given examples of occupational, personal and recreational activities carrying a fatal risk of 1 in 20 000 [46].

Activities carrying a fatal risk of 1 in 20 000
Smoking 75 cigarettes
Working in a typical factory for 1-2 years
Travelling 4023 km by motor car
Travelling 20 116 km by air

Table 10. Examples of occupational, personal and recreational activities carrying a fatal risk

The ICRP risk coefficients are age, and sex averaged for a normal population.

Exposed population	**Excess relative risk of cancer (per Sv)**
Entire population	5.5 % - 6.0 %
Adult only	4.1 % - 4.8 %
Relative risk values based on ICRP publications 103 (2007) and 60 (1990)	

Table 11. Nominal Risk for Cancer effects

For the age group corresponding to adult workers, the risk is reduced to 80 % of that for the whole population. For children, the risk is 2-3 times greater than for adults, and for persons aged over 50 years, the risk is 10-20% of that for younger adults. Nuclear medicine patients cannot be regarded as a normal group, and their skewed age distribution will produce a smaller increase in risk. In a study, in the United States, in 1982, one third of nuclear medicine patients were aged over 64 years [66]. The age-adjusted incidence rate in the US from 2001 to 2005 was 467 cancers per year per 100 000 men and women [68]. Quantifying their fatal risk in terms of loss of life expectancy has been suggested as providing a basis for the comparison of different activities [67]. However, it is not generally used as a means of explaining the risks of nuclear medicine procedure. It has been pointed out that loss of life expectancy does not provide an easy means of comparing the risk of acute death caused by an accident with death caused by cancer because of the long latency period associated with the latter [69].

2.8.4 General basis of risk assessment

2.8.4.1 Internal radiation

Estimates of organ absorbed doses are the primary basis of any form of internal risk assessment for nuclear medicine procedures [70] and are usually required by radiopharmaceutical licensing authorities. MIRD Committee has developed the method of estimating organ absorbed dose generally referred to as MIRD Shema [71]. Example from MIRDOSE software is given in Figure16.

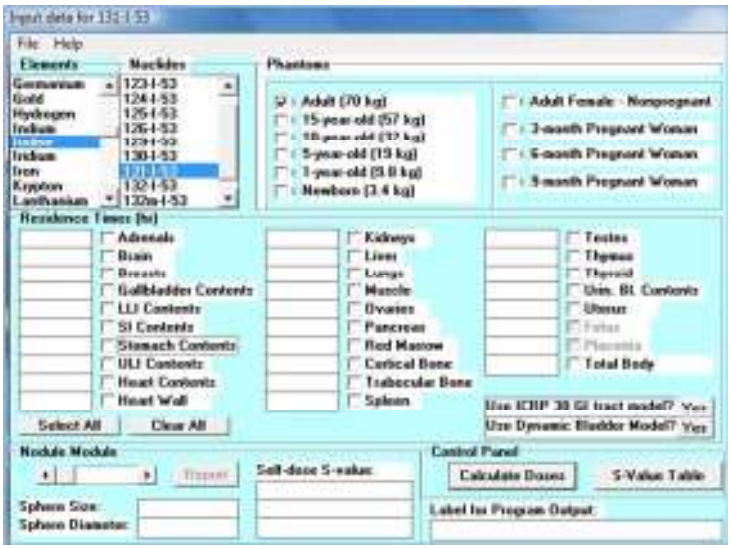

Figure 16. MIRD dose software

The body is considered to consist of source organs which accumulate a significant amount of radioactivity, and target organs which are irradiated by activity in the source organs. The calculation of mean absorbed dose to a target organ (t) from its exposure to a source organs is simple multiplication of the two quantities, cumulated activity (A) and the mean absorbed dose per unit cumulated activity, (S) by:

$$\mathrm{D}(\mathrm{t} \leftarrow \mathrm{s}) = \sum \mathrm{AS}(\mathrm{t} \leftarrow \mathrm{s}) \tag{65}$$

Where (S) is the tissue or organ emitting the energy (source organ) and (t) is the tissue or organ where the energy is absorbed (target organ).

The S-factor involves readily available parameters such as mass of the target tissue, the mean energy emitted per nuclear transition and the fraction of energy emitted from the source organ that is absorbed in the target organ. Given an appropriate anatomical model and biokinetics data, and by adding all the source organ contributory doses, the MIRD schema allows the total absorbed dose to every target organ to be derived including the situation of the target organ and source organ being the same. The list of organ absorbed dose for radiopharmaceuticals published by (ICRP) has been complied by this method [72].

ICRP has defined the risk to an irradiated individual as the effective dose (E) expressed in units Sievert (Sv). In 2008 Brenner in the study published in BJR proposed to replace effective dose, with “effective risk”, where summed organ doses will be replaced each weighted with actual epidemiologically-based cancer risks, instead with committee-generated numbers. The effective risk is thus a generic lifetime radiation - attributable cancer risk.

$$\text{Effective Risk} = \mathrm{R} = \sum_{w_T} \mathrm{H_T} = \sum w_T \sum w_R D_{T,R} \tag{66}$$

Where(r_T), lifetime radiation attributable organ specific cancer risks are estimates (per unit equivalent dose to tissue T). This equation is the same with Effective dose, the calculation will be no harder and any inherent assumptions will be the same for both (e.g. LNT).

For radiation protection purposes ICRP adopted in its Publication 26 (1977) for whole body exposures:

- Mortality risk factor for radiation-induced cancers: about 10^{-2} Sv^{-1} (average for both sexes and all ages).
- Average risk factor for hereditary effects (expressed in the first two generations) $4x10^{-3}Sv^{-1}$.

Calculation of dose limit for occupational exposure was based on judgment of the acceptability of the level of risk in radiation work by comparing it with that for other occupations recognized as having high standard of safety: average annual mortality due to occupational hazards lower than 10^{-4} per year. It was adopted an annual dose limit of 50 mSv for occupational exposure and the risk of $5x10^{-5}$ per year for fatal cancer and $2x10^{-5}$ for hereditary effects.

For the general public, exposure risk was in range 10^{-6} to 10^{-5} per year. Based on detriment of 10^{-2} Sv^{-1} the restriction on the lifetime dose would correspond to a 1mSv per year. Annual dose limit of 5 mSv was adopted for public exposure, assuming to result in average dose equivalents of less than 0.5 mSv.

The ICRP 60 contains reassessment of the risk according to evolution of the scientific knowledge on the follow up of atomic bomb survivors.

Morbidity and year of life lost are integrated in the calculation of health detriment. Dose limits are revised on the basis of the model tolerability of risk – **Risk informed approach.** In the Table 12 are presented the fatal probability coefficients compared within ICRP 26 and ICRP 60.

Fatal probability coefficient ($10^{-4}Sv^{-1}$)			Detriment
	ICRP 26	ICRP 60	ICRP 60
Bladder	-	30	29.4
Bone marrow	20	50	104.0
Bone surface	5	5	6.5
Breast	25	20	36.4
Colon	-	85	102.7
Liver	-	15	15.8
Lung	20	85	80.3
Esophagus	-	30	24.2
Ovary	-	10	14.6
Skin	-	2	4.0
Stomach	-	110	100.0
Thyroid	5	8	15.2
Remainder	50	50	58.9
Gonads			133.3
Total	**125**	**500**	**725.3**

Table 12. Evolution of risk estimates for fatal cancer

In recent ICRP Publication 103 are evident evolutions of scientific knowledge on cancer incidence that lead to base the calculation of the health detriment on incidence. There is the significant reduction of the part of severe hereditary effects in health detriment. The reference levels are introduced as guideline for managing the different exposure situation with risk consideration. The new formula to calculate the health detriment, cancer mortality based from ICRP 60 is changed in cancer incidence based. In the Table 13 are presented calculation of the health detriment

Health Detriment ($10^{-4}Sv^{-1}$)		
	ICRP 103	ICRP 60
Bladder	16.7	29.4
Bone marrow	61.5	104.0
Bone surface	5.1	6.5
Breast	79.8	36.4
Colon	47.9	102.7
Liver	26.6	15.8
Lung	90.3	80.3
Esophagus	13.1	24.2
Ovary	9.9	14.6
Skin	4.0	4.0
Stomach	67.7	100.0
Thyroid	12.7	15.2
Remainder	113.5	58.9
Gonads	25.4	133.3
Total	**574.3**	**500**

Table 13. Detriment

2.8.4.2 External radiation

After administration of radiopharmaceuticals, the radiation emitted from the patient acts as a potential mobile source of exposure to other individuals. Critical groups within the hospital are nuclear medicine staff, ward staff and visitors. Exposure of these groups is controlled by the designation of controlled areas, local rules and written systems of work. After the patient has left hospital members of the public who could be at risk are fellow travelers, colleagues at work and family members. Their exposure is controlled by keeping the patient in the hospital for an appropriate period of time, and after discharge from hospital by issuing instructions to modify their behavior inside and outside the home for a certain period of time.

To assess the dose to the critical group, from the radiation emitted by a patient, two methods can be used. Firstly, direct measurements can be made of the integral dose received by an individual in the critical group by securing a thermoluminiscent dosimeter (TLD) to the individual. This method satisfies the criteria of being sensitive to a decrease in dose rate with time. The other method that might be used is when the dose to an individual in the critical group is estimated by multiplying the dose rates measured at different distances from the patient by the times spent at each distance by that individual. Both methods have disadvantages but give the idea of approximately estimated dose rate at certain distances. The dose rate variations with distance from the patient will depend on the

anatomical distribution of the radioactivity and hence on the radiopharmaceutical administered. The extrapolations and interpolations will be much easier if the variation of dose rate with distance can be described by a simple mathematical function. TLD measurements and Monte Carlo calculations have shown that the inverse square law can be used to describe the variation of dose rate with distance beyond a distance which increases with the area of the source [73].

2.8.5 Potential groups exposed to ^{131}I patient

It is well known that patients treated with ^{131}I presents radiation hazard for the people that might come in close contact with them. The exposed groups are members of staff and members of the public. In the members of staff are included: nuclear medicine staff (physician, physicist, technologist, nursing staff). While in members of the public are included: (parents, children, the breast fed infant and other groups that might come in close contact with patient treated with ^{131}I).

2.8.5.1 Nuclear medicine staff

Nuclear medicine staff is exposed to radiation while performing the treatment to the patient either for treatment of hyperthyroidism or thyroid cancer. In both case, the physician and physicist are the most exposed staff. The therapy usually and in the most cases is performed with capsules and from radiation protection point it is much safer way than solution. Also, technologist is exposed during the scanning of patient, but in that case most of activity is gone because, in the case of thyroid cancer patients, the imaging is performed after ten days from received therapy [74].

2.8.5.2 Nursing staff

An in-patient who is undergoing a therapy procedure should be nursed in an isolation suite designated as the controlled area. The risk to staff can be assessed on an individual basis depending on measured dose rates and the level of care required. In the literature [75, 76, 77] it has been shown that from dose rate and occupancy data that the ward nurse would only exceed the control area limit of 60 μSv per day [75] if helping a totally helpless patient that had undergone one of the high activity procedure, for example, bone scan.

2.8.5.3 Children exposed to patients treated with radioiodine ^{131}I

When radiopharmaceutical is administered to a breastfeeding mother (Figure 17), radioactivity will be secreted into the milk, and the child will be necessary exposed on undesired radiation, and will receive certain radioactivity [78]. The activity concentration secreted in milk decreases exponentially with time after administration, and therefore assuming the volume per feed (V) and the time between feeds (τ) are constant the total activity ingested by infant (I) for all feeds can be calculated from the following formula.

$$I = \sum_{j=1}^{m} c_j \cdot V/\left[1 - \exp\left(-\lambda_j \cdot \tau\right)\right] \quad (67)$$

Where (m) is its number of exponential components for each of which (c_j) is its concentration of activity ingested in the first feed and (λ_j) is its effective decay constant. The effective dose (D) to the infant is given by:

$$D = Ie \quad (68)$$

Where (e) is effective dose to the infant per unit activity ingested.

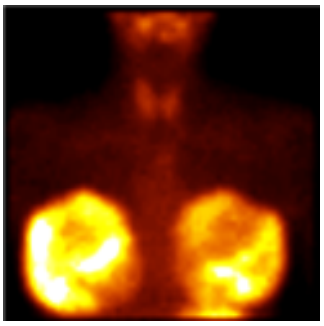

Figure 17. Activity in breast feeding woman (IAEA)

2.8.5.4. Parents exposed to child undergone ^{131}I therapy.

A parent looking after young children who have undergone nuclear medicine procedure will receive a dose from the radiation emitted from the radioactivity retained by child's organs. The critical group in this case will be the parents of young infants who require extended periods of close contact. Estimates of these doses have been made from maximum values of dose rate measured at 0.1 m from pediatric patients multiplied by the effective exposure times described in the literature. It was estimated that a parent could receive a dose of 1 mSv if the infant had been administered 500 MBq of ^{99m}Tc. It is the case that is based on the maximum dose rate per unit activity observed at 0.1 m (0.5 μSvh MBq^{-1}) and on the maximum reported period of close contact. For the parents caring for children treated as in-patients with ^{131}I-MIBG for neural crest tumors such as neuroblastoma, a thyroid blockade is unnecessary because the main risk is from external radiation rather than the ingested activity. In the case of thyroid radioiodine therapy, the youngest child in this study is 16 years old, and there was no so close contact with parents. Anyway the use of straightforward precautions it should be possible to limit the dose to parents from this external radiation to 1 mSv per treatment [79].

2.9 Radiation Protection and Regulations during performing therapy with ^{131}I

2.9.1 Dose Limits

In the context of radiation protection and radiation risk dose limits and reference levels are of importance. *Dose limits* refer to the maximum level of dose that the general public can receive from a source other than natural background radiation levels and those received by occupational workers in their job. The *reference levels* reflect the typical dose values expected in the majority of imaging studies [55].

Limits for exposure to radiation should be at a level below the threshold where deterministic effects occur (i.e. below 0.1 Gy) and the limit should exclude exposures from background radiation. Using the threshold dose as a starting point, dose limits are detriment using the Principles of Justification and Optimization. On the Graph 4 are presented the key elements of the radiation protection system:

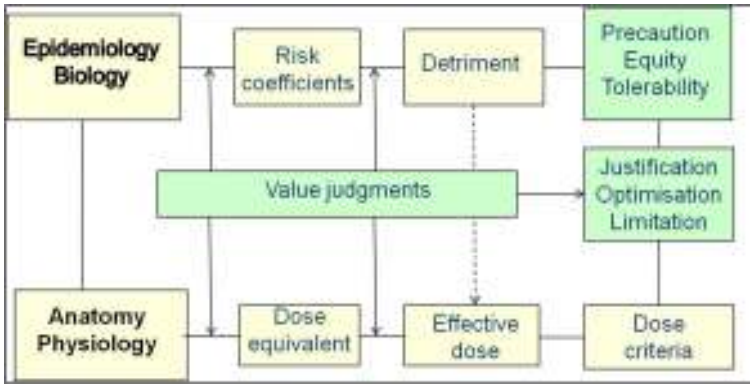

Graph 4. The main elements of the radiation protection

Principle of Justification: Any decision that alters the radiation exposure to an individual or population should have an outcome that does better than harm. This means that any radiation source should provide a benefit with its use; either to the individual or to society at large and the risk of any detrimental effects must be small relative to any benefit.

Principle of optimization: The application of radiation in any situation should be developed to minimize the risk of exposure while maximizing the benefit. When the medical benefit is retained or maximized, the risk should be as low as possible. The principle of optimization is analogous to the As Low As Reasonably Achievable (ALARA) concept.

To minimize radiation hazard International and national organizations have been established to set guidelines for the safe handling of radioactive materials. The ICRP and IAEA also National Safety regulatory authority set guidelines for all radiation workers to follow in handling radiation. According National regulations the annual limit of occupational dose to an individual adult is 20 mSv.

The cardinal principles of radiation protection from external sources are based on four factors: time, distance, shielding and activity.

Time

The total radiation exposure to an individual is directly proportional to the time of exposure to a radiation source. The longer the exposure, the higher the radiation dose is. Therefore, it is wise to spend no more time than necessary near radiation sources.

Distance

The intensity of the radiation source and hence the radiation exposure varies inversely as the square of the distance from the source to the point of exposure. It is recommended that an individual should keep as far away as possible from the radiation source. Procedures and radiation areas should be designed so that individuals conducting the procedures or staying in or near the radiation areas receive only minimum exposure.

Shielding

Various high atomic number (Z) materials that absorb radiations can be used to provide radiation protection. Because the ranges of α and β particles are short in a matter, the containers themselves act as shields for these radiations. γ – radiations, however, are highly penetrating. Therefore, highly absorbing material should be used for shielding of γ-emitting sources. For economic reasons, lead is most commonly used for this purpose. Shielding is very important means of protection from radiation. Radionuclides should be stored in a shielded area. The radiopharmaceutical dosages for patients should be carried in shielded syringes.

Activity

It should be obvious that the radiation exposure increases with the intensity of the radioactive source. The greater the source strength, the more the radiation exposure is. Therefore, one should not work unnecessarily with large quantities of radioactivity.

2.9.2 Personnel monitoring

Personal dosimeters are devices worn by individuals exposed to ionize radiation to evaluate and document their external radiation exposure level. Personnel monitoring usually employs film dosimeters, ring dosimeters, thermoluminescent, pocket ionization chambers etc. At the Institute of pathophysiology and nuclear medicine monitoring of workers is performed by using TLD's and ring dosimeters. The TLD gives accurate exposure reading and can be reused after proper heating (annealing).

2.9.3 Radioactive waste disposal

Radioactive waste generated in nuclear medicine (syringes, needles, contaminated papers etc.) are disposed of by the following methods according to national guidelines: decay in storage, release into the sewerage system, transfer to authorized recipient etc.

Decay in a storage

Radionuclides with half-lives less than 65 days usually are disposed of by this method. These radionuclides are allowed to decay in storage for a minimum of 10 half-lives and then surveyed. If the radioactivity of the waste cannot be distinguished from background, it can be disposed of as normal medical waste after removal of all radiation labels. This method is most appropriate for short-lived radionuclides.

Release into sewage system

Radiation safety directorate permits radioactive waste disposal into the sewage system provided the radioactive material is soluble or dispersible in water. Excreta from humans undergoing medical diagnosis or treatment with radioactive material are exempted from the limitation. To adopt this method of radioactive disposal one must determine the total volume and the flow of the sewer water in the institutions and the number of users for specific radionuclide.

2.9.4 Radioactive spill

Accidental spillage of radioactivity can cause unnecessary radiation exposure to personnel and must be treated cautiously and expeditiously. There are two types of spills: major and minor spill. A major spill usually occurs when the spilled activity cannot be contained in a normal way and can cause undue exposure to personnel. In the case of a major spill, the RSO should be notified immediately. Areas, personnel and equipment must be decontaminated. Survey and wipe tests must be performed after decontamination.

2.9.5 Record keeping

Records must be maintained for the receipt, storage and disposal of radioactive materials, as well as for various activities performed in the radiation laboratory. These records contain specific information and are kept for a period of five years specified by Radiation Safety Directorate.

2.9.6 Transportation of radioactive material

The radioactive packages must be labeled properly before transportation. There are three types of labels according to the exposure reading in μSv/h at 1m from the surface of the package (transport index). The transport index must be indicated on the label and the sign “RADIOACTIVE” must be placed on the package. The labels must identify the content and amount of radionuclide in Becquerels. The package must contain shipping documents inside, bearing the identity, amount and chemical form of the radioactive material and TI Figure 18.

Figure 18. Form of the package with ^{131}I

Chapter 3

3. MATERIAL AND METHOD OF RESEARCH

3.1 Patients

In this study were analyzed thyroid cancer and hyperthyroid patients for 5 years period (2007-2011) who were treated at the Institute of pathophysiology and nuclear medicine, Faculty of Medicine, Ss. Cyril and Methodius University in Skopje, the Republic of Macedonia. The total number of patients who were reviewed was 526 (136 male and 390 female) age between (15 and 80). Patients were evaluated by ultrasonography, in vivo and in vitro nuclear medicine techniques, and final diagnosis was documented by histopathology during or after operation. The demographic findings will be presented in the results chapter from this thesis.

At the group of thirty thyroids cancer and thirty hyperthyroid patients were performed external measurements at different distances with dose rate meter, after receiving iodine therapy.

Estimation of effective dose for different organs using Monte Carlo simulation was performed at 24 groups of patients divided according given activity. Patients were divided in 24 groups receiving average dose per group: 185 MBq; 370 MBq; 555 MBq; 1110 MBq; 1813 MBq; 2423 MBq; 2516 MBq 2756 MBq; 3009 MBq; 3145 MBq; 3237 MBq; 3349 MBq; 3441 MBq; 3515 MBq; 3614,2 MBq; 3737 MBq; 3838 MBq; 3959 MBq; 4033 MBq; 4440 MBq; 5106 MBq; 5476 MBq; 5550 MBq; 6105 MBq.

External measurements over gastric region on the surface of the skin were performed with TLD at fifteen patients.

Environmental release of iodine in the sewage system was performed with environmental radioactivity monitoring system.

3.2 Survey meter Dose Rate Test

A survey meter dose rate test was performed to determine if the dose rate measurements are consistent at all nominated distances. The aim of the test was to find out that the dose rate measurements are in accordance with inverse square law. Mathematically the inverse square law is expressed with following equation:

$$I \propto \frac{k}{d^2} \tag{69}$$

This law states that radiation exposure or intensity (I) at a distance (d) from a radioactive source is proportional to the inverse square of the distance and (k) is proportionality constant that depends on the type of the radioactive source and its activity. This statement is true for exposure from radioactive point source (a source that is very small when compared to the large distances from the source involved) which emits radiation that is not absorbed in the distances involved. The exposure from radioactive patient does not follow the simple inverse square law, but approximately we can afford to take the measurements and account patient as point source. The purpose was to find out if variations in the distance affect dose rate measurements. A syringe with 1100 MBq of ^{99m}Tc activity was placed at 145 cm height. The height was estimated for a normalized man's height of 170 cm minus 25 cm for thyroid location. Dose rate measurements were taken with the survey meter "mini-rad" series 1000 at 0.25 m; 0.5 m; 1.0 m; 2.0 m; at 145 cm height.

Figure 19. Survey meter "mini-rad" series 1000

3.3 Patient procedure

At a group consisted of sixty patients, were performed external dose rate measurements. The patients were interviewed and informed on the research aims by medical physicist and physician. They signed agreement for receiving a therapy and all patients feel positive about participating in the study. Thirty were hyperthyroid patients and thirty were thyroid cancer patients. The patient population consisted of 25 female and only 5 male at hyperthyroid group and 26 were female and 4 were male at thyroid cancer group. Age ranged between 15 years to 80 years old. Hyperthyroid patients were treated with 185 MBq to 1295 MBq of ^{131}I and thyroid cancer patients were given activities between 3700 MBq and 5550 MBq.

3.4 Radiation Dose Rate Measurement

The dose rate from the patient was monitored with external survey monitor “mini-rad” Series 1000 at horizontal distances of 0.25 m; 0.5 m; 1.0 m; and 2.0 m for hyperthyroid patient and 0.25 m; 0.5 m; 1.0 m; 2.0 m; and for thyroid cancer patients. The survey meter was calibrated by The Service from Public Health Protection Institution, Skopje, and the Republic of Macedonia using the known exposure rate from 740 GBq ^{137}Cs source primary gamma energy of 0.66 MeV. The distances from the source were 4.0 m; 2.0 m; 1.0 m and 0.5 m in order to obtain different exposure rates. The errors in all cases were 15%. The effective point of the patient measurements was taken to be in the centre of the detector. Vertical movement of the survey meter was utilized to obtain the maximum reading each time. The highest dose rate measurement depends on closest position of the survey meter to residual extra thyroidal functioning tissue, which retains radioactive radioiodine. A standard height was not used in order to reduce the error originating from variations in the patients’ heights and the locations of the target organ (thyroid).

The initial measurements were performed within 15 minutes following administration of the^{131}I dose. Thyroid cancer patients were measured during three very rare four days (every day at same time) until the measured level fall down to permitted limit (2.0 m – 8 μSv/h). The dose rate was determined at different distances: 0.25 m; 0.5 m; 1.0 m and 2.0 m from the patient. Distance 0.5 m, is relevant distance for partner sharing the same bed; 1.0 m is relevant distance for people who have their meal at the same table, watching television and being around the same house. The 1.0 m and 2.0 m distances would be relevant for people sharing the same office. The assumptions for distances were based on the previously published works of Culver et al and Barrington et al. The authors of this publication assumed that the dose received at a distance greater than 1.0 m was negligible. Author Babicheva in her work included a distance of 2.0 m in the patients survey form rather than make the same assumptions. I have also included the 2.0 m for thyroid cancer patients expecting that it would be the safe distance for first day measurement for thyroid cancer patients. For hyperthyroid patients, the measurements were performed within 15 minutes after administration of the dose at distances 0.25 m; 0.5 m; 1.0 m; and 2.0 m. Inverse square law ratios of dose rate were calculated for both groups of patients in order to assess consistency of the measurements at varying distances. The patient instructions form about therapy, and written following instructions were given to patients and also they have signed an agreement for therapy with radioiodine ^{131}I. Thyroid cancer patients stayed at hospital for three days. Medical physicist has done measurements every day until the dose rate of 8 μSv/h at 2.0 m was reached. That means that the residual activity is less than 800 MBq when patients were released to go home with orally given and written instructions for their further behavior in home conditions.

3.5 External measurements over gastric region using TLD

Effective dose measurements were done with thermoluminiscent dosimeters which contains hot pressed chips from phosphors or lithium fluoride (LiF) with property of thermal luminescence. TLDs were most appropriate to estimate radiation because the amount of ionizing radiation is directly proportional to the effective dose. The principle of thermo luminescence dosimetry is often described as a two step process: ionization of atoms into a metastable state and then recombination of the electron hole pair with the resulting emission of photons. When TLD material is irradiated an electron is excited to the conduction band creating a hole in the valence band. These electrons and holes are free to migrate and can also be trapped in shallow energy levels from which they can later decay without the TLD material being heated (fading). If the energy levels are deep enough (deep trap), then the electron or hole can remain in the trap for a long time. The number of electrons trapped in metastable level is proportional to the absorbed energy in the TLD material. If the TLD material is heated up these electrons may be excited to the conduction band and later recombine with holes emitting the excess energy as light (Figure 20). The light is detected by a PM-tube and resulting charge is correlated to an absorbed dose in TLD material.

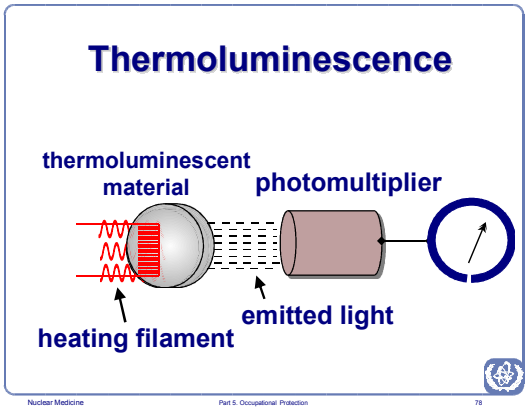

Figure 20. Process of thermoluminiscence

Used TLD's were type TLD 100 Thermo Fisher Scientific Inc. square shape dimensions 3 mm^2. LiF:Mg and Ti is approximately tissue-equivalent (Z_{eff} = 8.2) and has an photon energy response for gamma-rays that ranges from 15 keV - 3 MeV (IEC 1066). A detection threshold of the dosimetry system is 30,689 μSv, according ISO/12794 (S.5) Figure 21.

Figure 21. TLD

The controlled TLD was kept separately to measure background. The background readings were subtracted from the readings of estimated effective doses at surface of the skin above gastric region. The TLDs were prepared with standard instructions. TTP recommendation for Teflon card configuration for chip TLD type (TLD 100, LiF: Mg,Ti) for hot gas reader type for 6600 plus automatic are given in following Table 14.

Description	Settings
Preheat temperature	50 °C
Preheat time	0 s
Temperature rate	25 °C/s
Maximum temperature	300 °C
Acquire time	13 1/3 s
Annealing temperature	0 °C
Annealing time	0 s

Table 14. TTP

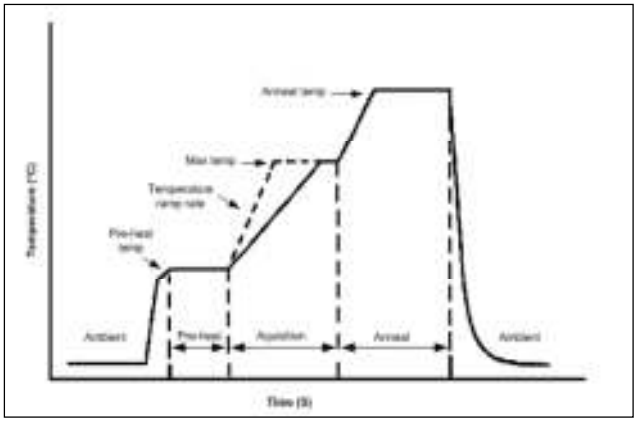

Graph 5. Heating cycle

The heating cycle normally consist of preheat, acquisition, anneal and cool segments. Preheat is applied to segregate the light generated from low energy traps to minimize fade effect. Significant dosimetry data are generated and stored during acquisition segment. To ensure current exposures do not contribute to subsequent measurements, the anneal cycle is applied. This has the effect of removing signal residual. The heating cycle applied helps to establish the reproducibility of the dosimeter. The combined standard uncertainty of a dosimetry system is less than 15 %. An automatic TLD reader (Thermo Harshaw 6600 plus) was used to evaluate the TLD chips Figure 22.

Figure 22. TLD Reader Thermo Harshaw 6600

The system uses Nitrogen gas to heat TLD pellets rather than a heater plate. The Win REMS System Software running on a Windows platform is used to analyze the read data. After annealing the TLD can be used again.

At fifteen, patients were performed external dose rate measurements at the surface (skin) over gastric region. Actually in these cases it was estimated Hp (0.07).These measurements were performed for a limited time of fifteen minutes and total time of three days until the patient left the hospital. The results will be presented in the next chapter.

3.6 Environmental measurements of released concentration of iodine in sewage system

Patients treated with ablation doses of ^{131}I are confined in the hospital for a few days to allow external radiation levels to decline to acceptable levels before release. Activity declines rapidly due to the biological elimination of ^{131}I from the body. As a result of this elimination, considerable amounts of radioactive ^{131}I are discharged within patient excreta into the local municipal sewer. The environmental network monitoring system was installed in the sewage system, to evaluate the concentration of ^{131}I during hospitalization of the patient. The measurement station consists of:

- an acquisition and processing board (PCB) allowing the connection of the detection probe, and the other optional measurement instruments,
- the gamma ray detection probe,
- the power supply and the telecommunication devices.

The gamma ray detection probe (Figure 23) has the following characteristics:

- 1 NaI(Tl) detector,
    - Energy resolution at 662 keV: $\pm$7%
    - Energy measurement range: 80-2000 keV,
    - Impermeable casing made of 316 l stainless steel or corrosion resistant HDPE,
    - 1 multi-channel analyzer (1024 channels).

The probe was installed by and calibrated at National Institute of Radioelements, Fleurus, Belgium.

The estimation of discharged levels was performed over five patients during their hospitalization at isolated room. The measurement was performed when there was treated one patient with 3700 MBq and two patient at the same time each of them treated with 3700 MBq. The results will be presented in the next chapter.

Figure 23. Monitoring system

3.7 Sampling

3.7.1 Radiopharmaceutical ^{131}I

Radioactive material in the form of ^{131}INa is purchased from CIS Biointernational, France (Figure 24). Usual radioiodine concentration supplied by the manufacturer is 1110 MBq/ml on the date of calibration. In the hospital measured the activity of the capsule is in the process of radiopharmaceutical preparation for administration. Activity was measured using dose calibrator Atom lab 100 (Figure 24) based on pressurized well type ionization chamber (14 bar Argon, inside well diameter 57 mm and length 270 mm). Energy range of the dose calibrator was between 25 keV and 3 MeV with resolution of 1 kBq. Electrometer accuracy was declared as $\pm$1% while chamber standard uncertainty for activity determination was estimated at less than $\pm$3%. Considering the data on the measurement uncertainties obtained from the manufacturer and our own measurements we can state that expanded uncertainty of radioiodine activity in solution is less than $\pm$10% (k=2) assuming a normal distribution for uncertainty Type B.

Figure 24. Dose calibrator Atom lab 100, Biodex

Radionuclide purity of Na^{131}I is not less than 99.9% (total radioactivity is due to ^{131}I). Capsule material and additional elements in the solution are not relevant for the purpose of these investigations. Volatility of radio pharmacy prepared Na^{131}I is neglected (on the order of 10^{-5} of the total activity) [81].

Figure 25. Lead container and vial for the capsule

According to our protocol a first ablation dose for residual thyroid tissue is 3700 MBq. Patients are usually administered into designated room with onsite bathroom facilities; visiting time being restricted to not more than 10 minutes a day at distance of more than 5.0 m. Daily monitoring and measurements were performed until the day of discharged with radiation levels acceptable under national regulation. The dose values for several organs of interest were compared for different administered doses.

3.7.2 Application of Monte Carlo software package

The use of Monte Carlo method to simulate radiation transport has become the most accurate means of predicting absorbed dose distributions and other quantities of interest in radiation treatments of cancer patients using either external or radionuclide therapy. The general idea of Monte Carlo analysis is to create a model, which is similar as possible to the real physical system of interest and to create interactions within that system based on known probabilities of occurrence with random sampling of the probability density functions (PDFs). As the number of individual events (histories) is increased, the quality of the reported average behavior of the system improves meaning that the statistical uncertainty decreases.

3.7.3 Estimation of effective dose for different organs using Monte Carlo simulation

General method for determination of effective dose in different organs and for estimation of additional risks is presented as three steps procedure:

- Dose equivalents in tissues or organs are calculated by appropriate radiation transport codes using a suitable mathematical anthropomorphic phantom;

- The effective doses E, on the basis of tissue weighting factors, has been calculated and
- Additional risks of lifetime mortality were assessed.

Geometry

The used radiation transport code MCNP4b [91] is appropriate for various complex geometries. The geometry is arranged in two major parts: surfaces and cells. Each surface is a two-dimensional plane with given parameters that are created for cell boundaries. These planes have many shapes including spheres, cylinders and spheroids, elliptical and curved plane.

Tallies

MCNP provides seven standard neutron tallies, six standard photon tallies and four standard electron tallies. The basic tallies can be modified by the user in many ways. Proper tally specification is very important in MCNP calculations. In the case of dose distribution calculation in different organs for gamma rays the tallies *F8 and F6 are applicable and therefore used. For beta particles, only *F8 can be used. These tallies give the absorbed energy in organs in units $MeVg^{-1}$ per disintegration. In the case of calculation of local dose distribution in the stomach wall, beside F6 and *F8 tallies just for gamma rays, F2 tally has been used to. Because this tally represents flux average over the surface, flux dose rate conversion coefficients have been used [80].

The basic concept of dose estimation using Monte Carlo calculations starts from input data and presumptions introduced into consideration. Input data are data determining the source (nuclear, radiological and shielding data), geometry and materials [81].

3.7.3.1 Source data

Iodine ^{131}I is boson with 53 p and 78 n. It is beta emitting radionuclide with complex beta decay scheme, a principal gamma ray of 364 keV and a principle beta particle with maximum energy of 0.61 MeV, an average energy of 0.192 MeV and a range in tissue of 0.8 mm. Each beta minus emission for ^{131}I has one or more corresponding gamma emissions. Reaction energy is Q = 0.97 MeV. Specific activity is 4600 TBq /g. In the case of ^{131}I beta particles and gamma ray transport should be taken into account. For the energies less than 2.5 MeV the range of beta particle is approximated by the following equation:

$$R = \frac{0.412}{\rho} E^{(1.265-0.0954 \ln E)} \quad (70)$$

Where (R) is range expressed in cm, (E) is the beta particle energy in MeV, (ρ) is material density in gcm^3. Conversion factors for radiation absorbed dose from Na ^{131}I are well known and are given in numerous literatures. In Table 15 there are given tabulate values from ICRP 53 [82], used in the simulation.

Organ	Conversion factor (mGy/MBq)	
	0% uptake	55% uptake
Bladder wall	0.610	0.290
Colon wall	0.043	0.058
Kidneys	0.065	
Ovaries	0.042	0.041
Testes	0.037	0.026
Stomach	0.034	
Thyroid		790.00

Table 15. ICRP conversion coefficient

3.7.3.2 Geometry and materials

The source of ^{131}I was considered as a point source placed in the middle of the soft tissue sphere. It was reasonable to presume the point source geometry as the small dried drop was deposited on the capsule holder. Self-absorption in such source should not be significant. The calculations performed during this study used a few various anthropomorphic organs due to the presence of the source in some other organ [85].

For our purposes, we used the new MIRD model. The phantom consists of three major sections:

- An elliptical cylinder representing the trunk and arms
- Two truncated circular cones representing the legs and feet
- A circular cylinder on which sits an elliptical cylinder capped by half an ellipsoid representing the neck and head.

The other organs are modeled by appropriate geometrical figures. The stomach wall is represented by the volume between two concentric ellipsoids and contents within the inner ellipsoid. Average stomach masses in grams are between 150 g for wall and 250 g for contents if it is not empty. The stomach is represented as the mass between two ellipsoids

$$\left(\frac{x-8}{4}\right)^2+\left(\frac{y+4}{3}\right)^2+\left(\frac{z-35}{8}\right)^2\leq 1 \tag{71}$$

$$\left(\frac{x-8}{3.387}\right)^2+\left(\frac{y+4}{2.387}\right)^2+\left(\frac{z-35}{7.387}\right)^2\geq 1 \tag{72}$$

In the case of adult male the parameters in former equation have the next values: a=4.00, b=3.00, c=8.00, d=0.613, x_0=8.00, y_0= -4.00, z_0=35.00 [85].

The axes are in cm; stomach volume is 151.9 cm^3 and the mass is 150 g. The thickness of the stomach wall is assumed to be about 0.613 cm. Only the case of the empty stomach is considered; therefore, we didn't put into calculation the stomach contents. This consideration is based upon clinical practice in our hospitals that all therapy procedures are given "at the empty stomach". According to this presumption the iodine capsule is at the bottom of the stomach lying at the stomach wall. The highest doses are delivered to an empty stomach because beta particles are absorbed in stomach content if present. Three phantom tissue types are recognized as skeletal, lung and all other tissue (soft tissue). The densities of those tissues are: 1.4 gcm^{-3}, 0.296 gcm^{-3} and 1.04 gcm^{-3} respectively. The exact compositions of each tissue type are given in ICRP reports 70 and ICRP 89 and ICRU-46, [86, 87, 88]. The soft tissue composition used is presented as 10.6%H+11.5%C+2.2%N+75.1%O+0.1%Na+0.1%P+0.1%S+0.2%Cl+0.1%K.

For organs with walls and with contents as a source (even the very small one) it can be considered that

$$\Phi_i(r_k \leftarrow r_h) = \frac{1}{2m_h} \tag{73}$$

The (m_h) is the mass of the source organ. Thus the dose to the wall sections of the gastrointestinal tract and to the urinary bladder from sources in the corresponding contents represents a surface dose for electrons and beta particles.

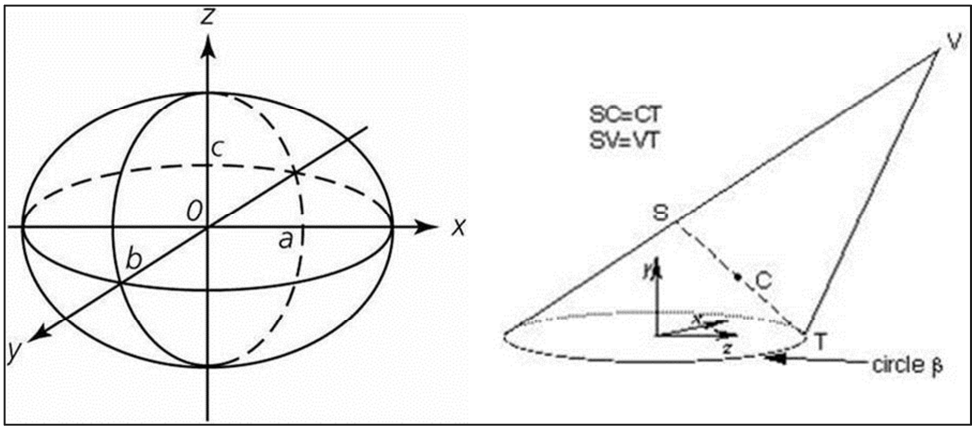

Figure 26. Elipsoid gastric model

3.7.3.3 Modeling of energy distributions of beta particles

Beta decay spectra which included internal conversion electrons were calculated using the Fermi model of beta decay with a relativistic correction for Coulomb Forces and the spectral factor correction for “forbidden” transitions was a set of polynomial function [89]. End point energies and activity data were acquired from Evaluated Nuclear Structure Data File (ENSDF) database at Brookhaven National Laboratory [90]. On Graph 6 is presented beta spectra of iodine 131.

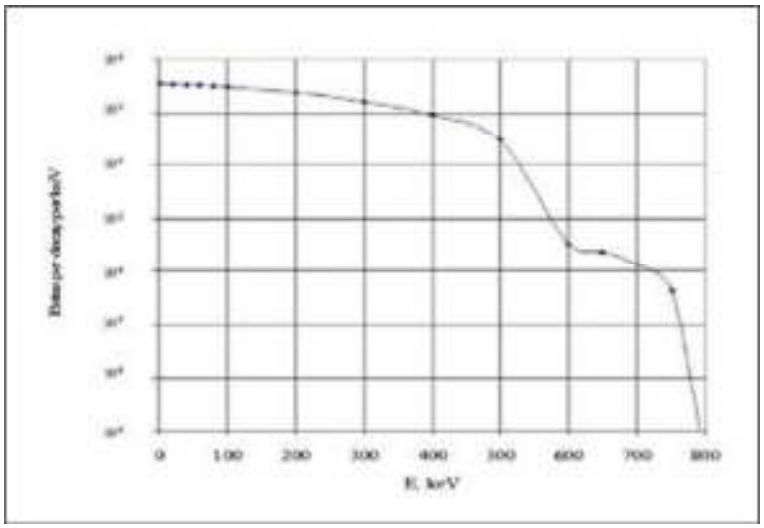

Graph 6. Beta spectra of ^{131}I

In the process of beta decay, either an electron or positron is emitted as well; there is a spectrum of energies for the electron or positron depending upon what fraction of the reaction energy (Q) is carried by the massive particle. The shape of this energy curve can be predicted from the Fermi theory of beta decay. Treating the beta decay as a transition that depended upon the strength of the coupling between the initial and final states, Fermi developed a relationship which is now referred to as Fermi, golden rule [89], where the transition probability is given by:

$$\lambda_{if} = \frac{2\pi}{\hbar}|M_{if}|^2\rho_f \tag{74}$$

Where (M_{if}) is the matrix element for the interaction and (ρ_f) is the density of the final states. A transition will proceed rapidly if the coupling between the initial (i) and the final (f) states is stronger. The matrix element can be expressed as integral final (f) and initial (i)

$$M_{if} = \int \varphi_f^* V \varphi_i dv \tag{75}$$

The (V) is operator for the physical interaction which couples initial and final states of the system. And (φ) is the wave function for final (f) and initial state (i). The transition probability is proportional to the

square of the integral of this interaction over all of the space appropriate to the problem. From the Fermi theory of beta decay the shape of distributions for the transitions is given approximately by the expression:

$$N(KE_e) = C\sqrt{KE_e^2 + 2KE_e m_e c^2}(Q - KE_e)^2(KE_e + m_e c^2)F(Z', KE_e) \quad (76)$$

Where F (Z",KEe) is called Fermi function. It accounts for nuclear coulomb interaction which shifts the distribution toward lower energies because of the Coulomb attraction between the daughter nucleus and the emitted electron. It shifts the distribution upward for positrons. Q represents the energy yield of the transition and as such is the upper bound on the kinetic energy of the electron, KEe. The relativistic momentum for the electron apparent complexity of the expression is partly because it is necessary to use relativistic momentum for the electron.

Chapter 4

4. RESULTS AND DISCUSSION

4.1 Five years follow up

In the thesis are presented the results for five year period (2007 - 2011) of patients treated with radioiodine 131, either for hyperthyroidism or thyroid cancer, at the Institute of pathophysiology and nuclear medicine in Skopje, Macedonia. The statistical analysis was performed by using SPSS 12.0 version. Proportions, means, medians etc. were calculated, and suitable tests of significance carried out.

Total number of treated patients in this period was 527 (329 hyperthyroidism and 198 thyroid cancer). Graph 7.

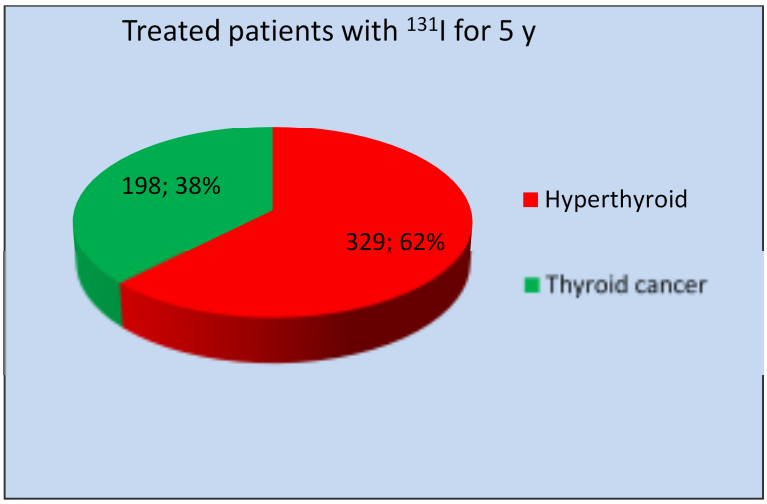

Graph 7. Treated patients for 5 years

The number of female patients was 391 (234 hyper and 157 cancer) and male 136 (95 hyper and 41 cancer). Our findings show that the number of the female population was more affected with thyroid diseases than a male population for both groups (hyperthyroid and thyroid cancer) or in percents (71.1% female and 28.9% male) for hyperthyroid and (79.3% female and 20.7% male) for thyroid cancer Graph 8. Total male to female ratio was 1:2.8. Mortality rate during these five years at thyroid cancer patients was 2%.

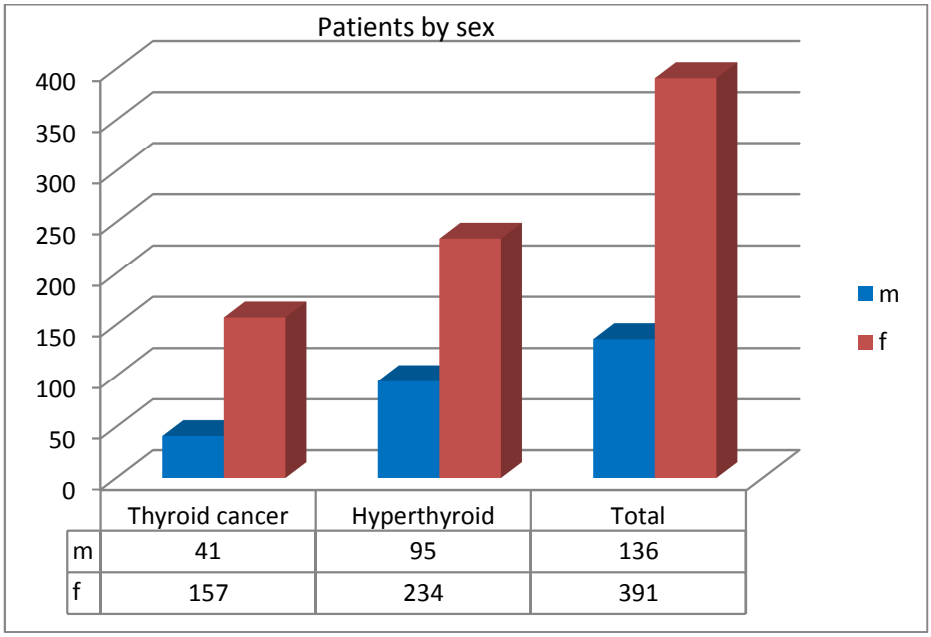

Graph 8. Treated patients by sex

Our findings are in good agreement with findings from the published results in the world literature. The gender distribution in this thesis is similar to that reported from other studies.

Tzavara et al. [97] have published a study in which the number of analyzed thyroid cancer patients was 677 during the period of 30 years. In that study 75% were female, 81% were with papillary and 22% had follicular thyroid carcinoma.

Another study by R. Sciuto et al. [98] followed cohort of 1503 patients with differentiated thyroid carcinoma. Median age at diagnosis was 46. Papillary cancer represented > 80% of cases, follicular cancer 14.7%. The female patients were 78.6% and male 21.4%. The age less than 45 were 49.6% and > 45 were 50.4%.

A study by Brig SS Anand et al. [99] reports retrospective analysis of 70 patients. Papillary carcinomas constituted 88% followed by follicular cancers at 9% of all cancers. Females were affected more than males in the ratio 2.2:1. Mean age of presentation for papillary cancer was 39 years and for follicular 50 years.

Totally administered activity for five years was 894 GBq. For hyperthyroid patients, the administered dose was 148 GBq, and for treatment of thyroid cancer 746 GBq Graph 9. Most of the delivered therapy was performed in the form of capsules, but there were a certain number of patients that received the therapy in the form of solution.

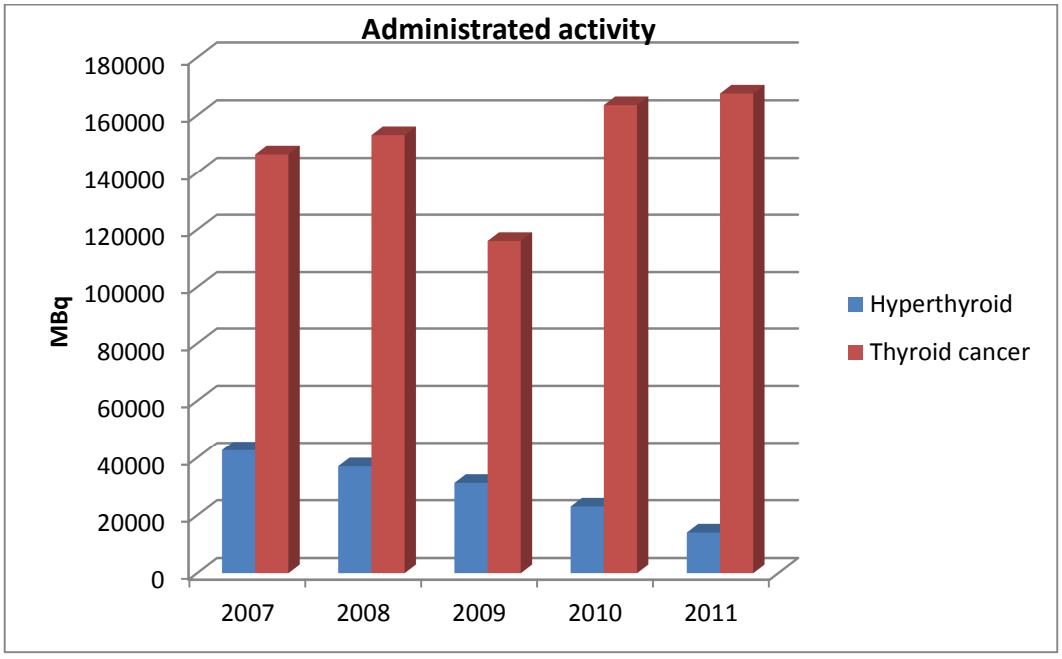

Graph 9. Administered activity per years

In the Table, 16 are presented administered activity during five years period. In the group of hyperthyroid patients the ratio male : female was 1 : 2,5. It is obvious that the number of patients is decreasing in the last years. It is the result of the changes in the public health system or better and improved triage of the patients before they have to be sent at tertiary institution.

Hyperthyroid patients					
Year	Number of patients	male	female	ratio	MBq
2007	90	21	69	3,3	42661
2008	91	26	65	2,5	37037
2009	70	18	52	2,9	31228
2010	45	18	27	1,5	23051
2011	33	12	21	1,8	14060
Total	**329**	**95**	**234**	**2,5**	**148037**

Table 16. Hyperthyroid patients

For the thyroid carcinoma patients the total male : female ratio is 1 : 5,0 and there is no evidence of decreased number of patients treated with radioiodine. The majority of well differentiated malignancies manifested between third and fifth decades of life.

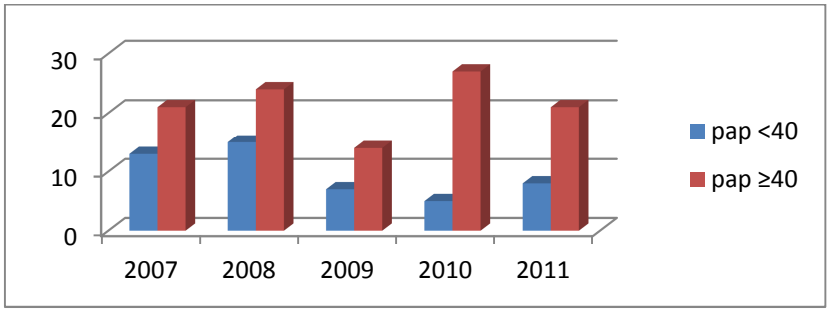

Graph 10. Age of papillary patients

Mean age was 44 ± 5 years (median 45, range 17 -74). On the Graph 10, 30.9% of the patients with papillary cancer were less than 40 years of age as compared with papillary/follicular cancer the percentage was 37.5%. However the difference was not statistically significant (p = 0.983)

Carcinoma patients					
Year	Number of patients	male	female	ratio	MBq
2007	39	12	27	2,3	146520
2008	40	5	35	7,0	153180
2009	32	8	24	3,0	116089
2010	45	9	36	4,0	163573
2011	42	7	35	5,0	167591
Total	**198**	**41**	**157**	**3,8**	**746953**

Table 17. Carcinoma patients

On the Graph11 are presented the number of patients during five years.

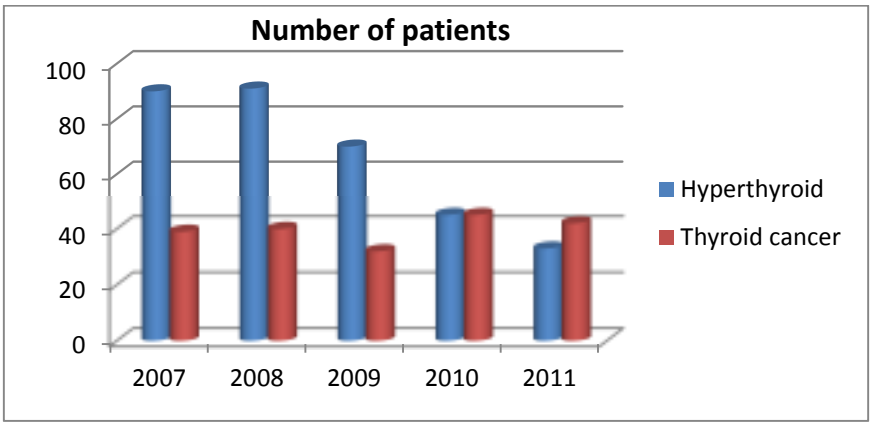

Graph 11. Number of patients

Table 18. Shows that papillary carcinoma were the commonest accounting for 79%, followed by follicular carcinoma (20%) and medullar carcinoma (1,5%). Table 17 also shows a comparison with the world literature [132]. 70.7% males had papillary carcinoma as compared to 80.2% of females. The difference between males and females for the type of cancer was not statistically significant (p value = 0.84)

Diagnosis	World (%)	Results (%)
Papillary carcinoma	60-80	79
Follicular carcinoma	5-25	20
Medullar carcinoma	5-10	1.5
Anaplastic carcinoma	4-10	1

Table 18. Distribution of malignant thyroid tumors amongst study group and the comparison with world literature

Our results are in consonance with that reported on other studies. The most present is papillary carcinoma (79%) and it is similar with the worldwide trend as iodine fortification of the salt has resulted in decreased prevalence of the iodine deficiency disorders.

4.2 Results for external dose rate measurements

At sixty patients (hyperthyroid and thyroid cancer) were performed dose rate measurements at distances 0.25 m; 0.5 m; 1.0 m; and 2.0 m.

4.3 Survey Meter Dose Rate

In order to validate the dose rate results of the survey meter, dose rate test was performed with activity of 1100 MBq ^{99m}Tc. The results are presented in Table 19

Activity MBq	Dose rate µSv/h	Dose rate µSv/h	Dose rate µSv/h	Dose rate µSv/h
	0.25 m	0.5 m	1.0 m	2.0 m
1100	420	110	30	7

Table 19. Dose rate results

The Table 20 and Graph 12 presents evaluation of the survey meter precision in regard to dose rate measurements at different distances. Ratio r^1 represents the dose rate at 0.25 m divided by the dose rate at 0.5 m distance. Ratio r^2 represents the dose rate 0.25 m divided by the dose rate at 1.0 m distance, and r^3 represents the dose rate 0.25 m divided by the dose rate at 2.0 m distance. The values R1, R2, R3 are the dose ratios corrected for the inverse square variation. In the best case, the results of those calculations should be equal to 1 in all three distances. The gained results in this case are all within acceptable limits.

r^1	r^2	r^3	$R1=r^1/4$	$R2=r^2/16$	$R3=r^3/64$
3.82	14.00	60.00	**1.0**	**0.9**	**0.9**

Table 20. Inverse Square Dose Rate Validation

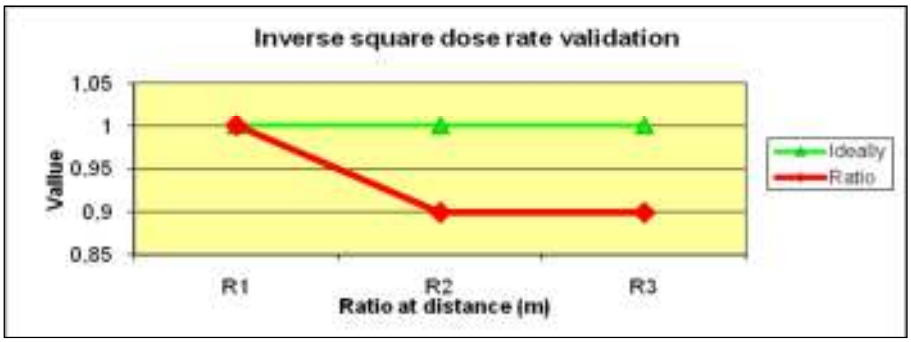

Graph 12. Inverse square dose rate validation

4.4 Hyperthyroid patients

All patients feel positive to participate in the study. Ten patients were with diagnosis Autonomous Functioning Thyroid Adenoma. Eight patients were with hyperthyroidism; six were with diagnosis SDT; two were with diagnosis SNT and Ca pap-follow up, and one patient was with diagnosis M. Basedow (Graph 13).

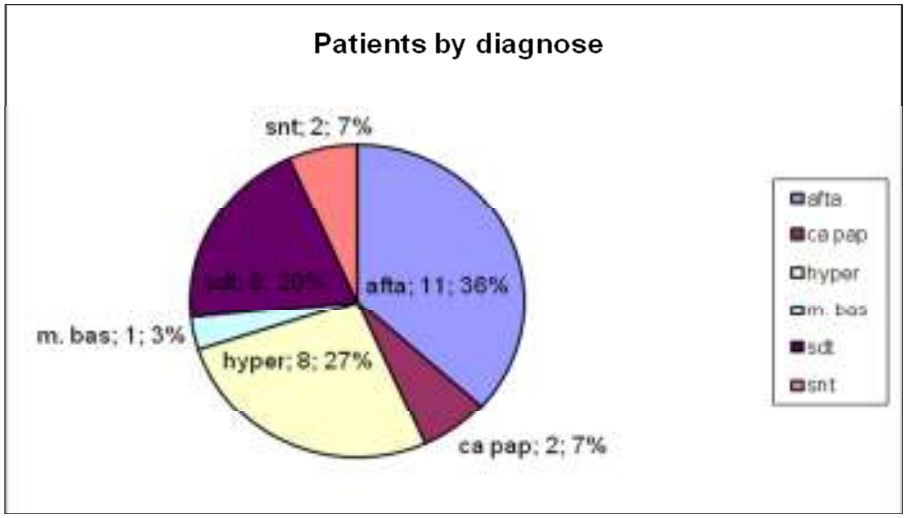

Graph 13. Patients by diagnose

Only five patients were male, and other twenty-five patients were female or in percent's 17% were male, and 83% were female (Graph 14).

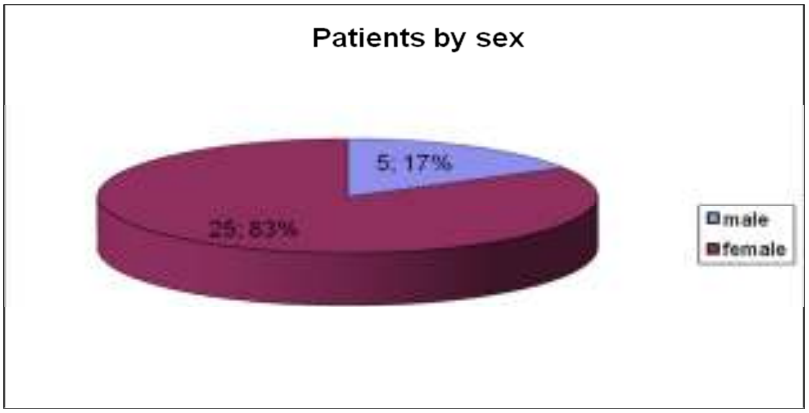

Graph 14. Patients by sex

The activity that was administered to patients was minimum 185 MBq and max 1295 MBq. The mean delivered dose was 683 MBq (Graph 15).

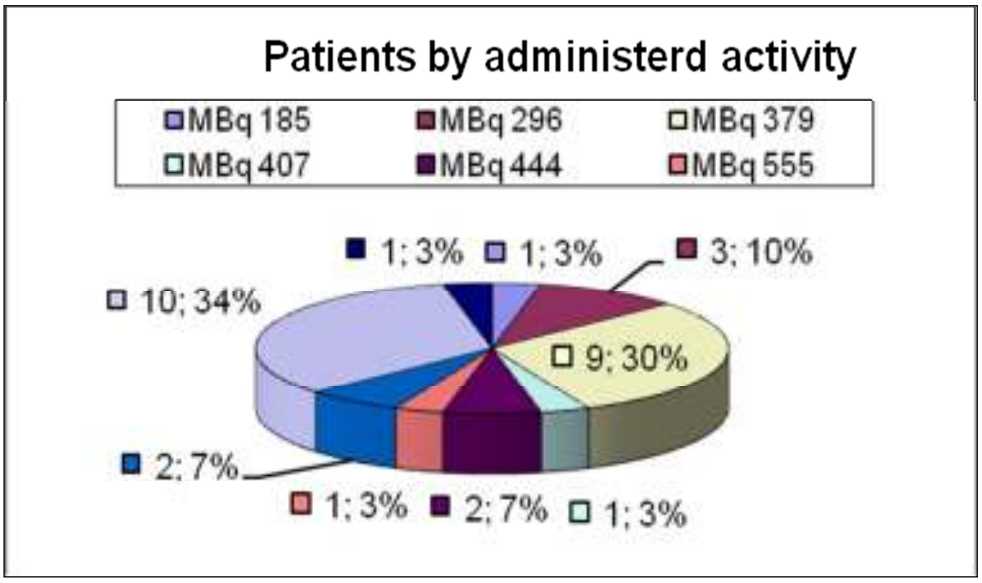

Graph 15. Patients by administrated activity

4.4.1 Hyperthyroid patient dose rate

Table 21 presents the measured dose rates on the first day of administered activity (185 MBq – 1295 MBq) for hyperthyroid patients.

No.	MBq	Dose rate (μSv/h)			
		0.25 m	0.5 m	1.0 m	2.0 m
1	925	380	90	40	15
2	1110	390	150	50	17
3	185	60	20	10	3
4	370	120	60	20	6
5	407	120	50	20	6
6	370	115	50	18	5
7	370	115	40	15	5
8	370	130	40	15	5
9	370	115	30	12	4
10	555	130	60	25	8
11	370	120	50	25	5
12	370	110	50	20	5
13	370	115	60	20	7
14	1110	420	150	50	15
15	1110	410	150	80	20
16	1110	400	100	50	15
17	296	100	50	20	4
18	1295	450	200	70	20
19	296	110	40	15	4
20	925	390	100	40	15
21	444	120	70	30	6
22	444	120	40	20	6
23	1110	400	130	50	20
24	296	110	40	20	7
25	370	120	40	20	6
26	1110	390	100	50	15
27	1110	400	100	60	17
28	1110	410	100	50	15
29	1110	420	100	60	20
30	1110	420	100	55	18

Table 21. Dose rates

The results for dose rate from Table 21 are shown on Graph 16.

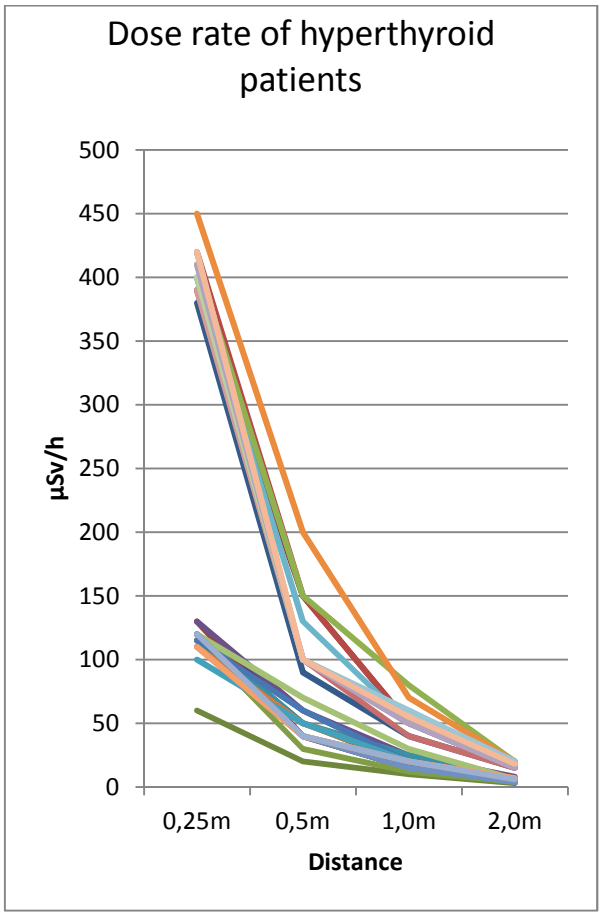

Graph 16. Dose rate of hyperthyroid patients

Table 22 Present the correlation between dose rate and administered activities for hyperthyroid patients on the first day. The correlation coefficients were positive and in the range from 0.30 to 0.44.

Coeficients at distances (m)			
0.25 m	0.5 m	1.0 m	2.0 m
0,34	0,36	0,44	0,30

Table 22. Coefficients at distances (m)

A linear correlation coefficient has an absolute value between 0 and 1. With one is indicated a perfect linear relationship exists, and zero means that no linear relationship exists. Generally, unless the

absolute value of the correlation is greater than 0.5 the relationship between two variables is not considered of importance unless the sample is large (45). In our case, there is a positive correlation of less than 0.5, and this is not significant (Graph 17).

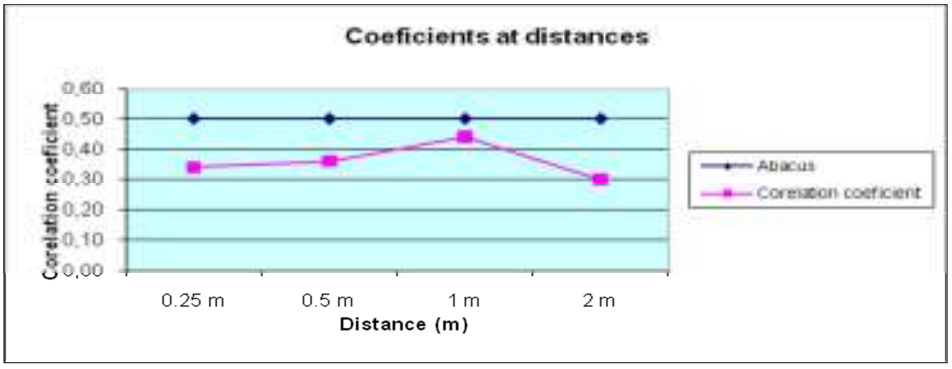

Graph 17. Coefficients at distances

Distance (m)	Mean dose rate (μSv/h)	Standard deviation	Dose rate range (μSv/h)
0.25	240	148.41	60 - 450
0.5	79	43.92	20 - 200
1.0	34	19.43	10 - 80
2.0	10	6.14	3 - 20

Table 23. Dose rate vs. distance for Hyperthyroid patients at time of treatment

Table 23 and Graph 18 presents the mean dose rate for hyperthyroid patients at the time of treatment for all 30 patients. The patients were treated with 185 MBq – 1295 MBq of ^{131}I activity on an outpatient basis. The maximum dose rate at the time of treatment was 450 μSv/h at a distance of 0.25 m and minimum was measured at 2.0 m only 3 μSv/h up to 20 μSv/h. The following Graph 18 presents the values of standard deviation, mean dose rate, minimum and maximum dose rate range.

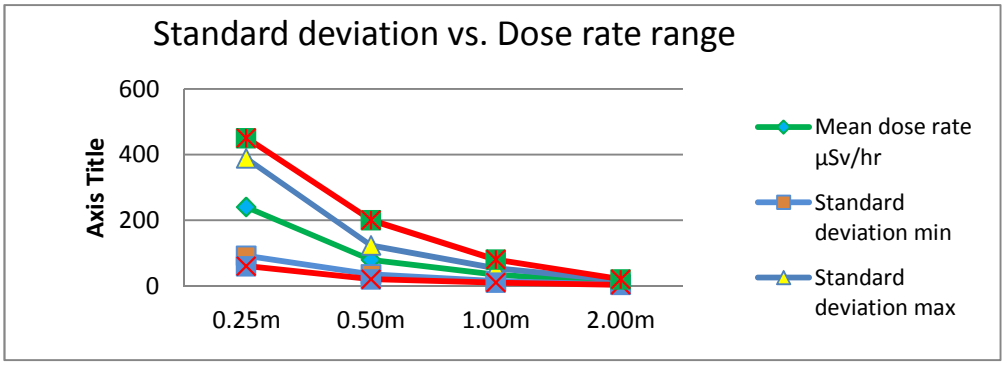

Graph 18. Standard deviation vs. Dose rate range

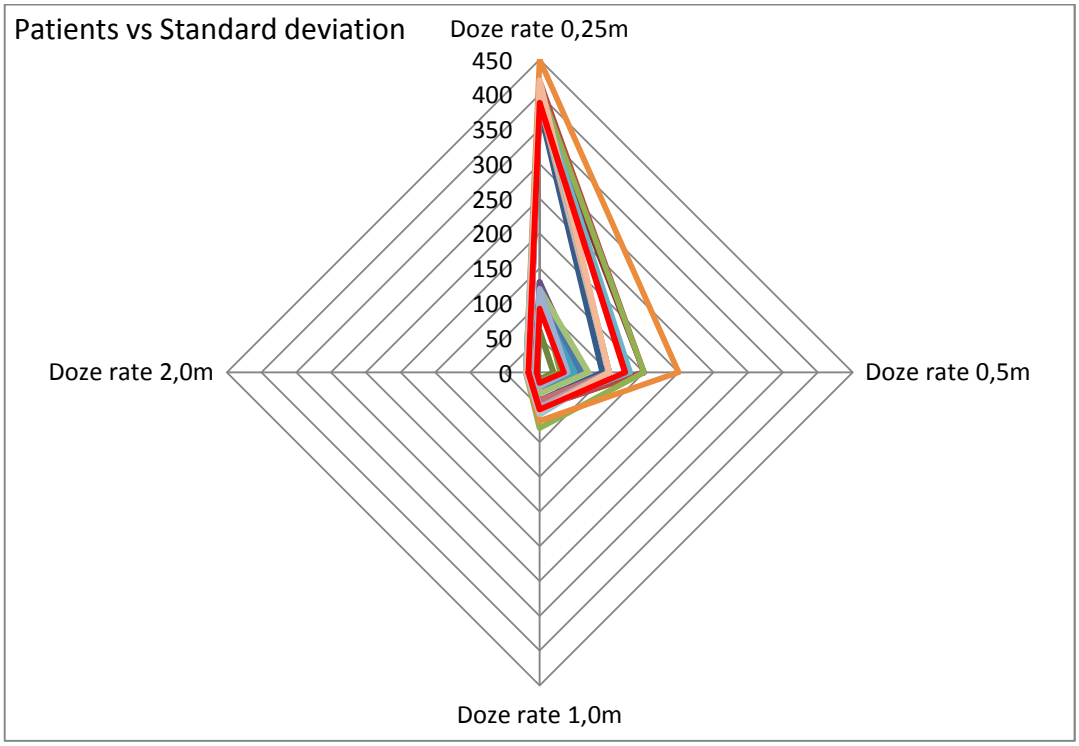

Graph 19. Dose rate measurements

The Graph 19 presents dose rate measurements for all thirty patients. With the red line is marked standard deviation, max and min.

The next Table 24 presents inverse square law validation for all patients at the day of administration. The given readings for dose rate at different distances should follow the inverse square law. Ratios were calculated with respect to that at 0.25 m. These then were divided by the value to allow variations to be seen. Overall the results followed the expected pattern of course there were exceptions, which are commented in the discussion part.

No.	Dose rate µSv/h				Ratio			Inverse square		
	A	B	C	D	r^1	r^2	r^3	R1	R2	R3
	0.25m	0.5m	1.0m	2.0m	A/B	A/C	A/D	$r^1/4$	$r^2/16$	$r^3/64$
1	380	90	40	15	4,2	9,5	25,3	1,1	0,6	0,4
2	390	150	50	17	2,6	7,8	22,9	0,7	0,5	0,4
3	60	20	10	3	3,0	6,0	20,0	0,8	0,4	0,3
4	120	60	20	6	2,0	6,0	20,0	0,5	0,4	0,3
5	120	50	20	6	2,4	6,0	20,0	0,6	0,4	0,3
6	115	50	18	5	2,3	6,4	23,0	0,6	0,4	0,4
7	115	40	15	5	2,9	7,7	23,0	0,7	0,5	0,4
8	130	40	15	5	3,3	8,7	26,0	0,8	0,5	0,4
9	115	30	12	4	3,8	9,6	28,8	1,0	0,6	0,4
10	130	60	25	8	2,2	5,2	16,3	0,5	0,3	0,3
11	120	50	25	5	2,4	4,8	24,0	0,6	0,3	0,4
12	110	50	20	5	2,2	5,5	22,0	0,6	0,3	0,3
13	115	60	20	7	1,9	5,8	16,4	0,5	0,4	0,3
14	420	150	50	15	2,8	8,4	28,0	0,7	0,5	0,4
15	410	150	80	20	2,7	5,1	20,5	0,7	0,3	0,3
16	400	100	50	15	4,0	8,0	26,7	1,0	0,5	0,4
17	100	50	20	4	2,0	5,0	25,0	0,5	0,3	0,4
18	450	200	70	20	2,3	6,4	22,5	0,6	0,4	0,4
19	110	40	15	4	2,8	7,3	27,5	0,7	0,5	0,4
20	390	100	40	15	3,9	9,8	26,0	1,0	0,6	0,4
21	120	70	30	6	1,7	4,0	20,0	0,4	0,3	0,3
22	120	40	20	6	3,0	6,0	20,0	0,8	0,4	0,3
23	400	130	50	20	3,1	8,0	20,0	0,8	0,5	0,3
24	110	40	20	7	2,8	5,5	15,7	0,7	0,3	0,2
25	120	40	20	6	3,0	6,0	20,0	0,8	0,4	0,3
26	390	100	50	15	3,9	7,8	26,0	1,0	0,5	0,4
27	400	100	60	17	4,0	6,7	23,5	1,0	0,4	0,4
28	410	100	50	15	4,1	8,2	27,3	1,0	0,5	0,4
29	420	100	60	20	4,2	7,0	21,0	1,1	0,4	0,3
30	420	100	55	18	4,2	7,6	23,3	1,1	0,5	0,4
mean	**240,3**	**78,7**	**34,3**	**10,5**	**3,0**	**6,9**	**22,7**	**0,7**	**0,4**	**0,4**

Table 24. Inverse square ratio

The mean value of dose rate at 0.25 m, 0.5 m, 1.0 m, 2.0 m was 240.3 µSv/h, 78.7 µSv/h, 34.3 µSv/h, and 10.5 µSv/h respectively.

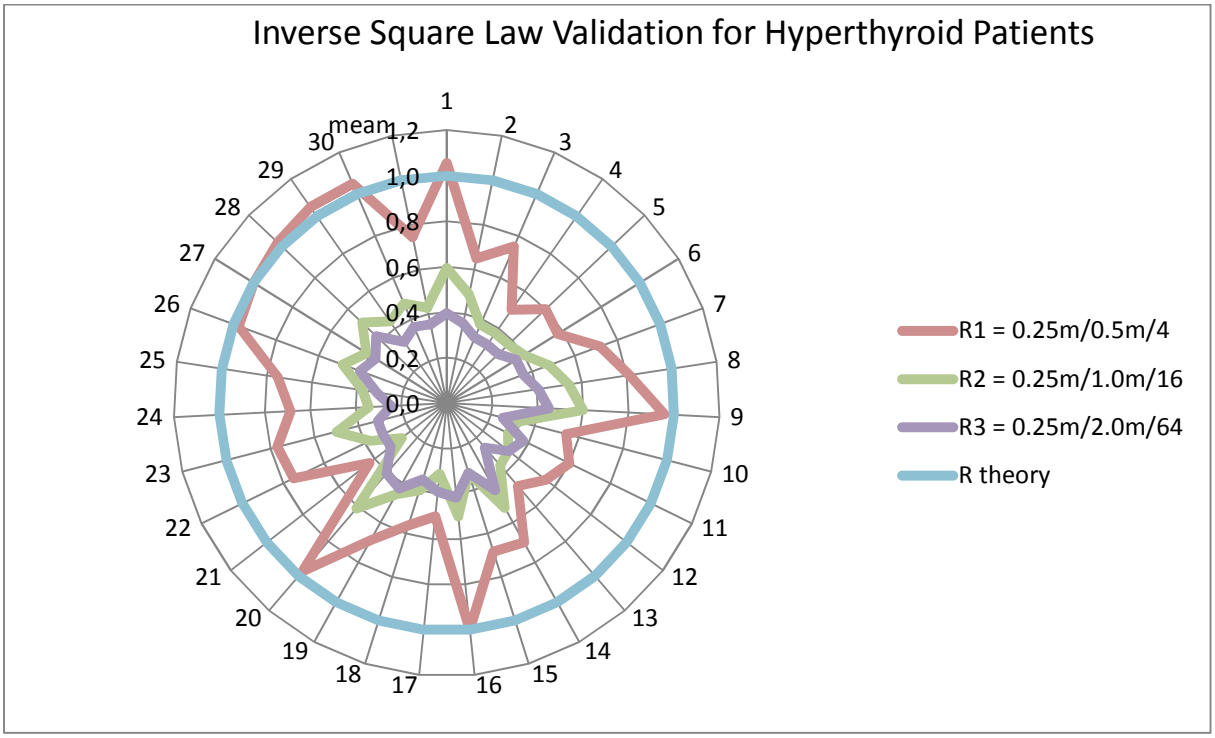

Graph 20. Inverse Square Law Validation for Hyperthyroid Patients

Graph 20 demonstrates inverse square law validation of dose rate for hyperthyroid patients. The mean value for dose rate at 0.25 m is very close (0.7) to the ideal value (1) given by theory for the inverse square law. Changing the distance to 0.5 m, 1.0 m, and 2.0 m the values for dose rates differ much more than proposed value by theory. The explanation is given in the part of the discussion, and it refers to that we treat patient as a point source in approximation which is very conservative, but in reality, the situation is very different and many other factors affect the results. Further measurements in the future can be made more realistic by using patient-specific parameters that are based on direct measurements and the modeling of the patient's lifestyle.

4.5 Thyroid cancer patients

4.5.1 Thyroid Cancer Patients Dose Rate

The group of thyroid cancer patients consisted of 30 patients. From thirty patients, 23 were with diagnosis Ca papillarae, three patients were with Ca follicular, the same number with Ca papillary/follicular and only one patient was with diagnosis Ca medullary. Graph 21 summarizes patients by diagnose.

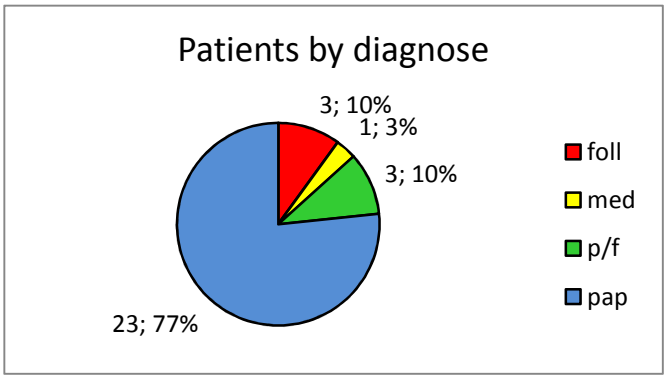

Graph 21. Patients by diagnose

Twenty six of patients were female, and only four were male (Graph 22).

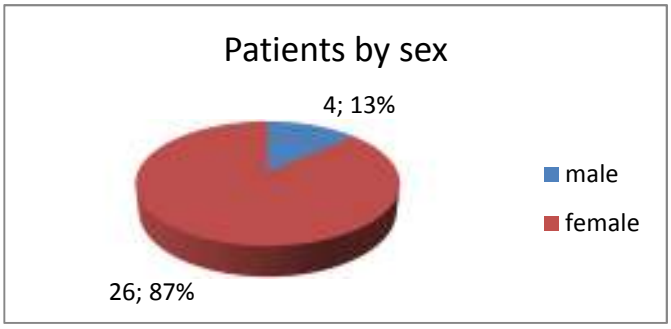

Graph 22. Patients by sex

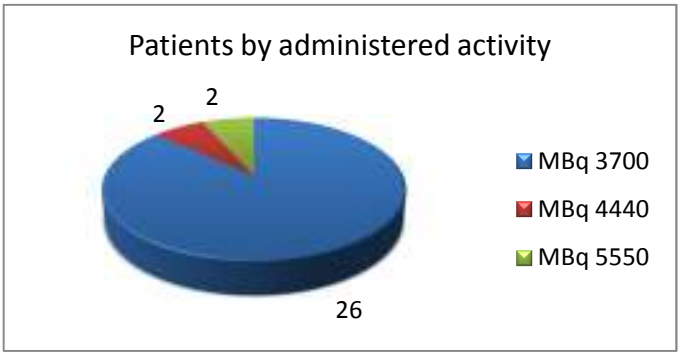

Graph 23. Patients by administrated activity

The administered activity varied between 3700 MBq to 5550 MBq (Graph 23). The meanly administered dose was 3539 MBq. The most of thyroid cancer patients stayed in the hospital for three days. There were 3 follow up patients who had received a second administration dose since the adequate ablation had not been achieved on the first treatment. A regularly calibrated sodium iodide scintillation survey meter was used. All dose rate measurements were made at anterior midline of the patients at about 15 min after radiopharmaceutical administration. The dose rate was determined every day during the stay at hospital at distance of 0.25 m; 0.5 m; 1.0 m and 2.0 m. The results are presented in the following Table 25.

No.	Dg.	Sex	Age	MBq	Dose rate (μSv/h)											
					day 1 (m)				day 2 (m)				day 3 (m)			
					0.25	0.5	1	2	0.25	0.5	1	2	0.25	0.5	1	2
1	pap	f	26	3700	450	200	100	40	300	90	50	15	170	60	20	7
2	pap	f	70	3700	440	180	100	50	270	80	40	15	90	12	8	3
3	pap	f	29	4440	470	220	150	50	310	120	90	25	240	50	30	8
4	pap	m	41	3700	420	220	150	50	310	100	80	21	280	90	70	15
5	pap	f	43	3700	410	230	150	40	300	100	50	15	250	50	15	6
6	p/f	f	33	3700	400	190	100	30	280	80	30	15	250	50	14	6
7	pap	m	35	3700	440	190	150	50	310	120	60	15	240	60	20	7
8	pap	f	15	3700	450	210	100	50	260	150	60	20	250	70	30	12
9	pap	m	35	3700	420	220	150	40	280	100	40	15	180	30	15	5
10	pap	m	75	3700	470	180	100	60	300	100	50	20	220	60	40	8
11	pap	f	30	3700	480	210	150	60	290	100	50	15	240	70	30	10
12	pap	f	73	5550	490	220	150	80	290	100	70	25	300	65	25	7
13	foll	m	66	5550	500	230	200	50	300	100	70	30	250	70	50	15
14	pap	f	42	3700	440	180	120	40	290	100	50	20	200	100	30	10
15	pap	f	21	3700	450	210	150	50	290	100	70	25	230	60	30	10
16	med	f	43	3700	460	220	150	50	290	90	40	15	240	50	25	8
17	foll	f	68	3700	420	250	200	50	300	110	60	20	190	40	15	7
18	pap	f	18	3700	430	260	200	50	290	100	50	15	200	50	20	8
19	p/f	f	25	3700	430	220	150	50	310	120	70	30	260	90	50	15
20	pap	f	39	3700	480	260	200	50	310	125	70	30	180	40	25	10
21	pap	m	61	4440	470	250	200	60	300	115	70	30	200	50	30	15
22	foll	f	40	3700	460	240	200	40	250	80	30	10	100	30	10	3
23	pap	f	62	3700	450	210	150	50	250	80	40	10	175	40	20	6
24	pap	f	45	3700	430	200	150	60	320	120	70	20	230	70	30	7
25	p/f	f	50	3700	490	220	160	80	240	70	50	20	170	30	5	2
26	pap	f	60	3700	470	240	150	60	240	70	45	20	140	20	8	4
27	pap	f	55	3700	420	190	140	50	310	120	50	15	150	25	12	8
28	pap	f	42	3700	430	210	140	45	300	110	55	20	190	30	15	7
29	pap	f	44	3700	410	200	140	40	280	110	55	20	170	20	10	6
30	pap	f	50	3700	430	210	160	50	270	100	50	15	180	40	12	7

Table 25. Dose rate

On the Graph 24 are presented the individual dose rates as measured at 0.5 m distance.

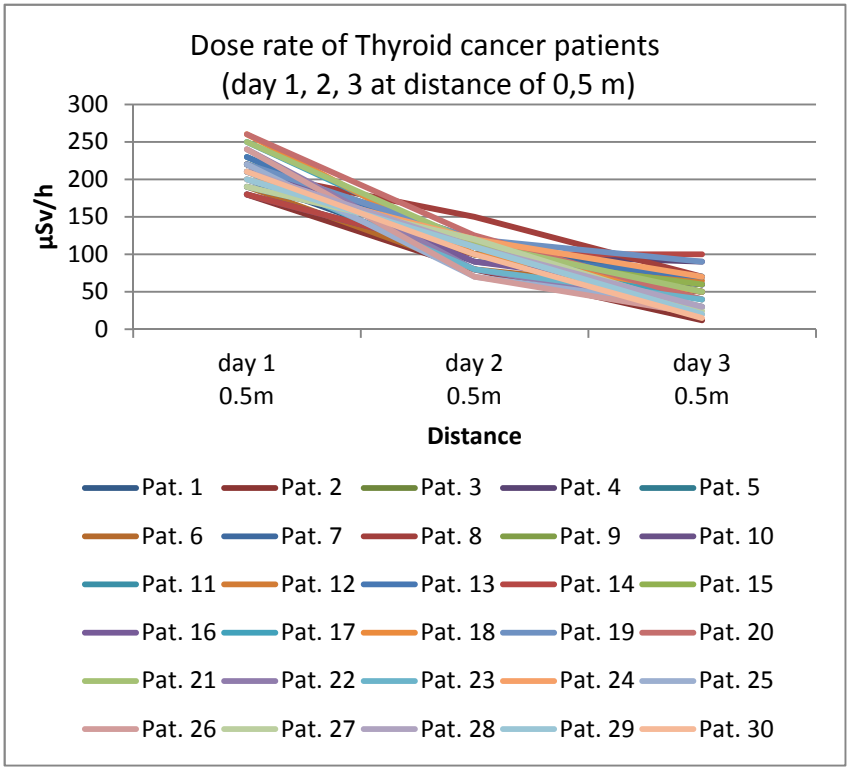

Graph 24. Dose rate of Thyroid cancer patients

Coefficients for three days were calculated at distance of 0.25 m and 0.50 m (Table 26, 27). The coefficients for 0.25 m were positive for all three days and ranged from 0.05 and 0.12. For the distance of 0.5 m, the coefficients were 0.24 for day 3 and 0.48 for the first day.

Coefficients, n=30, at distance of 0.25 m		
day 1	day 2	day 3
0,12	0,08	0,05

Table 26. Coefficients for 0.25 m

Coefficients, n=30, at distance of 0.50 m		
day 1	day 2	day 3
0,48	0,35	0,24

Table 27. Coefficients for 0.50 m

The mean dose rate was calculated for day 1, day 2 and day 3 and the values are given in following Tables 28, 29 and 30. In the same tables are given dose rate ranges for the distance 0.25 m, 1.5 m, 1.0 m and 2.0 m for thyroid cancer patients.

Day 1			
Distance (m)	Mean dose rate (μSv/h)	Standard deviation	Dose rate range(μSv/h)
0.25 m	447	27	410 - 500
0.50 m	198	29	150 - 200
1.00 m	150	31	100 - 200
2.00 m	51	11	40 - 80

Table 28. Mean dose rate

Day 2			
Distance (m)	Mean dose rate (μ Sv/h)	Standard deviation	Dose rate range (μ Sv/h)
0.25 m	288	22	250 - 320
0.50 m	102	18	70 - 125
1.00 m	56	14	30 - 90
2.00 m	19	6	10 - 30

Table 29. Mean dose rate

Day 3			
Distance (m)	Mean dose rate (μSv/h)	Standard deviation	Dose rate range (μSv/h)
0.25 m	206	49	90 - 280
0.50 m	50	23	12 - 100
1.00 m	24	14	5 - 50
2.00 m	8	3,5	2 - 15

Table 30. Mean dose rate

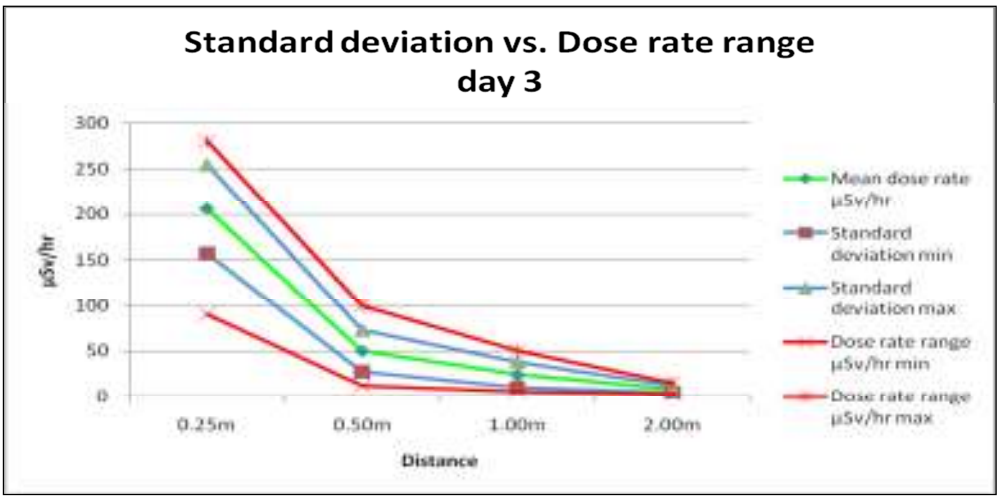

Graph 25. Standard deviation vs. Dose rate range

The maximum dose rate for day one was between 410 µSv/h - 500 µSv/h at 0.25 m and the minimum dose rate was between 90 µSv/h - 280 µSv/h at 0.25 m and from 2 µSv/h – 15 µSv/h at 2.0 m distance on day three. On Graph 25 are presented, the mean dose rates at day three. Compared with the values from the day one dose rates at day 3 are decreased from 447 µSv/h at 0.25 m to a mean dose rate 206 µSv/h, or from 52 µSv/h to 8 µSv/h at 2.0 m.

No.	Dose rate (day 3)				Ratio			Inverse square		
	A	B	C	D	r^1	r^2	r^3	R1	R2	R3
	0.25 m	0.5 m	1.0 m	2.0 m	A/B	A/C	A/D	$r^1/4$	$r^2/16$	$r^3/64$
1	170	60	20	7	2,8	8,5	24,3	0,7	0,5	0,4
2	90	12	8	3	7,5	11,3	30,0	1,9	0,7	0,5
3	240	50	30	8	4,8	8,0	30,0	1,2	0,5	0,5
4	280	90	70	15	3,1	4,0	18,7	0,8	0,3	0,3
5	250	50	15	6	5,0	16,7	41,7	1,3	1,0	0,7
6	250	50	14	6	5,0	17,9	41,7	1,3	1,1	0,7
7	240	60	20	7	4,0	12,0	34,3	1,0	0,8	0,5
8	250	70	30	12	3,6	8,3	20,8	0,9	0,5	0,3
9	180	30	15	5	6,0	12,0	36,0	1,5	0,8	0,6
10	220	60	40	8	3,7	5,5	27,5	0,9	0,3	0,4
11	240	70	30	10	3,4	8,0	24,0	0,9	0,5	0,4
12	300	65	25	7	4,6	12,0	42,9	1,2	0,8	0,7
13	250	70	50	15	3,6	5,0	16,7	0,9	0,3	0,3
14	200	100	30	10	2,0	6,7	20,0	0,5	0,4	0,3
15	230	60	30	10	3,8	7,7	23,0	1,0	0,5	0,4
16	240	50	25	8	4,8	9,6	30,0	1,2	0,6	0,5
17	190	40	15	7	4,8	12,7	27,1	1,2	0,8	0,4
18	200	50	20	8	4,0	10,0	25,0	1,0	0,6	0,4
19	260	90	50	15	2,9	5,2	17,3	0,7	0,3	0,3
20	180	40	25	10	4,5	7,2	18,0	1,1	0,5	0,3
21	200	50	30	15	4,0	6,7	13,3	1,0	0,4	0,2
22	100	30	10	3	3,3	10,0	33,3	0,8	0,6	0,5
23	175	40	20	6	4,4	8,8	29,2	1,1	0,5	0,5
24	230	70	30	7	3,3	7,7	32,9	0,8	0,5	0,5
25	170	30	5	2	5,7	34,0	85,0	1,4	2,1	1,3
26	140	20	8	4	7,0	17,5	35,0	1,8	1,1	0,5
27	150	25	12	8	6,0	12,5	18,8	1,5	0,8	0,3
28	190	30	15	7	6,3	12,7	27,1	1,6	0,8	0,4
29	170	20	10	6	8,5	17,0	28,3	2,1	1,1	0,4
30	180	40	12	7	4,5	15,0	25,7	1,1	0,9	0,4
mean	**205,5**	**50,7**	**23,8**	**8,1**	**4,6**	**11,0**	**29,3**	**1,1**	**0,7**	**0,5**

Table 31. Inverse square law validation

The Table 31 presents inverse square law validation for all patients at the day of discharge from hospital. Ratios were calculated with respect to that at 0.25 m.

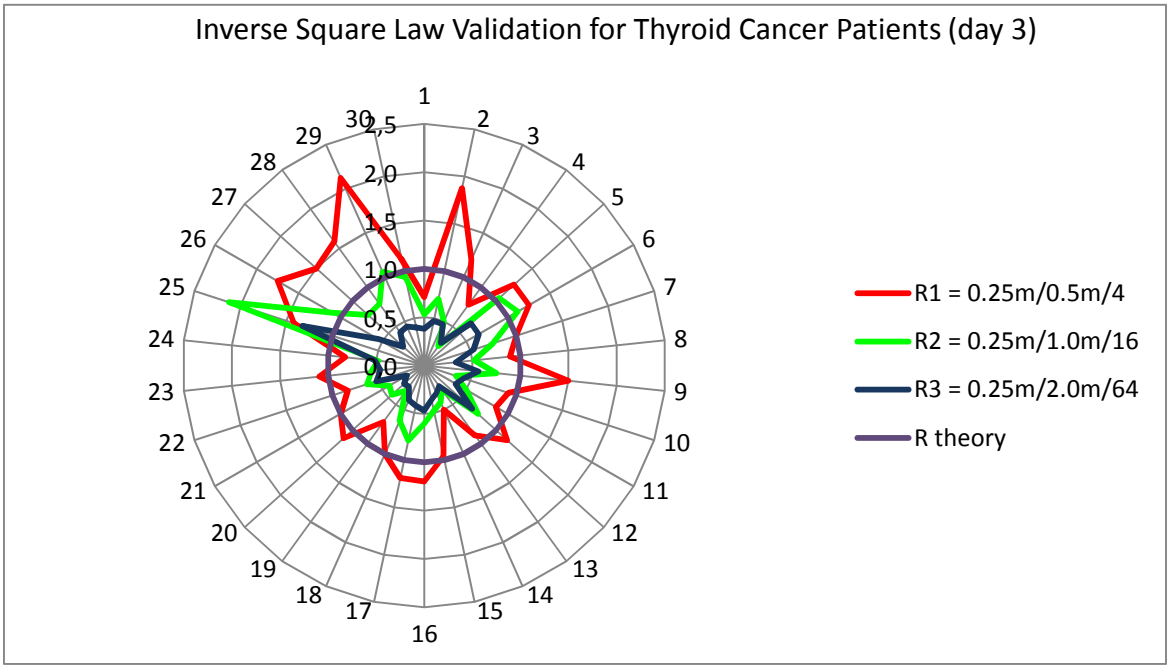

Graph 26. Inverse square law validation of dose rate for thyroid cancer patients

The mean value of dose rate at 0.25 m, 0.5 m, 1.0 m and 2.0 m was 205 μSv/h, 50.7 μSv/h, 23.8 μSv/h and 8.1 μSv/h.

Very little data has been published regarding the exposure rates near patients receiving diagnostic levels of radiopharmaceuticals, as concerns are generally lower. There are also not so many publications about dose rates from radioiodine therapy and other used radiopharmaceuticals. From the several published papers the findings confirm that calculated values from nuclear medicine patients produces significantly overestimated of real dose rates.

A study by author Yanling Yi et al. [94], from 2013 confirm the findings to others that the use of an unshielded point source method to model exposure rates near nuclear medicine patients produces significant overestimates of the real dose rates. For ^{131}I cancer patients, who typically have very small thyroid remnant uptakes and thus activity mostly distributed uniformly throughout the body, the exposure rates are overestimated by a factor of about three at 0.3 m and about two at 1.0 m. When using point source model with the appropriate factor, the model provides reasonable data for determining patient release criteria.

4.6 Results of calculated values of dose equivalent rate, effective dose and risk for different organs using MCNP 4b

By application of MCNP4b software, the absorbed energy in the most exposed organs as a consequence of ^{131}I solution/capsule retaining in the stomach has been calculated. Calculated values for imported energy per transformation for different organs are given in Table 32

Organ	Imparted energy (MeV)		
	Gamma	Beta	Gamma-Beta
Bone surface	6.02×10^{-3}	0	6.02×10^{-3}
Stomach	11.48×10^{-5}	2.59×10^{-1}	2.59×10^{-1}
Colon	8.35×10^{-3}	6.25×10^{-6}	8.35×10^{-3}
Kidneys	2.26×10^{-4}	0	2.26×10^{-4}
Liver	5.94×10^{-4}	8.88×10^{-7}	5.95×10^{-4}
Lungs	6.53×10^{-5}	2.48×10^{-7}	6.56×10^{-5}
Testes	2.02×10^{-4}	0	2.02×10^{-4}
Bladder	12.82×10^{-4}	0	12.82×10^{-4}
Skin	4.52×10^{-4}	0	4.52×10^{-4}

Table 32. Imparted energy per transformation for different organs

The dose equivalent – (radiation weighting factor equal unity) in different organs are calculated and presented in the Annex 3. for the capsule and solution activity of 185 MBq up to 6 105 MBq during 15 min of retaining in the stomach.

Using the tissue weighting factors, w_T [56], and calculated dose equivalent, the effective dose for different organs has been calculated and the results are presented in the following Table 33.

Organ	Quantity		
	Density(g/cm^2)	Volume (cm^3)	Dose per transformation (Gy)
Bone surface	1.40	2500	2.75×10^{-16}
Stomach	1.04	130	3.07×10^{-13}
Colon	1.04	331	3.88×10^{-15}
Kidneys	1.04	260	1.34×10^{-16}
Liver	1.04	1300	5.73×10^{-17}
Lungs	0.30	2800	1.25×10^{-17}
Testes	1.04	26	1.19×10^{-15}
Bladder	1.04	40	4.93×10^{-15}
Skin	1.04	1058	6.57×10^{-17}

Table 33. Calculated values of dose equivalent in different organs

The calculations were performed for all activities used in radioiodine diagnostic and therapy. The lowest value was 185 MBq; activity used for whole body scan, and the maximums delivered dose was 6105 MBq for thyroid cancer therapy. The values of effective doses for stomach and other organs around the stomach such as skin, lungs, liver, colon, bladder and ovary, gonads are presented in Graph 27. In the Graph 28 are given the compared values for 1 minute and 15 minutes for ovary, gonads.

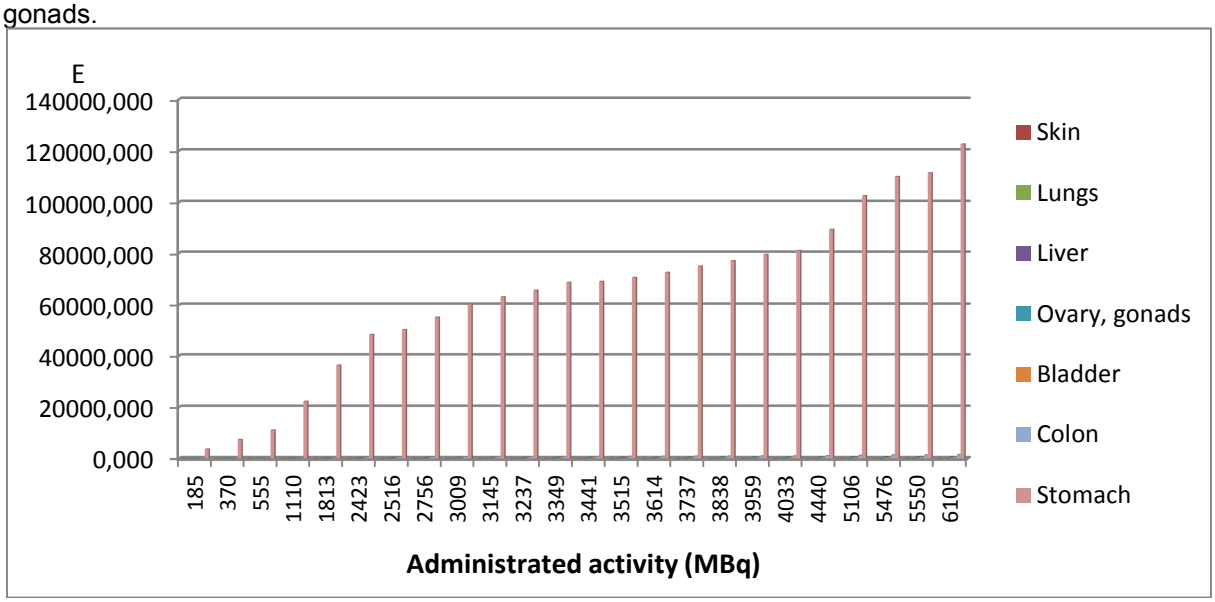

Graph 27. Effective doses

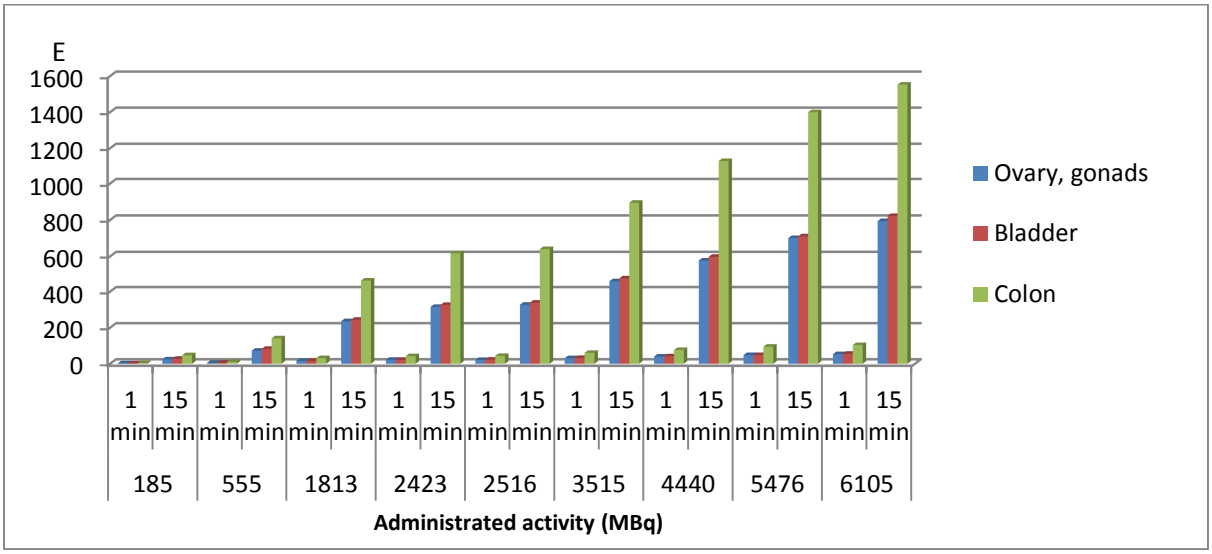

Graph 28. Comparison of effective doses for given activity for one and 15 minutes

The calculated results are for administered activity from 185 MBq up to 6105 MBq, and for the time of absorption of 1 minute and 15 minutes. The total number of histories during the simulation was one million. Due to sphere symmetry estimated uncertainties for calculation of local stomach doses are less than 0.1%, and they are negligible. The relative uncertainty of simulation for all results was not higher than 5%. The normal Gaussian probability distribution is applied on uncertainty determination. Considering the number of histories obtained uncertainties of Monte Carlo calculations of energy imparted in organs (MeV per disintegration) are acceptable.

The lowest effective dose is received by Skin, Lungs and Liver. The results are given in Table 32 and on the Graph 29, also the results are presented in Annex 2.

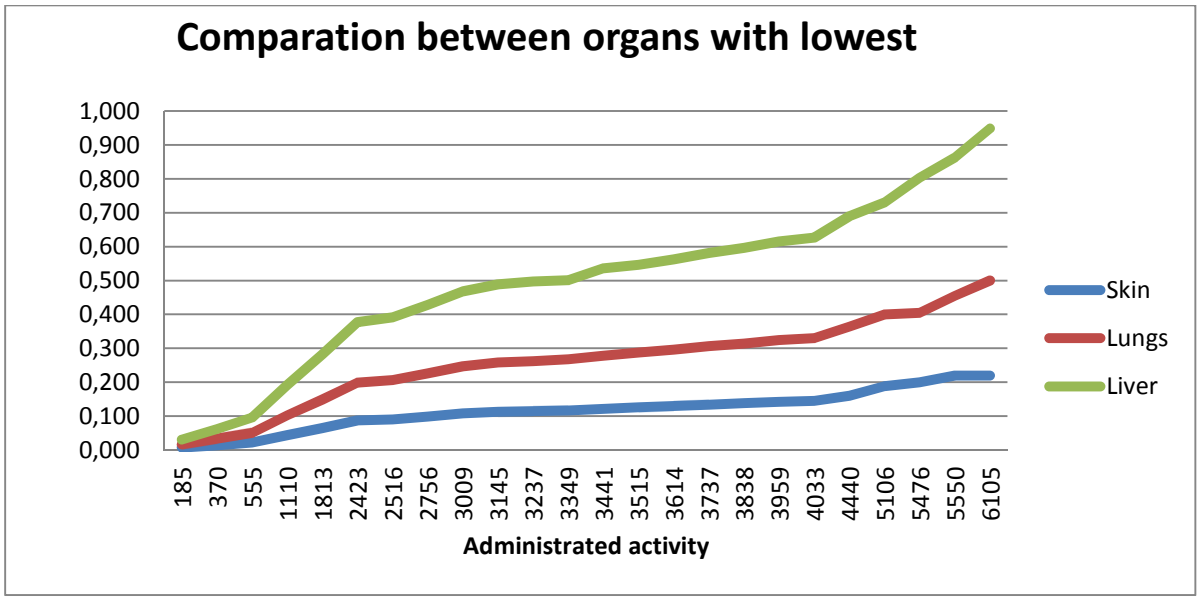

Graph 29. Effective doses for Skin, Lungs and Liver

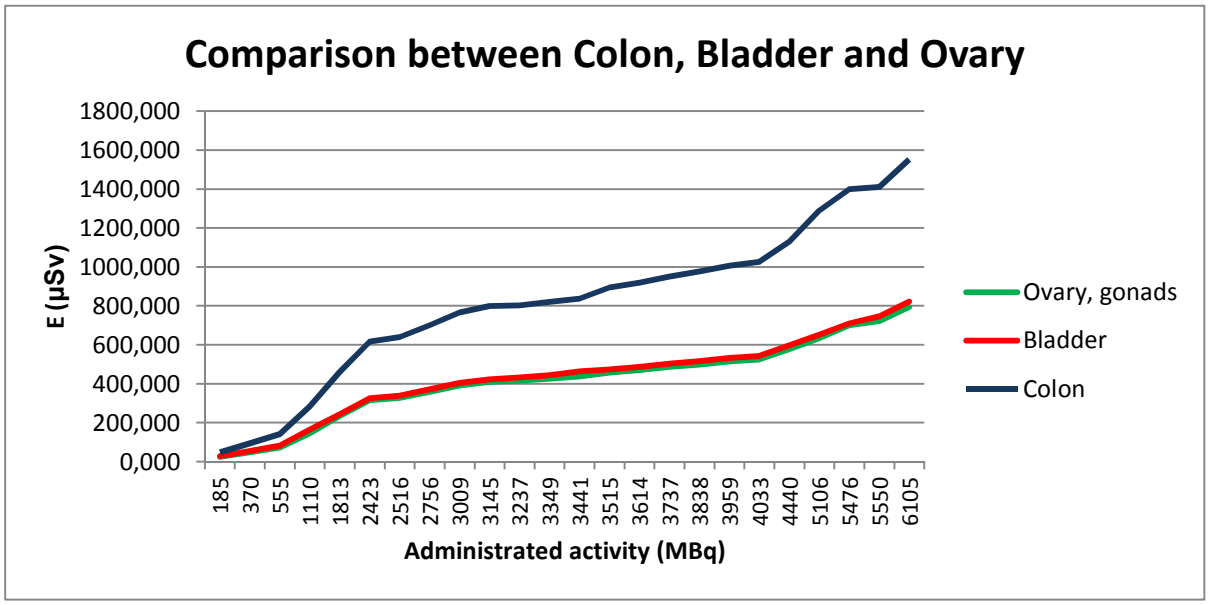

Graph 30. Effective doses for Ovary, gonads, bladder and colon

The Graph 30 shows that ovary and bladder receive approximately the same effective doses, while from this group the effective dose for colon is much higher., For the maximum, given activity 6105 MBq, colon receives maximum effective dose.

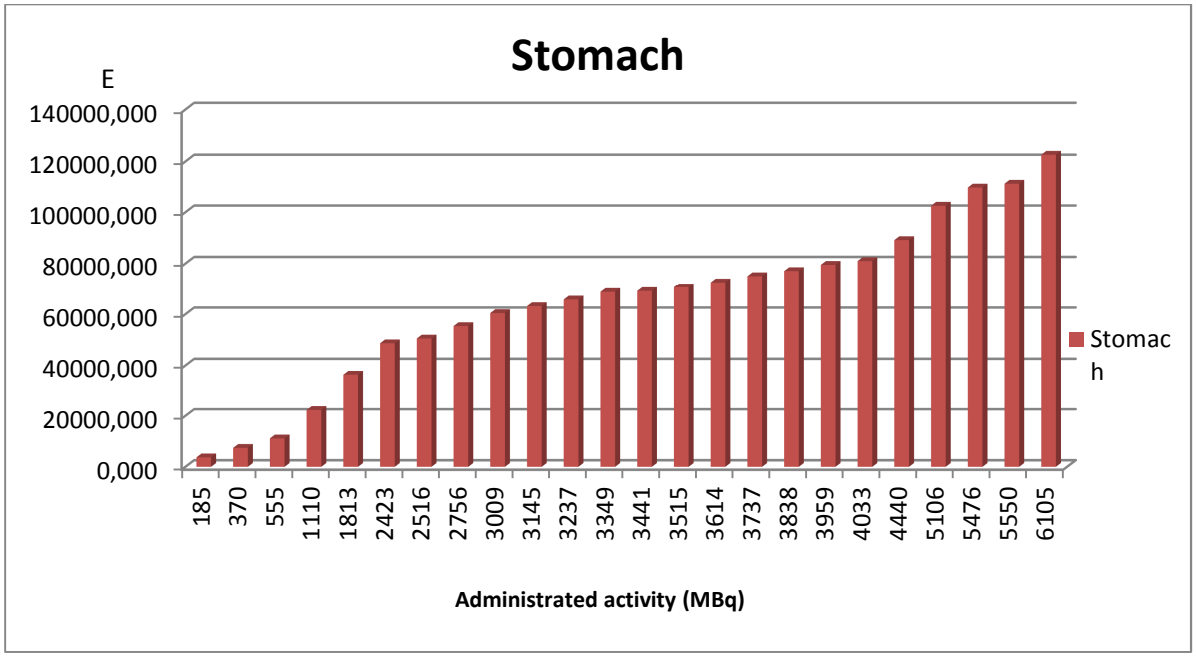

Graph 31. Effective doses for stomach

Normally the effective dose from radioiodine is completely dominated by the absorbed dose to the thyroid. Under certain circumstances, however, the uptake in the thyroid may be very small, and in these cases the absorbed dose due to iodide taken up in the stomach may be of more interest. A

diminished thyroid uptake may be e.g. a result of thyroid blocking or surgical removal of the gland. Recent biokinetics models for radioiodine [100, 72,101] include the stomach wall as a compartment where an increased concentration of iodine can be seen shortly after intake. Assuming that the residence time in the stomach is 15 to 30 minutes, the absorbed dose to the stomach increases by at least 30% for ^{131}I [102]. The dose to the stomach wall is a factor of 2-3 higher if the source is located entirely within the wall itself compared to when it is found only in the contents. Assuming that the uptake in the stomach is located to the wall, we performed all calculations using Monte Carlo simulation as an input parameter. We simulate the situation in the very first one minute and 15 minutes after radioiodine administration when the thyroid uptake has not yet started.

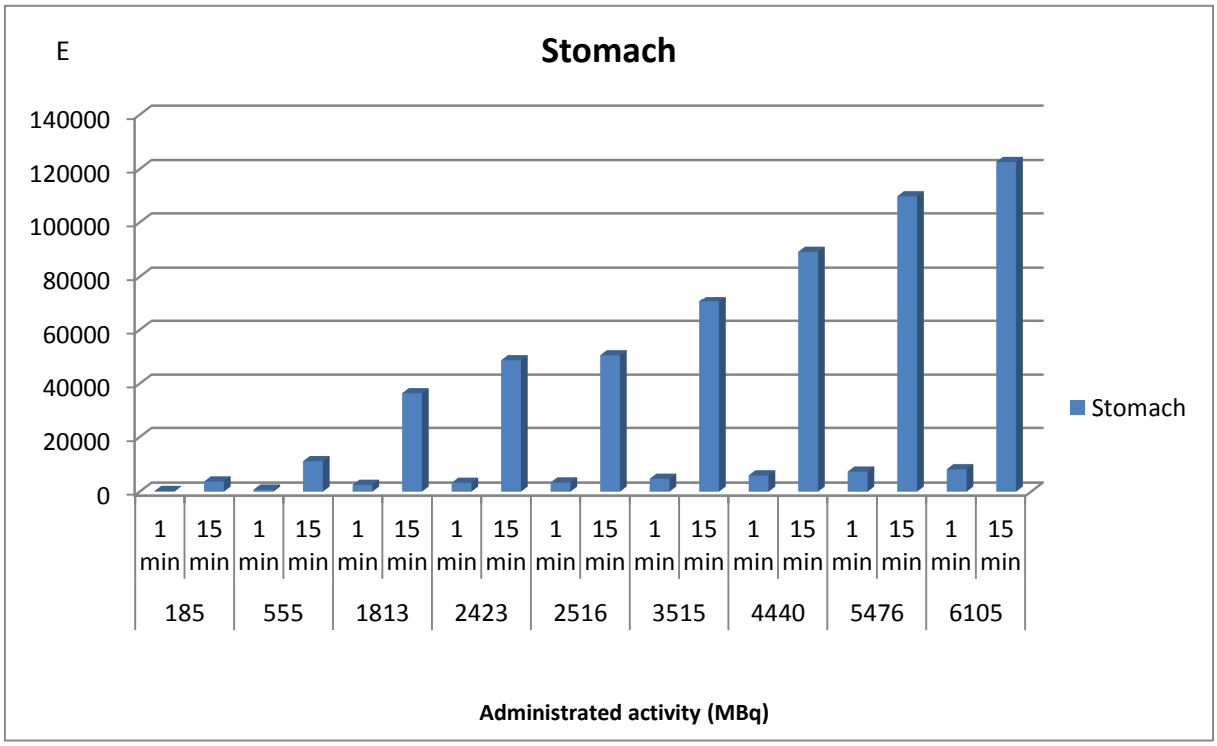

Graph 32. Compared values for 1 and 15 minutes, stomach

The highest stomach doses were expected concerning the beta-gamma nature of ^{131}I decay. The beta particles and secondary electrons created into interaction of gamma rays deposit their energies in short path-lengths. These energy depositions result in absorbed doses to the stomach in which the radionuclide is localized and to organs in its vicinity. Taking into account all of these we performed the calculation for both beta and gamma emission [102]. The investigation and calculations were started with the assumption that the values of additional effective doses of risks during the 15 min of ^{131}I capsules retaining in the stomach before their absorption are not negligible neither for stomach wall neither surrounding organs. This fact was the main reason for our prediction about the necessity of a precise dose and additional risk estimation. Obtained results indicate that the values of local doses in the stomach wall could not be ignored.

4.6.1 Calculated risk

From clinical practice, it is obvious that radioiodine therapy is safe and that the level of risk is smaller than that of other therapeutic modalities routinely used in oncology (external beam radiotherapy and chemotherapy). But also it is very important to support this impression with indisputable data. While the risk is obviously small, fear of the unknown is the worst enemy of the medical use of radionuclides. The accurate and objective evaluation of risk is thus an important primary task of nuclear medicine community. The most common acute complications of ^{131}I therapy radiation thyroiditis, gastrointestinal discomfort and nausea, xerostomia are usually mild and self-limiting. Among the late effects permanent myelosuppression and pulmonary radiation fibrosis are dose dependent, and thus only the minority of patients treated with very high cumulative doses is at risk. In contrast to these risks, the potential hazards from ^{131}I therapy which have the greatest impact on the decision to utilize this modality are the induction of second tumors [103, 104] and genetic damage [105]. These are considered to be stochastic effects with no threshold; virtually every patient treated with any dose of ^{131}I is exposed to some potential risk. In such cases, it is necessary to ensure that the risks of the radiation are less than from the disease itself [102]. For stochastic effects, the probability of their occurrence is believed to be proportional to the dose (linear dose effect relationship in the low dose/low dose rate range). Therefore, the probability of their induction should be reduced as far as possible by keeping the dose as low as possible. Epidemiological studies report a higher incidence of stomach cancer in patients receiving ^{131}I. After higher activities, typically those used in the treatment of thyroid malignancies, an increased incidence of leukemia has been observed. There may also be a small increase in bladder and breast cancers. Radiation doses to specific organs which may not be the target organ of therapy can be influenced significantly by the pathophysiological changes induced by the disease process.

Incidence of secondary malignancies and leukemia might increase with higher doses. A Swedish report found that organs that were estimated to have received more than 1 Gy had a significantly increased risk of subsequent malignancy [104]. They studied a cancer risk for 834 patients with an average dose of 4551 MBq. A dose related increased risk of cancer was observed. For patients receiving the dose of less than 1850 MBq, there was no significantly elevated risk of subsequent malignancy [104].

From this aspect, it was very important to compare the effective doses for stomach and surrounding organs for different nine values of administered activities. In the Table 34, are presented calculated risks for bladder, colon and ovary compared with the risk for stomach. The risk is calculated for one and fifteen minutes and forgiven different activities. Our results show that the stomach has the highest risk among the other organs. From statistical analysis the correlation coefficient (r) among the estimated risk was found to be very significant ($p<0,00001$) for stomach-bladder, stomach-colon and stomach-ovary.

The study from Ahmed S. et al. indicates that the significant uptake of radioiodine by stomach of thyroid cancer patients carries additional risks of probabilistic fatal occurrence in this organ compare to other organs. These warrants long-term follow up of thyroid carcinoma patients.

MBq	Time (min)	**Bladder**	**Colon**	**Ovary, gonads**	**Stomach**
185	1 min	1.00×10^{-9}	0.90×10^{-7}	0.80×10^{-8}	0.024×10^{-3}
	15 min	0.149×10^{-7}	0.131×10^{-5}	0.120×10^{-6}	0.340×10^{-3}
555	1 min	3.01×10^{-9}	2.64×10^{-7}	2.43×10^{-8}	0.08×10^{-3}
	15 min	0.448×10^{-7}	0.396×10^{-5}	0.362×10^{-6}	1.022×10^{-3}
1813	1 min	1.007×10^{-7}	7.54×10^{-7}	7.92×10^{-8}	0.24×10^{-3}
	15 min	1.465×10^{-7}	1.112×10^{-5}	1.176×10^{-6}	3.337×10^{-3}
2423	1 min	0.14×10^{-7}	0.11×10^{-5}	0.11×10^{-6}	0.31×10^{-3}
	15 min	1.959×10^{-7}	1.487×10^{-5}	1.572×10^{-6}	4.461×10^{-3}
2516	1 min	0.14×10^{-7}	0.11×10^{-5}	0.12×10^{-6}	0.32×10^{-3}
	15 min	2.033×10^{-7}	1.544×10^{-5}	1.632×10^{-6}	4.631×10^{-3}
3515	1 min	0.21×10^{-7}	0.16×10^{-5}	0.16×10^{-6}	0.46×10^{-3}
	15 min	2.841×10^{-7}	2.157×10^{-5}	2.281×10^{-6}	6.471×10^{-3}
4440	1 min	0.25×10^{-7}	0.19×10^{-5}	0.25×10^{-6}	0.58×10^{-3}
	15 min	3.588×10^{-7}	2.724×10^{-5}	2.880×10^{-6}	8.172×10^{-3}
5476	1 min	0.31×10^{-7}	0.23×10^{-5}	0.24×10^{-6}	0.74×10^{-3}
	15 min	4.385×10^{-7}	3.309×10^{-5}	3.470×10^{-6}	10.079×10^{-3}
6105	1 min	0.34×10^{-7}	0.26×10^{-5}	0.27×10^{-6}	$\mathbf{0.76\times10^{-3}}$
	15 min	4.934×10^{-7}	3.746×10^{-5}	3.960×10^{-6}	$\mathbf{11.237\times10^{-3}}$

Table 34. Total risk

In general there are no reports of an increased risk of neoplasias, genetic damage or infertility with the doses used in hyperthyroidism. Doses obtained for 1813 MBq do not have a significant impact in risk assessment. Also calculated risk for one minute even for higher values of administered activity also are not significant. Since 1946, millions of adults have been treated with ^{131}I, without an increase in cases of leukemia or other forms of cancer. In addition, no increased risks of congenital malformations in children of treated parents have been reported.

ICRP 60 suggests that, in the case of internal exposure, the annual limits on intake based on a committed effective dose equivalent of 20 mSv will be ensured so that the lifetime dose equivalent in any single organ must not exceed 20 Sv, which is sufficient to avoid deterministic effects in unspecified tissues and organs [125].

From the distribution of probabilities of fatal sites, specific cancers for male and female over age 0-90 y for four countries (Japan, US, UK and Puerto Rico) the average factor was found to be maximum for stomach (0.225) over other organs [ICRP 60].
The risk coefficients are presented in Table 35

Organ	Risk coefficient $[10^{-2}Sv^{-1}]$
Bladder	0.30
Bone surface	0.05
Colon	0.80
Liver	0.15
Lungs	0.85
Ovary, gonads	0.10
Skin	0.02
Stomach	1.10

Table 35. Risk coefficient

The use of Monte Carlo calculations allowed this task to be completed successfully, which have been extremely complicated with conventional mathematics due to the complex geometries.
Even though these doses were representative, there are some factors that must be considered. The approximate model of gastric, the time of 15 minutes for dissolving the capsule, biokinetics of radioiodine and determination of effective half life is individual and different for every patient. Than the size and shape of residual tissue of the thyroid also affects the absorbed dose to other organs.

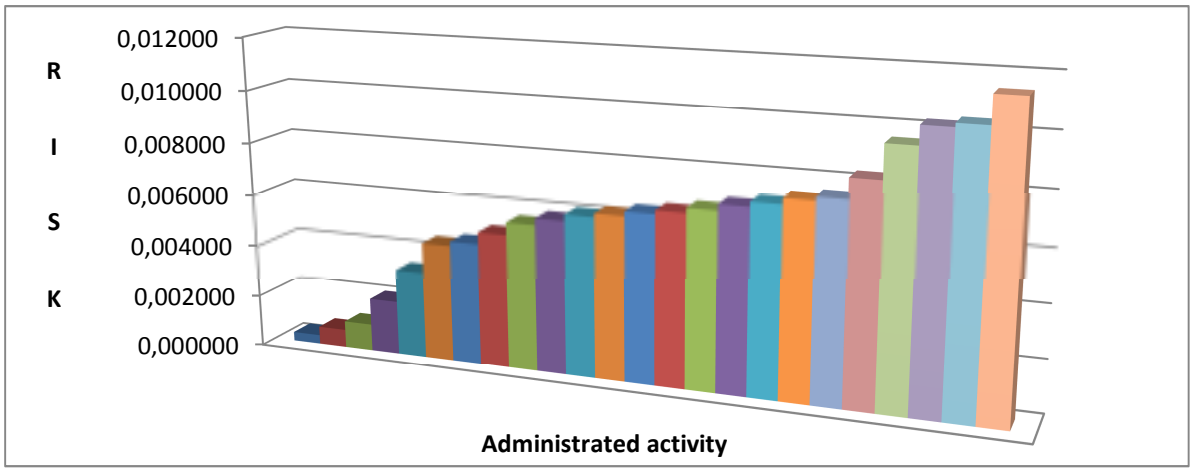

Graph 33. Risk according administered activity

Presently, health effects are neither a concern to the patients, nor to the physicians because of the overall effect in treating tumors. Although there may be a risk of getting secondary cancers over many decades, this therapy is generally preferred over the certainty of dying from thyroid cancer. If thyroid cancer occurs during the later years of individual's life, the probability of adverse health effects from this treatment would not be a major concern for the patients, especially because the treatment is very effective, and it will increase the years of life of the patients. But in the latest years our findings are that thyroid cancer occurs at very young population aged below 16. So in these cases it is of great importance to estimate the risk of getting fatal cancer. However, risk assessment can be performed by considering the risk of getting secondary cancer and risk coefficients provided by the International Commission on Radiation Protection (ICRP 1990). Using these coefficients and the calculated doses to each of the organs, the risk of getting fatal cancer can be calculated for each organ as well as for the individual. Because the energies emitted were due to photons, the dose is equal to the dose equivalent. The radiation weighting factor is one, so one Gray equals 1Sievert (Sv).

There are several epidemiological studies that reports that it appears to be no risk of cancer from radioiodine therapy [118]. There are factors in the studies that might have an effect on the results:

- The patients were followed less than 15 years, which might not be long enough to develop cancer.
- The absorbed dose calculations were based upon the model, usually ICRP Publication 53, and not the individual biokinetics data. For example, the absorbed dose to the red marrow is 50 % overestimated in average, using ICRP Publication 53.
- The age limit for radioiodine treatment is lowered. More young people, women of childbearing age and even children are prescribed radioiodine therapy today [119].

In a study by Franklyn et al. [118] the relative cancer mortality was decreased after radioiodine therapy, but there was a significant increase and mortality for cancer in the small intestine and a positive association between bladder cancer incidence and cumulatively administered activity ^{131}I.

In another study by Holm et al.1991 [111], an elevated risk for stomach, kidney and brain cancer was seen. The risk for stomach cancer increased with dose although it was not statistically significant. These findings are in accordance with our investigations. The incident of thyroid carcinoma is higher in patients with Graves' disease treated with antithyroid drugs than in patients treated with radioiodine or surgery. The explanation might be that more thyroid tissue is persistent after drug treatment than after radioiodine treatment or surgery [108].

The cancer risk has also been estimated using biological dosimetry [120]. Micronuclei originate when radiation disrupts the DNA and chromosome fragments fail to incorporate in the nucleus during next cellular division. The number of micronuclei in blood lymphocytes after ^{131}I-iodide therapy was

studied, and the cancer mortality was estimated to less than 1%. The patients studied though were all over 40 years.

Thirty years ago radioiodine therapy was less attractive in younger and fertile patients due to the potentially higher risk of secondary malignancies. Today after several papers indicating no risk of cancer after ^{131}I-iodide therapy, young people and even children are more likely to receive the therapy. A higher risk for thyroid cancer has been seen in children after the Chernobyl accident and the increase of thyroid cancer is seen in the children that were born or in the fetal stage at the time of the accident [121]. For childhood leukemia, no such increase has been seen [122].

In 1962 twenty six institutions, 25 in the United States and one in the United Kingdom performed prospective follow up of the hyperthyroid patients treated with radioiodine with activity (from 70 to 600 MBq). Reports of the first results were based on follow up of approximately 22, 000 patients treated with radioiodine and 14.000 patients treated with antithyroid drugs. The results revealed a small increase in leukemia in ^{131}I subjects when compared to age matched U.S rates, but the rates in the ^{131}I- treated patients were less than those observed in the surgically treated patients [106, 107]. A high rate of hypothyroidism was seen in all groups of treated subjects, regardless of therapy; there was a strong relationship between the amount of ^{131}I activity and the frequency of hypothyroidism. The study clearly demonstrated the importance of inclusion of an appropriate comparison group; because without it a small leukemia increase observed would have been attributed to the then estimated 50 to 100 mGy, marrow dose from ^{131}I rather than to thyrotoxicosis. Additional information was gathered on the frequency of benign and malignant thyroid neoplasm [108]. No evidence of an increase in malignant thyroid tumors was observed when disease observed in the first 5 years of follow – up was excluded. By excluding these 5 years, the co-occurrence of already present thyroid cancer, was not attributed to the ^{131}I therapy. In 1974, 497 nodules were present when the paper by Dobyns et al. was published [108]. The charts of these patients were reviewed in the mid -1980s by the physicians at the four largest centers, and more than 95% of the cases were instances in which one reviewer noted a nodule, which was not subsequently noted in the patient's chart. As a result to limited information on the biological turnover of ^{131}I in the subjects in the original thyrotoxicosis therapy study, organ doses could not be estimated, and therefore administered activity, was used as a measure of exposure. The amount of activity administered in single doses ranged from <185 MBq to >555 MBq. Assuming 25-50% uptake in adults and given a mean activity of 330 MBq of ^{131}I administered to the patients who developed leukemia. The bone marrow dose is estimated using ICRP data to lie between 13 and 67 mGy. A later follow-up of cancer mortality was conducted on this same patient population [109]. The study showed that the total number of cancer deaths was close to that expected based on mortality rates in the general population (2950 compared to 2857), but there was a small excess of mortality from cancers of the lung, breast, kidney and thyroid. A deficit of deaths was noted for cancers of the uterus and the prostate gland. Radioactive iodine was not linked to total cancer deaths or to any specific cancer with the exception of thyroid cancer, however, thyroid

cancer risk was not elevated when the first 5 years of follow-up were excluded. While this study does not provide compelling evidence for an association between ^{131}I therapy given to adult patients and thyroid cancer mortality, it should be noted that because thyroid cancer is rarely fatal, mortality is not good measure of effects of ^{131}I on the thyroid gland [107].

While a British study of hyperthyroid patients found a small but significant increased risk of thyroid cancer incidence and mortality among ^{131}I treated patients [110], another Swedish study reported that the risk of thyroid cancer was not significantly elevated 10 or more years after treatment [111, 112].

Thyroid cancer risk also has been examined in cohorts of patients treated with iodine for diagnostic purposes. No significant excess risk of thyroid cancer were examined for reasons other than a suspected thyroid tumor, even the mean doses at thyroid are about 0.9 -1 Gy [113, 114, 115, 116]. In most recent follow-ups of hyperthyroid patients, neither leukemia risk nor other malignancies have been significantly linked to ^{131}I therapy and the doses to organs other than thyroid are quite low.

The thyroid doses for cancer therapy are extremely high with the aim of killing all of the cells in thyroid tissue. The doses to other organs are generally small. In a follow up of Swedish thyroid cancer patients treated with ^{131}I the red bone marrow dose was estimated to be about 251 mGy. Cohort study in three European countries (Sweden, France and Italy) was conducted. The meanly administered activity was 6 (0.2-56) GBq. The risk of leukemia was elevated, but it didn't reach statistical significance (RR= 1.9; 95% CI=0.8-3.6) GBq. There was also suggestive evidence of an increased risk of cancers of the salivary gland, bone and soft tissue and uterus. No evidence of genetic effects in the offspring of women treated with ^{131}I for thyroid cancer has been detected, but the recommendation that conception is delayed for 1 year after therapy is still advocated.

It is generally agreed that no evidence of significant germ cell damage has been noted among subsequently conceived offspring of treated hyperthyroid patients. Gonad damage and transiently impaired fertility may occur occasionally among thyroid cancer patients treated with much larger amounts of iodine ^{131}I.

4.6.2 Future work

Although this research involved the use of actual thyroid therapy cases, they do not necessarily represent the exact doses the patients are receiving due to geometric factors and distances and sizes of the organs. Because of these factors, there is a recommendation for future work. Patient monitoring during first twenty four hours of administering radioiodine is very important, because most of the administered radioiodine is excreted during this period. Calculation of individual doses should be established. Collecting data about external exposure rate using GM counter is very well established

and recognized method of measuring distribution and tracer uptake inside body, and it should be continued and implemented in routine.

4.7 Results of external TLD measurements on the surface of the skin above gastric region

The measurements over the skin above gastric region were performed by using TLD. In the Table 36 are presented results from the measurements. The measurements were performed for a limited time of fifteen minutes and the period of stay in hospital of 3 and 4 days. All patients were female, aged (17 up to 67) mean 47.6.

Pat. No	MBq	15 min (mSv) Hp(0.07)	3 days (mSv) Hp(0.07)	Type	f/m	age
1	3589	3.55	76.45	pap	F	50
2	3552	3.72	83.23	pap	F	17
3	3145	2.61	60.96	pap	F	45
4	2960	2.1	91.42	pap	F	43
5	5550	4.93	157 (4day)	pap	F	17
6	1850	0.95	39.4 (24h)	pap	F	48
7	3700	4.11	95.33	pap	F	55
8	3711	4.32	94.25	pap	F	60
9	3700	2.60	82.8	pap	F	45
10	3552	11.98	195	pap	F	56
11	3700	4.24	92.5	pap	F	62
12	3589	3.20	93.34	pap	F	54
13	3552	3.80	94.87	pap	F	67
14	3700	4.64	97.34	pap	F	50
15	3700	4.57	94.32	pap	F	46
Mean	**3570**	**4.36**	**96.54**	pap	F	**47.6**

Table 36. External TLD measurements

The meanly administered activity was 3570 MBq. Estimated value of Hp (0.07) for fifteen minutes was 4.36 mSv, and for all period during the hospitalization of patients was 96.54 mSv. These results give useful information about the values of effective doses measured over gastric and total effective dose during the hospitalization of the patients. The minimum value of effective dose was estimated at patient who was treated with 1850 MBq and the patient was hospitalized only for one day, while the maximum was estimated at 195 mSv. These investigations from radiation protection of view are of great importance. From gained results, we could conclude and confirm that thyroid cancer patients

after receiving radiotherapy should stay hospitalized for several days. Otherwise, they could deliver high effective dose if someone is in their close proximity.

Collecting data about external exposure rate using GM counter is very well established and recognized method of measuring distribution and tracer uptake inside body, and it should be continued and implemented in routine practice.

4.8 Results from environmental measurements of released concentration of iodine in sewage system

Patients, when treated with ablation doses of ^{131}I, are confined in a hospital for a few days to allow external radiation levels to decline to acceptable levels before release. The relatively rapid decline in activity is due primarily to the biological elimination of ^{131}I from the body. Elevated concentration of ^{131}I has been observed in the air nearby waste water following the application of therapy doses [95, 96]. The release limit for radioactive waste liquid according EU rules is 1 Bq/ml or 1000 Bq/l. The authorized limit dose air concentration is 400 Bq/m^3. The measurements were performed in case one when only one patient was hospitalized and the case two when in the room were treated two patients. The result from the probe was taken for the period of three days during their stay at hospital. Elevated concentrations of ^{131}I have been observed in air for the period of three days after administration of the therapy. The higher concentration was registered during first 24 hours. That is the time that 80% of activity is released in this period. The estimated doses are below the limit proposed by EU regulative.

Case	MBq	1 day Bq/m^3	2 day Bq/m^3	3 day Bq/m^3
Without patient	0	15	-	-
One patient	3700	150	95	25
Two patients	2 X 3700	320	170	43

Table 37. Results from environmental measurements

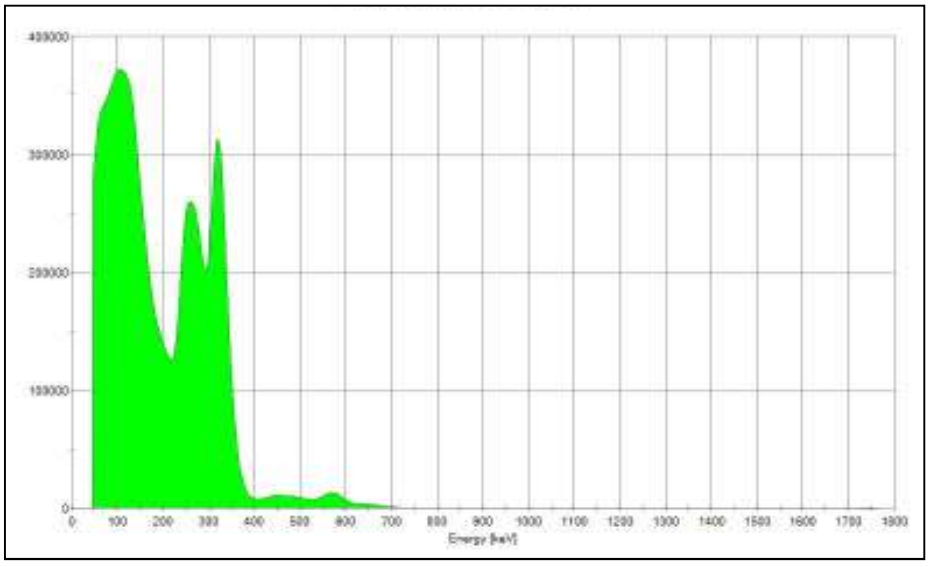

Graph 34. Energy spectrum of detected radionuclide by probe

Chapter 5

5. CONCLUSIONS

The development and use of radioactive isotopes of iodine have improved medical care substantially. Many clinical applications were an outgrowth of the development of the technology and the biological knowledge it engendered. Concern regarding the safe and effective use of radiation in medicine led to the development of standardized procedures and methods for calibrating the amount of activity administered to patients. This included much attention to quality control of the radionuclides administered, their chemical and radionuclide purity, and their stability in the body.

^{131}I is well used radionuclide for the treatment of both hyperthyroidism and differentiated thyroid cancer. It is well tolerated, simple to administer and has been proved in multiple follow up studies to be safe and effective. Regulations for the use of radioiodine remain extremely variable throughout the world, although there is a general acceptance of the basis radiation protection measures.

In latest years, there are developed dosimetry systems for intake of radionuclides. These systems evolved from simple mathematical models to complex computer based systems that provide high accuracy. These methods are in routine use, in all major medical centers. With these tools, many investigations have led to the publication of high – quality data on radiation dose to patients, to workers and to the public from environmental releases of many radionuclides. ^{131}I has received the greatest emphasis because of its unique applications in medicine [107].

In this study were performed external dose rate measurements of sixty patients and based on the gained results we can conclude the following:

1. The hyperthyroid patients are discharged from hospital with higher dose rate than the thyroid cancer patients, especially the group of patients treated for autonomous functioning thyroid adenoma. They should continue to be treated on out - patient basis, because it has several advantages: lower health costs, lower doses to nursing staff and psychologic benefits for patients and family members. Emphasizing adherence to the new written instructions for radiation protection is very important.
2. The thyroid cancer patients were released according dose rate measurements at third day with dose rate less than 8 μSv/h, at a distance of 2.0 m. During the three day stay in the hospital room, it is considered that the distance of 2.0 m from the patient could reduce the occupational exposure to nurse, physicist and physician who enter the room to visit treated patients. Also reducing the time of stay near the radioactive patient will reduce the effective doses to the other person and will improve better radiation protection.
3. Radiation dosimetry deals with the determination of the amount and the spatial and temporal distribution of energy deposited in matter by ionizing radiation. Internal radionuclide radiation

dosimetry specifically deals with the deposition of radiation energy in tissue to a radionuclide within the body. However unlike external radiation dose which can be often measured, internal radiation dose must be calculated. These procedures have evolved over more than 60 years from relatively simple approaches to those with a high level sophistication. Internal dosimetry has been applied to the determination of tissue doses and related quantities for occupational exposures in radiation protection, and diagnostic and therapeutic exposures in nuclear medicine. In this study by using MCNP 4b method were determined internal effective doses of several internal organs.

From the current investigation, the most exposed organ in this created model was stomach. The value of extra effective dose due to 1 minute solution and to 15 minutes $Na^{131}I$ therapeutic capsules staying in the stomach from the current official radiation protection point of view is significant. This warrants long term follow up of such patients.

The Monte Carlo method is considered to be the most accurate method presently available for solving radiation transport problems. It is very useful and unique method for the dosimetry of internal organs which is impossible to be calculated with any other method. It is extremely expensive computationally, because this method should simulate individual particles and simulating the average behavior of the particles in the system. For complex problems that the probability is small that a particle will contribute to the interest region, some form of variance reduction must be applied to reduce required computer time to obtain the results with sufficient precision

From the gained results, the effective dose equivalent is intended to be directly proportional to the risk from the exposure. The investigations were started with the assumption that the values of additional effective doses of risks during 15 minutes of ^{131}I capsules retaining in the stomach before their absorption are not negligible. Application of the solution has some advantages as the absorption in stomach wall is immediate but also has a lot of disadvantages. Capsules containing $Na^{131}I$ are widely used as they are more comfortable for administration and there is less possibility for local contamination of the patient and medical staff. During that time a large amount of radioactivity needlessly expose a part of a stomach and several surrounding organs. The significant uptake of radioiodine by stomach and urinary bladder of thyroid cancer patients carries additional risks of probabilistic fatal occurrences in them as compare to other organs. This fact was the main reason for our predication about the necessity of additional risk estimation. This warrants long term follow – up of such patients. Availability of risk estimates will help reduce psycho emotional distress for a patient.

4. According to the obtained results we recommended some corrections of the traditional concept of risk estimation in our hospitals and we emphasized the necessity to create the concept which is able to cover the higher risks under presented circumstances. We strongly

recommend the estimation of additional risks for each type of the procedure as a part of QA programs for $Na^{131}I$ capsules application. This investigation will become actual and important for the case of high doses administrated during radiotherapy treatments. We expect that estimated risks will be higher and therefore more significant for patient protection as well as for radiation protection in general. Risk assessment and effective dose estimation for wide range of administered activities of ^{131}I based radiopharmaceutical will give us a good basis for creation of suitable quality assurance and quality control programs in clinical practice. It also will enable design of appropriate programs for manufacturers and distributors of radiopharmaceuticals. Designed quality programs will be useful also for regulatory and accreditation bodies in the process of accreditation and radiation protection strategy.

We hope that the results of our investigation will improve safety culture in our health care system and also among authorities who make regulatory decision.

5.1 Team collaboration between patient, physician and physicist

The patient-physician relationship is a special one, involving trust, weighing and balancing of very significant decisions exposure of highly personal information. Decision about medical procedures and follow-up, use of medications, planning and lifestyle are very personal and often difficult. The role of physicist, who provide just one piece of information that physician must weigh and convey to his patient, is very peripheral, but nonetheless pivotal in the case of therapeutic use of radiation. These three individuals must work closely, however in this ongoing process to provide the highest quality medical care possible in every circumstance. Ultimately, the patient makes the final decisions about the progress of medical care and must be given the high quality information, clearly and unambiguously communicated by the physician and/or physicist.

It is very important that radiopharmaceutical therapy begin to involve the physicist more than it has in the past, as is modeled in external beam radiotherapy.

Chapter 6

REFERENCES

1. B.Karanfilski, D.Arsov, I.Tadzer; Iskustva vo lekuvanjeto na hipertireozata so radiojod 131, Godisen zbornik na Medicinski fakultet, VI.1959,113-115, Interna klinika i Institut za patofiziologija – Medicinski fakultet Skopje.

2. Briesmeister J: "MCNP – A general Monte Carlo N-Particle Transport Code, Version 4B", Report LA-12625-M. Los Alamos, NM; 1997.

3. Stabin MG. Fundamentals of nuclear medicine dosimetry, Springer, New York, 2008.

4. Dendy.P.P & Heaton. B.:(1999). Physics for Diagnostic Radilogy. 2nd edition Bristol Philadelphia:U.S.A: Institute of physics (IOP) Publishing. ISBN: 0-7503-0591-6

5. Klevenhagen, S.C.: (1993). Physics and Dosimetry of Therapy Electron Beams. Madison Wisconsin: Medical Physics (IOP) Publisher. ISBN: 0-944838-36-7.1993.

6. Friedell, H.L., Thomas, C.I.& Krohmer, J.S.: "Beta-Ray Applicationto the Eye woith the Descriptionof an Applicator Utilizing Sr90 and its Clinical use". Am. J. Ophtalmol. 33:525-535.

7. Donnald, T.G.;(1996) Principles of Radiological Physics. 3rd edition, New York;Churchill Living Stone. ISBN:0-4430-4816-9.

8. Johns, H.E. & Cunningham, J.R.: (1983) The Physics of Radiology. 4th edition. Springfield U.S.A: Chareles C Thomas, Chapter 3,5,13. ISBN: 0-398-04669-7.

9. Khan. F.M.:(2003). The Physics of Radiation Therapy. 3rd edition. Philadelphia U.S.A.: Lippincott Williams & Wilkonsin. ISBN: 0-7817-3065-1.

10.Podgorsak, E.B.; (2006). Radiation Physics for medical Physicists. Berlin Heilderberg New York: Springer. ISBN: 3-540-25041-7.

11. James, E.M.: (2006). Physics for Radiation Protection 2nd edition. Germany: Weinheim Wiley-VCH. ISBN: 3-527-40611-5.

12. IAEA: (2003). Review of Radiation Oncology Physics: AHandbook for Teachers and Students. Vienna Austria.

13. Cherry.S.R.,Sorenson. J.A.& Phelps, M.E.; (2003). Physics in Nuclear Medicine.3rd edition. Philadelphia U.S.A.; Saunders, ISBN: 0-7216-8341-X.

14. International Commission on Radiation Protection Publication: Release of patients after therapy with unsealed radionuclides. ICRP 94.pp.80, 2005, Elsevier, Oxford.

15. International Atomic Energy Agency, Safety Reports Series N0. 63 Release of Patients after Radionuclide Therapy, Vienna,2009.

16.H.R. Maxon, S.R. Thomas, R.C. Samaratunga, "Dosimetric considerations in the radioiodine treatment of macrometastases and micrometastases from differentiated thyroid cancer", Thyroid, 7(2):183-187,(1997).

17. C. Kobe, W. eschner, F. Sudbrock, I. Weber, k. Marx, M. Dietlein, H. Schicha. “Graves’ disease and radioiodine therapy: Is success of ablation dependent on the achieved dose above 200 Gy” Nuklearmedizin,47:14,(2007).

18. Maboe, D.P.A,: (2001). Radiation Detector Modelling with Monte Carlo N-Particle Code. Msc. Thesis, University of Limpopo (MEDUNSA).3-23.

19.International Commisssion on Radiological Protection. Radionuclide transformations-Energy and Intensity of Emissions. ICRP 38. Pergamon Press, Oxford, 1983.

20. Young, M.E.J; (1983). Radiological Physics. 3th edition. London;H.K. Lewis&CoLtd. ISBN:0-7186-0452-0.

21. Hamilton, J. Seaborg,G. (1939), Studies in iodine metabolism by use of a new radioactive isotope of iodine, Am J Physiol 127,557,1939.

22.Early PJ, landa ER. Use of therapeutic radionuclides in medicine. Health Phys 1995; 69(5):677-694.

23. Seidlin S, Oshry E, Yallow A. Spontaneous and experimentally induced uptake of radioactive iodine in metastases from thyroid carcinoma, J. Clin Endocrinol Metab. 1948;8:423-425.

24. B. Karanfilski, I. tadzer; Iskustva u testiranju tiroidne funkcije radijodom. Med. Glasnik XIV, 2a,1960, 126-131.

25. Nystrom E, Berg G, Jansson S, Lindstedt G, Torring O, Valdemarsson S, Warin B. Thyrotoxokos hos vuxna. ISBN: 91-630-7674-8, Ljungbergs Teyckeri AB, Klippan, Sweden, 1999.

26. Felliciano DV. Everything you wanted to know about Grave’s disease. Am J Surg 1992; 164(5): 404-411.

27. Reinwein D, Benker G, Konig MP, Pinchera Q, Schatz H, Schleusene A. The different types of hyperthyroidism in Europe. Results of prospective survey of 924 patients. J Endocrinol Invest 1988; 11(30:193-200.

28. Ingbar S.H. Braerman, L.E., Werner’s The Thyroid – A Fundamental and clinical Text, J.B. Lippincot Company, Philadelphia, 1986.

29.International Commisssion on Radiological Protection.Publication 30, Part 1, Limits for Intakes of radionuclides by Workers. Pergamon Prewss, Oxford, 1979.

30. G. Saha, Basic of PET Imaging – Physics, Chemistry and Regulation; Springer, 2004.

31. Kowalsky R. Perry J., Radiopharmaceuticals in nuclear medicine practice Appleton & Lange, Prentice Hall, Connecticut, USA, 1987.

32. Bernier D., Christian P., Langan J., Nuclear Medicine – technology and techniques; Mosby, 1993.

33. Kocher, David C., Radioctive Decay data tables, Springfield: National Technical Information Service, 1981 DOE/TIC-11026.

34. Kaplan, Irving, Nuclear Physics, New York: Addison-Wesley, 1964.

35. Ernest Mazzaferri, Clive Harmer, Ujjal K. Mallian Pat Kendall Taylor editors; Practical management of Thyroid Cancer.

36. International Commisssion on Radiological Protection. Publication 94: release of patients after therapy with unsealed radionuclides. ICRP.pp.80, 2005, Oxford.

37. International Atomic Energy Agency, Safety reports Series No. 63 release of Patients after Radionuclide Therapy, Vienna, 2009.

38. International Atomic Energy Agency, Basic Safety Standards for Protection against Ionizing Radiation and for the Safety of Radiation Sources, 1996.

39. Murray, I.P.C. Ell. P.J., Nuclear medicine clinical diagnosis and treatment, Edinburgh: Churchill Livingstone, 1994.

40. V. Spasic Jokic, M. Orlic, Monte Carlo Estimation of Patient Effective Dose in Diagnostic Procedures Using 131I; Journal of Physics: Conference Series 238 (2010) 012054.

41. S. Mattsson and C. Hoechen (eds.), Radiation Protection in Nuclear Medicine, DOI 10.1007/978-3-642-31167-3_2, Springer – Verlag Berlin Heidelberg 2013.

42. Bergonie J, Tribondeau L. De quelques resultants de la Radiotherapie, et esaie de fixation d'une technique rationelle. Comptes Rendu des Seances de l'Academie des Sciences 143:983-985, 1906.

43. Luckey TD. Radiation Hormesis. CRC Press.Boca Raton, FL, 1991.

44. Humm JL, Howell RW, Rao DV. AAPM Report No. 49, Dosimetry of Auger-Electron-Emitting Radionuclides, Med Phys 21(12), 1994.

45. Brooks AL. Evidence for "bystander effects" in vivo. Human Exp Toxicol 23:67-70, 2004.

46. Hall EJ. The bystander effect, Health Phys 85:31-35, 2003.

47. National academy of sciences, Health Risks from Exposure to Low Levels of Ionizing Radiation: BEIR VII Phase 2. The National Academies Press, Washington DC, 2006.

48. NCRP. The Relative Biological Effectiveness of Radiations of a different Quality. NCRP Report No 104. National Council on radiation Protection and Measurements, Bethseda, MD, 1990.

49. G. Saha., Springer-Verlag: Physics and radiobiology of nuclear medicine, 1993.

50. International Commission on Radiation Units and Measurements (2011) Fundamental Quantities and Units for Ionizing Radiation (Revised). ICRU report 85a. J ICRU 11 (1a).

51. International Commission on Radiation Units, Quantities and Units in radiation Protection Dosimetry, ICRU, Report 51, 1993

52. International Commission on Radiation Units. 1971 Radiation quantities and units ICRU Report 19 (Bethesda, MD: ICRU 1973 Dose equivalent Supplement to Report 19 (Bethesda, MD, USA: ICRU).

53. Rames Chandra; Nuclear medicine Physics: Basics, 7th edition, Lippincott & Wilkins,2011, ISBN 1451109415.

54. International Commission on Radiological Protection. 2007 The Recommendations of the International Commission on Radiological Protection. ICRP Publication 103 (2007).
55. International Commission on Radiological Protection. Basic anatomical and physiological data for use in radiological protection: reference values. ICRP Publication 89. Ann ICRP32(3-40 (2002).
56. International Commission on Radiological Protection. 1990. Recommendations of the International Commission on radiological Protection ICRP Publication 60. Ann. ICRP 21 (1-3) (Oxford: Pergamon Press) (1991).
57. International Commission on Radiation Units and Measurements, 2002, "Absorbed-dose specification in medicine nuclear", Oxford: Pergamon Press: ICRU Publication 67.
58. G. Sgouros, K.S. Kolbert, A. sheikh, K.S. Pentlow, E.F.Mun, A. barth, R.J. Robbins, S.M. Larson. Patient-Specific Dosimetry for 131I Thyroid Cancer Therapy Using 124iPET and 3-Dimensional-Internal Dosimetry (3D-ID) Software. J Nucl Med 45:1366-1372,(2004).
59. Zanzonico PB. Radiation dose to patients and relatives incident to 131I THERAPY. Thyroid 1997;7(2):199-204.
60. Lima, F.F. DE,2002, Otimizacao da dose terapeutica com 131I para carcinoma diferenciado da tiroide. Tese de D.Sc, Universidade Federal de Pernambuco, PE,Brasil.
61.Intermational Commission on Radiation Units and Measurements, 1998, "Fundamental quantities and units for ionizing radiation", Oxford: Pergamon Press: ICRU Publication 60.
62. M. C.Cantone, C. Hoeschen; Radiation Physics for Nuclear Medicine, Springer,2011.
63. Andreo, P., 1991, "Monte Carlo techniques in medical radiation physics", Phys. Med. Biol., v.36,n.7,pp.861-920.
64. National Radiological Protection Board. Board Statement on Diagnostic Medical Exposures to Ionising Radiation During Pregnancy, Documents of the NRPB 4(4). London:HMSO, 1993.)
65. Mountford P.J., Risk assessment of the nuclear medicine patient, The British Journal of Radiology, July 1997.
66. Mettler FA, Chrisitie JH, Williams JG, et al. Population characteristics and absorbed dose to the population from nuclear medicine:united States-1982. Health Phys 1986; 50: 619-28.)
67. Cohen BL. Catalog of risks extended and updated. Health Phys 1991; 61; 317-35.
68. Donald J. Peck, Ehsan samei,; How to understand and communicate Radiation Risk, Image Wisely,www.imagewisely.org.
69. Overbeek F, Pauwels EKJ, Broerse JJ. Carcinogeniic risk in diagnostic nuclear medicine: biological and epidemiological considerations. Eur J Nucl Med 1994;21:997-1012.
70. Stabin M, Stubbs J, Watson E. Recent controversy in radiation dosimetry. Eur J Nucl Med 1993;20:371-2.
71. Loevinger R, Budinger Tf, Watson EE(eds). MIRD primer for absorbed dose calculations. New York: Society of Nuclear medicine, 1989.

72. International Commission on Radiological Protection. Radiation Dose to Patients from Radiopharmaceuticals (including Addendum 1), ICRP Publication 53 Oxford: Pergamon Press, 1994.
73. Mountford PJ, Green S, Jones K, et al. Variation of dose rate with distance from extended sources of 99mTc. J Radiol Prot 1996;16:51-5.
74. Harding LK, Mostafa AB, Thomson WH. Staff radiation doses associated with nuclear medicine procedures – a review of some recent measurements. Nucl Med Commun 1990;11:271-7.
75. Mountford PJ,O'Doherty MJ, Forge NI. Radiationdose rates from adult patients undergoing nuclear medicine investigations. Nucl Med Commun 1991;12:767-77.
76. Harding LK, Mostafa AB, Roden L, et al. Dose rates from patients having nuclear medicine investigations. Nucl Med Commun 1985;6:191-4.
77. Mountford PJ, O'Doherty MJ, Harding LK, et al. Radiation dose rates from paediatric patients undergoing 99mTc investigations. Nucl Med Commun 1991;12:709-18.
78. Mountford PJ, Coakley AJ. A review of the secretion of radioactivity in human breast milk: data quantitative analysis and recommendations. Nucl Med Commun 1989;10:15-27.
79. Marcuse HR, Van der Steen J, Maessen HJM, et al. Radiation exposure to parents nursing their child during treatment with I-131-metaiodobenzylguanidine for neuroblastoma. In:Schlafke-Stelson AT,Watson EE, editors. Fourth International Radiopharmaceutical Dosimetry Symposium, CONF-851113. Oak Ridge, TN: Office of Science and Technological Information, 1986:181-5.
80. International Commission on radiological Protection. ICRP 74, Conversion coefficients for use in Radiological Protection against External Radiation, Annals of the ICRP 26,1997.
81. V. Spasic Jokic, M.Orlic, Monte Carlo estimation of patients effective dose in diagnostic procedures ising 131I, J.Phys:Conf.Ser. 238(1) (2010)1-6.
82. International Commission on radiological Protection.Radiation dose to patients from radiopharmaceuticals. ICRP Publication 53.Ann ICRp 18(1-40 (1987).
83. I.G.Zubal, C.R. Harrell, E.O. Smith, Z. Rattner, G. Gindi, P.B. Hofer, Computerized 3-dimensional segmented human anatomy, Med. Phys. 21 (1994) 299-302.
84. W.P. Segears, D.S.Lalush, B.M.W. Tsui, Modeling respiratory mechanics in the MCAT and spleen –based MCAT phantoms, IEEE Trans. Nucl. Sci. 48 (2001) 89-97.
85. K.F.Eckerman, M.Cristy, J.C.Ryman, The ORNL Mathematical phantoms Series, Oak Ridge National Labaratory, 1996.
86. International Commission on radiological Protection.ICRP 70, Basic Anatomical & Physiological Data for use in Radiological Protection., Annals of the ICRP 26, 1996.
87. International Commission on Radiological Protection. ICRP 89, Basic Anatomical & Physiological Data for use in Radiological Protection., Annals of the ICRP 32 (3-4), 2002.
88. International Commission on Radiation Units and Measurements, ICRU Report 46, Photon, Electron, Proton and Neutron Interaction data for body tissues, Bethesda, MD, 1992.

89. H. Behrens, L. Szybisz, Physics Data 6-1, zetralstelle Fur Atomkernenergie- Dokumentation, Germany, 1976.

90. Evaluated Nuclear Structure data File (ENSDF) database at the Brookhaven National Laboratory, 2002.

91. J.F. Briesmeister, A General Monte Carlo N-particle transport Code, Version 4B, LA-12625-M Report, Los Alamos national laboratory, Los Alamos., N.Mex., USA, 1977.

92. Hunt, J.G, Da Silva, F.C.A. Dos Santos, D.S, malatova, I., Dantas B.M, Azerdo A., 2000, "Visual Monte Carlo for Rdaiation Physics, particle Transport Simulation and Applications, Proceedings of the Monte Carlo 200 Conference, Lisbon, October 23-26, 2000, edited by A. Kling, F. Barao, M. Nakagawa, L. tavora, and P. Vaz. Springer-Verlag, Berlin, pp. 345-350.

93. Sherbini, S.S. and Decicco, J.E., 2005, "The use of radiation surveys to estimate the radiation effective dose to visitors of hospitalized patients – A theoretical study", Health Phys., v. 89, n.3, pp.216-223.

94. Yi, Y.; Stabin, M.G.; McKaskle, M.H.; Shone, M.D.; Johnson,A.B."Comparison of Measured and Calculated Dose Rates Near Nuclear Medicine Patients", Health Physics Society, March, 2013.

95. Larsen. I.L., E.A. Stetar and K.D. Glass, "In-House screening for Radioactive Sludge at a municipal Wastewater Treatment Plant", *Radiation Protection Management*, 12(4):29-38,1995.

96. Larsen. I.L., E.A. Stetar, B.G.Giles, and B.Garrison "Concentration of Iodine -131 Released from a Hospital Into a Municipal Sewer", RSO Magazine January/February 2001, Vol6, No1.

97. Tzavara I, Vlassopoulou B, Alevizaki C, Koukoulis G, Tzanela M, Koumoussi P, Sotsiou F, Thalassinos N, "Differentiated thyroid cancer: a retrospective analysis of 832 cases from Greece.;PMID 10468931, Pubmed – indexed foe MEDLINE.

98. R. Sciuto, L. Romano, S. Rea, F. Marandino, I. Sperdurti, and C.L. Maini;''Natural history and clinical outcome of differentiated thyroid carcinoma: aretrospective analysis of 1503 patients treated at a single institution., Annals of Oncology (2009) 20 (10) 1728-1735, Oxford Journals.

99. Brig SS Anand, V Sood, Lt Col PG. Kumar, Lt Col I. Sinha, Lt Col A. Kotwal, "Retrospective Analysis of Thyroid Cancer Patients", MJAFI, Vol 64, No1, 2008.

100. L. Johansson, S. Leide-Svegborn, S. Mattsson, B. Nosslin, Biokinetics of iodide in man:refinement of current ICRP dosimetry models, Cancer Biother. Radiopharrm. 18(2003) 445-450.

101. International Commission on Radiological Protection, ICRP 88 Doses to the Embryo and Fetus from Intakes of Radionuclides by the mother, International Commission on Radiological Protection, Pergamon Press, Oxford, 2001.

102. Vesna Spasic Jokic, Marina Zdraveska Kocovska,"New technique for effective dose estimation using Monte Carlo simulation for the patients undergoing radioiodine therapy", Measurement 46(2013) 795-802.

103. Brincker H. Hansen HS, Andersen AP. Induction of leukaemia by I131 treatment of thyroid carcinoma. Br J Cancer 1973:28:232-237.

104. Jall P, Holm LE, Lundell G, et al. Cancer risks in thyroid cancer patients. Br J Cancer 1991; 64:159-163.

105. Sobels FH. Estimation of the genetic risk resulting from the treatment of women with I131.Strahlentherapie 1968:138:172-177

106. E. L. Saenger, G. E. Thoma and E. A. Tompkins, Incidence of leukemia following treatment of hyperthyroidism: Preliminary report of the cooperative thyrotoxicosis therapy follow-up study. J.Am.Med.Assoc.205.855-862 (1968).

107. A.B.Brill, M.Stabin, A. Bouville, and E. Ron,"Normal Organ Radiation Doseimetry and Associated Uncertainties in Nuclear medicine, with Emphasis on Iodine-131.Radiation Research, 16691): 128-140.2006.

108. B. M. Doybyns, G. E. Sheline, J.B. Workman, E. A. Tompkins, W. M. McConahey and D. V. Becker, Malignant and benign neoplasms of the thyroid in patients treated for hyperthyroidism: A report of the cooperative thyrotoxicosis therapy follow up studyJ. Clin. Endocrinol. Metab. 38, 976-998 (1974).

109. E. Ron, M. M. Doody, D. V. Becker, A. B. Brill, R. E. Curtis, M. B. Goldman, B. S. H. Harris, D. A. Hoffman, W. M. McConahey and J. D. Boice, Cancer mortality following treatment for adult hyperthyroidism. J. AM. Med. Assoc. 280, 347-355 (1998).

110. J. A. Franklyn, P. Maiaonneuve, M. C. Sheppard, J. Betteridge and P. Boyle, Mortality after the treatment of hyperthyroidism with radioactive iodine. New Engl. J. Med. 338, 712-718 (1998).

111. L. E. Holm, P. Hall, K. Wiklund, G. Lundell, G. Berg, G. Bjelkengren, E. Cederquist, U. B. Ericsson, A. Hallquist and L. G. Larsson, Cancer risk after iodine-131 therapy for hyperthyroidism, J. Natl. Cancer Inst. 83, 1072-1077 (1991).

112. P. Hall, G. Berg, G. Bjelkengren, J. D. Boice, Jr., U. B. Ericsson, A. Hallquist, M. Lindberg, G. Lundell, J. Tennvall and L. E. Holm, Cancer mortality after iodine 131 therapy for hyperthyroidism. Int. J.Cancer 50,886-890 (1992).

113. P. W. Dickman, L. E. Holm, G. Lundell, J. D. Boice, Jr. and P. Hall, Thyroid cancer risk after thyroid examination with I131: A population based cohort study in Sweden. Int. J. cancer 106, 580-587 (2003).

114. K. Hahn, p. Schnell-Inderst, B. Grosche and L.E. Holm, Thyroid cancer after diagnostic administration of iodine in childhood. Radiat. Res. 156,61-70 (2001).

115. L. E. Holm, K. E. Wiklund, G. E. Lundell, N. A. Bergman, G. Bjelkengren, E. S. Cederquist, U. B. Ericsson, L. G. Larsson, M. E. Lidberg and R. S. Lindberg, Thyroid cancer after diagnostic doses of iodine 131: A retrospective cohort study, J. Natl. cancer Inst. 80, 1132-1138 (1998).

116. B. Globel, H. Globel, and E. Oberhausen, Epidemiologic studies on patients with iodine-131 diagnostic and therapy. In Radiation - Risk – Protection, Vol,II, pp. 565-568. Fcahhverband fur Strahlenschutz e. V., Koln, 1984.

117. Clark OH, Dah QY. Thyroid Cancer. Med Clin North Am 1991;75:211-34.

118. Franklyn JA, Maisonneuve P, Sheppard M, Betteridge J, Boyle P. Cancer incidence and mortality after radioiodine treatment for hyperthyroidism: a population-based cohort study. Lancet 1999; 353:2111-2115.

119. Wartofsky L, Glinoer D, Solomon B, Lagasse R. differences and similarities in the treatment of diffuse goiter in Europe and the ibnited states. Exp Clin End 1991; 97:243-251.

120. Monsieurs MA, Thierens HM, Van de Wiele C, Vrasl AM, Mierlaen IA, De winter HA, de Sadeleer CJ, De ridder I, Kaufman JM, Dierckx RA. Estimation of risk based on biological dosimetry for patients treated with radioiodine. Nucl Med Comm 1999;20:911-917.

121. Astakhova LN, Anspaugh LR, Beebe GW, Bouville A, Drozdovitch VV, Garber V, Gavrilin YI, Khrouch VT, Kuvshinnikov AV, Kuzmenkov YN, Minenko VP, Moschik KV, Nalivko AS, Robbins J, Shemiakina EV, Shinkarev S, Toschitskaya SI, Waclawiw MA. Chernobil-related thyroid cancer in children of Belarus :a case control study. Radiat Res 1998; 150(3):349-356.

122. Gapanovich VN, Laroshevich RF, Shuvaeva LP, Becker SI, Nekolla EA, Kellerer AM. Childhood leukemia in Belarus before and after the Chernobyl accident: continued follow up. Radiat environ Biophys 2001; 40(4):259-267.

123. Chandra,R., (1992), Introductory physics of nuclear medicine, 4th edition, Lea Febiger, Philadelphia,1992.

124. Edwards,M.S., 1977,"Dose Estimate Techniques", In:ROLLO, F.D., Nuclear Medicine Physics, Instrumentation, and agents, Chapter 14,Ed.Mosby Company.

125. Ahmed S, Jahan QM, Demir M, Zalaria GA, Study on Radioiodine distribution over several organs of the Thyroid cancer patients to determine the effective dose equivalent that relates to fatal occurrences: A clinical perspective. World J Nucl Med 2004;3: 131-136.

LIST OF FIGURES

LIST OF TABLES

LIST OF GRAPHS

Graph 34. Energy spectrum

Annex 1

Central Limit theorem

Define sets of a discrete random variable ξ,

$$M_{\xi=} \sum_{i=1}^{n} x_i \, p_i$$

And continuous ξ random variable at interval (a, b)

$$M_{\xi=} \int_{a}^{b} xp(x)dx$$

The variance of a discrete random variable ξ is defined by the number

$$D\xi = M[(\xi - M\xi)^2]$$

And continuous random variable ξ at an interval (a, b)

$$D\xi = \int_{a}^{b} x^2 \, p(x)dx - (\int_{a}^{b} xp(x)dx)^2$$

If $\xi_1,\xi_2,\ldots..\xi_N$ is a long sequence of values assumed by ξ the average of this will be the next Mʒ,

$$M\xi \approx \frac{1}{N} (\xi_1 + \xi_2 + \ldots..\xi_N) = \frac{1}{N} \sum_{i=1}^{N} \xi_i$$

$$SN = \sum_{1}^{N} A_{i(x_i, y_i, z_i \ldots)} = \overline{A}$$

Considering ξ_1, ξ_2, ξ_3…….N, independent random variables equally distributed. The distribution of the variables is the same as their variances. Thus we can write

$$M\xi_1 = M\xi_2 = \ldots\ldots M\xi_N = m$$

$$D\xi_1 = D\xi_2 = \ldots\ldots..D\xi_N = b^2$$

Knowing that for any random variable ξ and η and take place

$$M\ (\xi + \eta) = M\xi + M\eta$$

$$D\ (\xi + \eta) = D\xi + D\eta$$

If we denote with ρ_N the sum of the variables

$\rho_N = \xi_1 + \xi_2 + \ldots\ldots + \xi_N$ follows

$$M\rho_N = M(\xi_1 + \xi_{2\ldots\ldots\ldots} + \xi_N) = Nm$$

$$D\rho_N = D(\xi_1 + \xi_{2\ldots\ldots\ldots} + \xi_N) = Nb^2$$

Assuming ξ_N, denotes a normal random variable by individual parameters

$$a = Nm \text{ and } \sigma^2 = Nb^2$$

The Central Limit Theorem states that for any range (a' b') and N sufficiently large it.

$$P\{a' < \rho_N < b'\} \approx \int_{a'}^{b'} P\xi_N\,(x)dx$$

Thus the sum of a large number of independent variables also is approximately normal distributed

$$(P\rho_N(x) \approx P\xi_N(x))$$

Annex 2 – tables with results

MBq	*Skin*	*Lungs*	*Liver*
185	0,007	0,016	0,031
370	0,014	0,033	0,062
555	0,022	0,050	0,096
1110	0,044	0,102	0,192
1813	0,065	0,149	0,282
2423	0,087	0,199	0,377
2516	0,090	0,206	0,391
2756	0,099	0,226	0,428
3009	0,108	0,247	0,468
3145	0,113	0,258	0,489
3237	0,115	0,262	0,497
3349	0,117	0,268	0,501
3441	0,121	0,278	0,536
3515	0,126	0,288	0,546
3614	0,130	0,296	0,562
3737	0,134	0,306	0,581
3838	0,138	0,314	0,596
3959	0,142	0,324	0,615
4033	0,145	0,330	0,627
4440	0,160	0,364	0,690
5106	0,188	0,400	0,731
5476	0,200	0,405	0,803
5550	0,220	0,455	0,863
6105	0,220	0,500	0,949

Table A2-1. Results of organ effective dose for given activity

MBq	*Ovary, gonads*	*Bladder*	*Colon*
185	24,040	27,429	47,028
370	48,079	54,858	94,061
555	72,121	82,288	141,084
1110	144,244	164,581	282,100
1813	235,690	244,020	461,060
2423	315,060	326,190	616,360
2516	327,080	338,640	639,880
2756	358,350	371,010	701,050
3009	391,250	405,070	765,410
3145	408,850	423,300	799,850
3237	416,100	433,100	801,900
3349	426,100	443,100	819,900
3441	437,100	463,100	836,900
3515	457,050	473,200	894,140
3614	469,840	486,450	919,170
3737	485,810	502,980	950,410
3838	498,890	516,530	976,010
3959	514,670	532,860	1006,870
4033	524,290	542,820	1025,690
4440	577,200	597,600	1129,200
5106	632,200	650,600	1289,200
5476	700,030	709,880	1399,500
5550	721,500	747,000	1411,500
6105	793,650	821,700	1552,650

Table A2-2. Effective doses for ovary, bladder and colon

MBq	*Stomach*
185	3713,514
370	7427,062
555	11140,544
1110	22281,091
1813	36407,000
2423	48666,500
2516	50524,000
2756	55353,500
3009	60435,620
3145	63155,000
3237	65740,640
3349	68727,500
3441	69099,000
3515	70599,900
3614	72576,240
3737	75043,000
3838	77063,960
3959	79501,000
4033	80987,000
4440	89160,000
5106	102534,000
5476	109964,000
5550	111450,000
6105	122595,000

Table A2-3. Effective doses for different activity for stomach

Annex 3

Administrated activity: 185 MBq

Organ	$\bar{H}$[µSv/s]	$\bar{H}$[mSv/1 min]	*E*[µSv]	Risk
Bladder	0.555	0.04	1.84	1.00×10^{-9}
Colon	0.435	0.03	3.22	0.90×10^{-7}
Ovary, gonads	0.133	0.01	1.62	0.80×10^{-8}
Stomach			247.76	0.024×10^{-3}

Administrated activity: 555 MBq

Organ	$\bar{H}$[µSv/s]	$\bar{H}$[mSv/1 min]	*E*[µSv]	Risk
Bladder	1.665	0.11	5.61	3.01×10^{-9}
Colon	1.306	0.09	9.56	2.64×10^{-7}
Ovary, gonads	0.400	0.02	4.83	2.43×10^{-8}
Stomach			743	0.08×10^{-3}

Administrated activity: 1813 MBq

Organ	$\bar{H}$[µSv/s]	$\bar{H}$[mSv/1 min]	*E*[µSv]	Risk
Bladder	5.439	0.33	16.56	1.007×10^{-8}
Colon	4.268	0.27	31.01	7.54×10^{-7}
Ovary, gonads	1.308	0.09	15.87	7.92×10^{-8}
Stomach			2502	0.24×10^{-3}

Administrated activity: 2423.5 MBq

Organ	$\bar{H}$[µSv/s]	$\bar{H}$[mSv/1 min]	*E*[µSv]	Risk
Bladder	7.271	0,48	22.02	0.14×10^{-7}
Colon	5.705	0.36	42.07	0.11×10^{-5}
Ovary, gonads	1.749	0,14	21,67	0.11×10^{-6}
Stomach			3254.44	0.31×10^{-3}

Administrated activity: 2516 MBq

Organ	$\bar{H}$[µSv/s]	$\bar{H}$[mSv/1 min]	*E*[µSv]	Risk
Bladder	7.548	0.46	22.66	0.14×10^{-7}
Colon	5.923	0.37	43.27	0.11×10^{-5}
Ovary, gonads	1.816	0.11	21.08	0.12×10^{-6}
Stomach			3371.08	0.32×10^{-3}

Administrated activity: 3515.7 MBq

Organ	$\bar{H}$[µSv/s]	$\bar{H}$[mSv/1 min]	*E*[µSv]	Risk
Bladder	10.547	0.64	32.05	0.21×10^{-7}
Colon	8.276	0.51	60.09	0.16×10^{-5}
Ovary, gonads	2.537	0.16	30.88	0.16×10^{-6}
Stomach			4710.61	0.46×10^{-3}

Administrated activity: 4440 MBq

Organ	$\bar{H}$[µSv/s]	$\bar{H}$[mSv/1 min]	*E*[µSv]	Risk
Bladder	13.320	0.81	41.02	0.25×10^{-7}
Colon	10.452	0.64	76.28	0.19×10^{-5}
Ovary, gonads	3.142	0.21	39.82	0.25×10^{-6}
Stomach			5951	0.58×10^{-3}

Administrated activity: 5476 MBq

Organ	$\bar{H}$[µSv/s]	$\bar{H}$[mSv/1 min]	*E*[µSv]	Risk
Bladder	16.050	1.01	48.34	0.31×10^{-7}
Colon	13.009	0.78	94.34	0.23×10^{-5}
Ovary, gonads	3.995	0.25	48.03	0.24×10^{-6}
Stomach			7343.67	0.74×10^{-3}

Administrated activity: 6105 MBq

Organ	$\bar{H}$[µSv/s]	$\bar{H}$[mSv/1 min]	*E*[µSv]	Risk
Bladder	18.315	1.12	55.08	0.34×10^{-7}
Colon	14.372	0.87	103.61	0.26×10^{-5}
Ovary, gonads	4.406	0.27	53.01	0.27×10^{-6}
Stomach			8200	0.76×10^{-3}

Administrated activity: 185 MBq

Organ	$\bar{H}$[µSv/s]	$\bar{H}$[mSv/15min]	*E*[µSv]	Risk
Bladder	0.555	0.497	27.429	0.149×10^{-7}
Bone surface	0.031	0.013	27.789×10^{-5}	0.139×10^{-10}
Colon	0.435	0.392	47.028	0.131×10^{-5}
Liver	0.007	0.004	0.031	0.865×10^{-8}
Lungs	0.001	0.001	0.016	1.007×10^{-8}
Ovary, gonads	0.133	0.120	24.040	0.120×10^{-6}
Skin	0.007	0.007	0.007	0.132×10^{-8}
Stomach			3713.514	0.340×10^{-3}
TOTAL				0.346×10^{-3}

Administrated activity: 370 MBq

Organ	$\bar{H}$[µSv/s]	$\bar{H}$[mSv/15min]	*E*[µSv]	Risk
Bladder	1.110	0.994	54.858	0.298×10^{-7}
Bone surface	0.062	0.026	55.601×10^{-5}	0.278×10^{-10}
Colon	0.871	0.800	94.061	0.262×10^{-5}
Liver	0.014	0.008	0.062	1.736×10^{-8}
Lungs	0.002	0.002	0.033	2.015×10^{-8}
Ovary, gonads	0.267	0.241	48.079	0.241×10^{-6}
Skin	0.014	0.014	0.014	0.265×10^{-8}
Stomach			7427.062	0.681×10^{-3}
TOTAL				0.693×10^{-3}

Administrated activity: 555 MBq

Organ	$\bar{H}$[µSv/s]	$\bar{H}$[mSv/15min]	*E*[µSv]	Risk
Bladder	1.665	1.492	82.288	0.448×10^{-7}
Bone surface	0.094	0.040	83.367×10^{-5}	0.418×10^{-10}
Colon	1.306	1.176	141.084	0.396×10^{-5}
Liver	0.022	0.013	0.096	2.596×10^{-8}
Lungs	0.003	0.003	0.050	3.022×10^{-8}
Ovary, gonads	0.400	0.361	72.121	0.362×10^{-6}
Skin	0.022	0.022	0.022	0.397×10^{-8}
Stomach			11140.544	1.022×10^{-3}
TOTAL				1.0384×10^{-3}

Administrated activity: 1110 MBq

Organ	$\bar{H}$[µSv/s]	$\bar{H}$[mSv/15min]	*E*[µSv]	Risk
Bladder	3.331	2.983	164.581	0.898×10^{-7}
Bone surface	0.189	0.080	166.720×10^{-5}	0.837×10^{-10}
Colon	2.613	2.354	282.100	0.800×10^{-5}
Liver	0.044	0.026	0.192	5.194×10^{-8}
Lungs	0.006	0.006	0.102	6.046×10^{-8}
Ovary, gonads	0.794	0.724	144.244	0.724×10^{-6}
Skin	0.044	0.044	0.044	0.800×10^{-8}
Stomach			22281.091	2.045×10^{-3}
TOTAL				2.0770×10^{-3}

Administrated activity: 1813 MBq

Organ	$\bar{H}$[µSv/s]	$\bar{H}$[mSv/15min]	*E*[µSv]	Risk
Bladder	5.439	4.876	244.02	1.465×10^{-7}
Bone surface	0.302	0.124	272.44×10^{-5}	1.362×10^{-10}
Colon	4.268	3.842	461.06	1.112×10^{-5}
Liver	0.063	0.036	0.282	8.477×10^{-8}
Lungs	0.014	0.012	0.149	9.874×10^{-8}
Ovary, gonads	1.308	1.176	235.69	1.176×10^{-6}
Skin	0.072	0.065	0.065	1.299×10^{-8}
Stomach			36407	3.337×10^{-3}
TOTAL				3.389×10^{-3}

Administrated activity: 2423.5 MBq

Organ	$\bar{H}$[µSv/s]	$\bar{H}$[mSv/15min]	*E*[µSv]	Risk
Bladder	7.271	6.517	326.19	1.959×10^{-7}
Bone surface	0.404	0.364	364.18×10^{-5}	1.821×10^{-10}
Colon	5.705	5.135	616.36	1.487×10^{-5}
Liver	0.084	0.075	0.377	11.332×10^{-8}
Lungs	0.018	0.017	0.199	13.198×10^{-8}
Ovary, gonads	1.749	1.572	315.06	1.572×10^{-6}
Skin	0.096	0.087	0.087	1.736×10^{-8}
Stomach			48666.5	4.461×10^{-3}
TOTAL				4.531×10^{-3}

Administrated activity: 2516 MBq

Organ	$\bar{H}$[µSv/s]	$\bar{H}$[mSv/15min]	*E*[µSv]	Risk
Bladder	7.548	6.766	338.64	2.033×10^{-7}
Bone surface	0.420	0.378	378.08×10^{-5}	1.890×10^{-10}
Colon	5.923	5.331	639.88	1.544×10^{-5}
Liver	0.087	0.078	0.391	11.764×10^{-8}
Lungs	0.019	0.017	0.206	13.702×10^{-8}
Ovary, gonads	1.816	1.632	327.08	1.632×10^{-6}
Skin	0.100	0.091	0.090	1.802×10^{-8}
Stomach			50524	4.631×10^{-3}
TOTAL				4.704×10^{-3}

Administrated activity: 2756.5 MBq

Organ	$\bar{H}$[µSv/s]	$\bar{H}$[mSv/15min]	*E*[µSv]	Risk
Bladder	8.270	7.413	371.01	2.228×10^{-7}
Bone surface	0.460	0.414	414.22×10^{-5}	2.071×10^{-10}
Colon	6.489	5.841	701.05	1.691×10^{-5}
Liver	0.095	0.086	0.428	12.889×10^{-8}
Lungs	0.021	0.019	0.226	15.012×10^{-8}
Ovary, gonads	1.989	1.788	358.35	1.788×10^{-6}
Skin	0.110	0.099	0.099	1.974×10^{-8}
Stomach			55353.5	5.073×10^{-3}
TOTAL				5.153×10^{-3}

Administrated activity: 3009.3MBq

Organ	$\bar{H}$[µSv/s]	$\bar{H}$[mSv/15min]	*E*[µSv]	Risk
Bladder	9.029	8.093	405.07	2.432×10^{-7}
Bone surface	0.509	0.452	452.25×10^{-5}	2.261×10^{-10}
Colon	7.085	6.377	765.41	1.846×10^{-5}
Liver	0.104	0.094	0.468	14.072×10^{-8}
Lungs	0.023	0.020	0.247	16.390×10^{-8}
Ovary, gonads	2.172	1.952	391.25	1.952×10^{-6}
Skin	0.120	0.108	0.108	2.156×10^{-8}
Stomach			60435.62	5.539×10^{-3}
TOTAL				5.626×10^{-3}

Administrated activity: 3145 MBq

Organ	$\bar{H}$[µSv/s]	$\bar{H}$[mSv/15min]	*E*[µSv]	Risk
Bladder	9.435	8.458	423.30	2.542×10^{-7}
Bone surface	0.525	0.473	472.60×10^{-5}	2.363×10^{-10}
Colon	7.404	6.664	799.85	1.930×10^{-5}
Liver	0.109	0.098	0.489	14.705×10^{-8}
Lungs	0.024	0.021	0.258	17.128×10^{-8}
Ovary, gonads	2.270	2.040	408.85	2.040×10^{-6}
Skin	0.125	0.113	0.113	2.253×10^{-8}
Stomach			63155	5.789×10^{-3}
TOTAL				5.880×10^{-3}

Administrated activity: 3237.5 MBq

Organ	$\bar{H}$[µSv/s]	$\bar{H}$[mSv/15min]	*E*[µSv]	Risk
Bladder	9.599	8.5007	433.10	2.547×10^{-7}
Bone surface	0.536	0.461	479.10×10^{-5}	2.391×10^{-10}
Colon	7.596	6.903	801.90	1.957×10^{-5}
Liver	0.111	0.099	0.497	15.001×10^{-8}
Lungs	0.025	0.022	0.262	17.773×10^{-8}
Ovary, gonads	2.300	2.080	416.10	2.088×10^{-6}
Skin	0.129	0.113	0.115	2.408×10^{-8}
Stomach			65740.64	6.026×10^{-3}
TOTAL				6.120×10^{-3}

Administrated activity: 3349.25 MBq

Organ	$\bar{H}$[µSv/s]	$\bar{H}$[mSv/15min]	*E*[µSv]	Risk
Bladder	9.885	8.856	443.10	2.550×10^{-7}
Bone surface	0.546	0.406	489.10×10^{-5}	2.441×10^{-10}
Colon	7.896	7.001	819.90	1.977×10^{-5}
Liver	0.115	0.100	0.501	15.409×10^{-8}
Lungs	0.025	0.022	0.268	18.003×10^{-8}
Ovary, gonads	2.398	2.101	426.10	2.100×10^{-6}
Skin	0.135	0.113	0.117	2.318×10^{-8}
Stomach			68727.5	6.163×10^{-3}
TOTAL				6.260×10^{-3}

Administrated activity: 3441 MBq

Organ	$\bar{H}$[µSv/s]	$\bar{H}$[mSv/15min]	*E*[µSv]	Risk
Bladder	10.107	9.156	463.10	2.554×10^{-7}
Bone surface	0.561	0.508	503.10×10^{-5}	2.541×10^{-10}
Colon	8.176	7.260	836.90	2.001×10^{-5}
Liver	0.118	0.101	0.536	16.409×10^{-8}
Lungs	0.026	0.023	0.278	18.669×10^{-8}
Ovary, gonads	2.458	2.201	437.10	2.179×10^{-6}
Skin	0.135	0.113	0.121	2.488×10^{-8}
Stomach			69099	6.333×10^{-3}
TOTAL				6.433×10^{-3}

Administrated activity: 3515.7 MBq

Organ	$\bar{H}$[µSv/s]	$\bar{H}$[mSv/15min]	*E*[µSv]	Risk
Bladder	10.547	9.454	473.20	2.841×10^{-7}
Bone surface	0.586	0.528	528.31×10^{-5}	2.642×10^{-10}
Colon	8.276	7.450	894.14	2.157×10^{-5}
Liver	0.122	0.109	0.546	16.439×10^{-8}
Lungs	0.027	0.024	0.288	19.147×10^{-8}
Ovary, gonads	2.537	2.281	457.05	2.281×10^{-6}
Skin	0.140	0.126	0.126	2.518×10^{-8}
Stomach			70599.9	6.471×10^{-3}
TOTAL				6.573×10^{-3}

Administrated activity: 3614.2 MBq

Organ	$\bar{H}$[µSv/s]	$\bar{H}$[mSv/15min]	*E*[µSv]	Risk
Bladder	10.842	9.719	486.45	2.921×10^{-7}
Bone surface	0.603	0.543	603.93×10^{-5}	2.716×10^{-10}
Colon	8.508	7.658	919.17	2.217×10^{-5}
Liver	0.125	0.112	0.562	16.899×10^{-8}
Lungs	0.027	0.025	0.296	19.683×10^{-8}
Ovary, gonads	2.608	2.344	469.84	2.344×10^{-6}
Skin	0.144	0.130	0.130	2.589×10^{-8}
Stomach			72576.24	6.652×10^{-3}
TOTAL				6.757×10^{-3}

Administrated activity: 3737 MBq

Organ	$\bar{H}$[µSv/s]	$\bar{H}$[mSv/15min]	*E*[µSv]	Risk
Bladder	11.211	10.050	502.98	3.020×10^{-7}
Bone surface	0.623	0.562	561.56×10^{-5}	2.808×10^{-10}
Colon	8.797	7.918	950.41	2.293×10^{-5}
Liver	0.129	0.116	0.581	17.473×10^{-8}
Lungs	0.028	0.026	0.306	20.352×10^{-8}
Ovary, gonads	2.697	2.424	485.81	2.424×10^{-6}
Skin	0.149	0.134	0.134	2.677×10^{-8}
Stomach			75043	6.878×10^{-3}
TOTAL				6.986×10^{-3}

Administrated activity: 3838 MBq

Organ	$\bar{H}$[µSv/s]	$\bar{H}$[mSv/15min]	*E*[µSv]	Risk
Bladder	11.513	10.320	516.53	3.101×10^{-7}
Bone surface	0.640	0.577	576.68×10^{-5}	2.883×10^{-10}
Colon	9.034	8.132	976.01	2.354×10^{-5}
Liver	0.133	0.119	0.596	17.944×10^{-8}
Lungs	0.029	0.026	0.314	20.900×10^{-8}
Ovary, gonads	2.769	2.489	498.89	2.489×10^{-6}
Skin	0.153	0.138	0.138	2.749×10^{-8}
Stomach			77063.96	7.063×10^{-3}
TOTAL				7.174×10^{-3}

Administrated activity: 3959MBq

Organ	$\bar{H}$[µSv/s]	$\bar{H}$[mSv/15min]	*E*[µSv]	Risk
Bladder	11.872	10.647	532.86	3.199×10^{-7}
Bone surface	0.660	0.595	594.92×10^{-5}	2.975×10^{-10}
Colon	9.320	8.389	1006.87	2.429×10^{-5}
Liver	0.137	0.123	0.615	18.511×10^{-8}
Lungs	0.030	0.027	0.324	21.561×10^{-8}
Ovary, gonads	2.857	2.568	514.67	2.568×10^{-6}
Skin	0.157	0.142	0.142	2.836×10^{-8}
Stomach			79501	7.287×10^{-3}
TOTAL				7.401×10^{-3}

Administrated activity: 4033 MBq

Organ	$\bar{H}$[µSv/s]	$\bar{H}$[mSv/15min]	*E*[µSv]	Risk
Bladder	12.099	10.846	542.82	3.259×10^{-7}
Bone surface	0.673	0.606	606.04×10^{-5}	3.030×10^{-10}
Colon	9.494	8.546	1025.69	2.474×10^{-5}
Liver	0.140	0.125	0.627	18.857×10^{-8}
Lungs	0.031	0.028	0.330	21.964×10^{-8}
Ovary, gonads	2.910	2.616	524.29	2.616×10^{-6}
Skin	0.160	0.145	0.145	2.889×10^{-8}
Stomach			80987	7.423×10^{-3}
TOTAL				7.540×10^{-3}

Administrated activity: 4440 MBq

Organ	$\bar{H}$[µSv/s]	$\bar{H}$[mSv/15min]	*E*[µSv]	Risk
Bladder	13.320	11.940	597.6	3.588×10^{-7}
Bone surface	0.740	0.667	667.20×10^{-5}	3.336×10^{-10}
Colon	10.452	9.408	1129.20	2.724×10^{-5}
Liver	0.154	0.138	0.690	20.760×10^{-8}
Lungs	0.034	0.030	0.364	24.180×10^{-8}
Ovary, gonads	3.142	2.880	577.2	2.880×10^{-6}
Skin	0.176	0.160	0.160	3.180×10^{-8}
Stomach			89160	8.172×10^{-3}
TOTAL				8.300×10^{-3}

Administrated activity: 5106 MBq

Organ	$\bar{H}$[µSv/s]	$\bar{H}$[mSv/15min]	*E*[µSv]	Risk
Bladder	15.620	14.004	650.60	4.004×10^{-7}
Bone surface	0.856	0.767	767.20×10^{-5}	3.836×10^{-10}
Colon	12.452	10.408	1289.20	3.104×10^{-5}
Liver	0.184	0.157	0.731	23.760×10^{-8}
Lungs	0.040	0.032	0.400	28.180×10^{-8}
Ovary, gonads	3.801	3.199	632.2	3.190×10^{-6}
Skin	0.204	0.182	0.188	3.378×10^{-8}
Stomach			102534	9.398×10^{-3}
TOTAL				9.545×10^{-3}

Administrated activity: 5476 MBq

Organ	$\bar{H}$[µSv/s]	$\bar{H}$[mSv/15min]	*E*[µSv]	Risk
Bladder	16.050	14.825	709.88	4.385×10^{-7}
Bone surface	0.920	0.809	799.00×10^{-5}	4.00×10^{-10}
Colon	13.009	11.260	1399.5	3.309×10^{-5}
Liver	0.190	0.165	0.803	25.050×10^{-8}
Lungs	0.041	0.036	0.405	29.625×10^{-8}
Ovary, gonads	3.995	3.501	700.03	3.470×10^{-6}
Skin	0.218	0.193	0.200	3.598×10^{-8}
Stomach			109964	10.079×10^{-3}
TOTAL				10.237×10^{-3}

Administrated activity: 5550 MBq

Organ	$\bar{H}$[µSv/s]	$\bar{H}$[mSv/15min]	*E*[µSv]	Risk
Bladder	16.650	14.925	747.00	4.485×10^{-7}
Bone surface	0.926	0.834	834.00×10^{-5}	4.170×10^{-10}
Colon	13.065	11.760	1411.5	3.405×10^{-5}
Liver	0.192	0.173	0.863	25.950×10^{-8}
Lungs	0.042	0.038	0.455	30.225×10^{-8}
Ovary, gonads	4.005	3.600	721.5	3.600×10^{-6}
Skin	0.221	0.200	0.220	3.975×10^{-8}
Stomach			111450	10.215×10^{-3}
TOTAL				10.376×10^{-3}

Administrated activity: 6105 MBq

Organ	$\bar{H}$[µSv/s]	$\bar{H}$[mSv/15min]	*E*[µSv]	Risk
Bladder	18.315	16.418	821.70	4.934×10^{-7}
Bone surface	1.018	0.918	917.40×10^{-5}	4.587×10^{-10}
Colon	14.372	12.936	1552.65	3.746×10^{-5}
Liver	0.211	0.190	0.949	28.545×10^{-8}
Lungs	0.046	0.042	0.500	33.248×10^{-8}
Ovary, gonads	4.406	3.960	793.65	3.960×10^{-6}
Skin	0.243	0.220	0.220	4.373×10^{-8}
Stomach			122595	11.237×10^{-3}